





# Plasticity in *Caenorhabditis elegans*

## Plasticiteit in *Caenorhabditis elegans*

Proefschrift

ter verkrijging van de graad van doctor aan de  
Erasmus Universiteit Rotterdam  
op gezag van de rector magnificus  
Prof.dr. S.W.J. Lamberts  
en volgens besluit van het College van Promoties

De openbare verdediging zal plaatsvinden op  
woensdag 12 maart 2008 om 11:45 uur  
door **Martinus Petrus Josephus Dekkers**



## **Promotiecommissie**

Promotor: Prof.dr. F.G. Grosveld

Overige leden: Prof.dr. J.G.G. Borst  
Dr.ir. N.J. Galjart  
Dr. D.N. Meijer

Copromotor: Dr. G. Jansen

# Contents

<b>1</b>	<b>Introduction</b>	<b>7</b>
1.1	Introduction . . . . .	8
1.2	Plasticity of G-protein signalling . . . . .	8
1.3	Synaptic plasticity . . . . .	9
1.4	Structural plasticity . . . . .	10
1.5	Correlating cellular responses to behaviour . . . . .	10
1.6	<i>C. elegans</i> in neurobiology . . . . .	11
1.7	Cilia in signalling . . . . .	13
1.8	Cilia in <i>C. elegans</i> . . . . .	14
1.9	Behavioural repertoire of <i>C. elegans</i> , and its plasticity . . . . .	15
1.10	Gustatory plasticity . . . . .	18
1.11	Food signals are important for establishing gustatory plasticity . . . . .	19
1.12	Dauer formation . . . . .	19
1.13	Single cell studies & techniques . . . . .	20
1.14	Conclusion . . . . .	21
<b>2</b>	<b>Altered sensitivity of ASE and ASH neurons explains gustatory plasticity in <i>C. elegans</i></b>	<b>23</b>
2.1	Abstract . . . . .	24
2.2	Results . . . . .	24
2.3	Materials & Methods . . . . .	31
<b>3</b>	<b>Expression of mammalian receptors in <i>C. elegans</i> generates novel behavioural responses</b>	<b>33</b>
3.1	Abstract . . . . .	34
3.2	Introduction . . . . .	34
3.3	Results . . . . .	37
3.4	Discussion . . . . .	45
3.5	Materials & Methods. . . . .	48

<b>4</b>	<b>Mutation of the MAP kinase DYF-5 affects docking and undocking of kinesin-2 motors and reduces their speed in the cilia of <i>C. elegans</i></b>	<b>51</b>
4.1	Abstract . . . . .	52
4.2	Introduction . . . . .	52
4.3	Results . . . . .	54
4.4	Discussion . . . . .	64
4.5	Materials and Methods . . . . .	66
<b>5</b>	<b>Environmental cues and G protein signalling regulate intraflagellar transport and cilia length</b>	<b>69</b>
5.1	Abstract . . . . .	70
5.2	Introduction . . . . .	70
5.3	Results . . . . .	72
5.4	Discussion . . . . .	84
5.5	Materials & Methods . . . . .	86
<b>6</b>	<b>Discussion</b>	<b>89</b>
6.1	Plasticity in <i>C. elegans</i> . . . . .	90
6.2	Constructing circuits for behaviour . . . . .	92
6.3	Technical opportunities and challenges . . . . .	93
6.4	Are all forms of plasticity equal? . . . . .	96
6.5	Structural plasticity of the cilia . . . . .	97
6.6	Conclusion . . . . .	99
<b>7</b>	<b>References</b>	<b>101</b>
<b>8</b>	<b>Appendix</b>	<b>115</b>
8.1	Summary . . . . .	116
8.2	Samenvatting . . . . .	117
8.3	Dankwoord . . . . .	118
8.4	Curriculum Vitae . . . . .	120

*In the beginning there was nothing. God said: "let there be light!". And there was light. There was still nothing, but you could see it a whole lot better.*

Ellen Degeneres (attrib.)

# 1

## Introduction

## 1.1 Introduction

All animals have the ability to perceive and respond to external cues. Cues may signify the presence of good things, such as food, a potential mate or shelter, or bad things, such as predators, competitors, or a hazardous environment. Typically, an organism will be exposed to a mixture of positive and negative cues, requiring the animal to weigh the inputs and subsequently determine its behavioural response based on that information. However, the response may vary: a certain stimulus may elicit different behavioural responses, depending on the context of the stimulus, previous experiences of the organism, its age or developmental stage. This variability is called plasticity, and is well known in many animal species. The ensuing flexibility is thought to enhance the chances of survival and to be essential for memory formation and for many aspects of development. It has even been proposed to be one of the driving forces of natural selection and evolution (Price et al., 2003; Agrawal 2001). However, despite the broad impact of behavioural plasticity, the cellular and molecular mechanisms are thus far poorly understood.

## 1.2 Plasticity of G-protein signalling

Cells have many different ways to detect and respond to external cues. In general, cues are perceived by receptors, which transmit a signal to downstream molecules that amplify it. Eventually this results in a cellular response: an alteration of membrane potential, activation of certain enzymes, *de novo* protein synthesis, or entry in a different developmental stage.

A well studied example of such a signalling cascade is the G-protein signalling route. A broad array of external signals, as varied as chemical compounds to light are perceived by specific G-protein coupled receptors (GPCRs). The width of the panel of signals that GPCRs can sense is reflected in the fact that they comprise the largest and most diverse family of genes in the human genome. GPCRs are bound to heterotrimeric G-proteins. When a ligand binds the receptor, GPCRs allows the G-protein  $\alpha$ -subunit to exchange GDP for GTP, and to dissociate from the receptor and from the  $\beta/\gamma$  subunits. The  $\alpha$  and  $\beta/\gamma$  subunits subsequently activate a myriad of downstream effector proteins, such as adenylate cyclase, guanylate cyclase, phospholipase C, mitogen activated protein (MAP) kinases and ion channels. This results in a massive amplification of the signal, and eventually a cellular response.

Plasticity can be established at all levels in the signalling cascade. For G-protein



signalling systems it is well established that they are not constant but exhibit a memory of prior activation (Hausdorff et al., 1990). This regulated response level allows the cell to modulate its sensitivity to be maximal for ambient stimuli. The strength at which G-protein coupled receptors can signal depends mainly on two factors: the number of receptors present on the cell surface, and the efficiency with which they can transmit their signals. The number of GPCRs on the surface of the cell is governed by a balance of synthesis versus degradation and of shuttling between endosomal pools and the cell surface (Gainetdinov et al., 2004). A common way to downregulate sensitivity after signalling is internalizing receptors that have bound a ligand. This process depends on the phosphorylation of the C-terminal tail by G-protein coupled receptor kinases (GRK), in conjunction with beta arrestins (Gainetdinov et al., 2004). After internalization, the GPCRs can either be targeted for degradation, or recycled back to the cell surface. In addition to a role in dampening GPCR signalling, GRKs have been suggested to play an activating role in signalling in *C. elegans* (Fukuto et al., 2004).

The efficiency of GPCR signalling can be altered by modulating the responses of the G-proteins as well. RGS (Regulators of G-protein signalling) proteins normally function to limit signalling by  $G\alpha$  subunits, by promoting hydrolysis of GTP. It has been proposed that by changing the stoichiometry of this reaction, either by altering the localisation or by promoting transcription, cells can fine-tune G-protein signalling (Willars, 2006; Yu 2006).

### 1.3 Synaptic plasticity

After activation of a single cell, the signal is relayed to other cells. In neurons, information is generally transferred via specialized cell-cell contacts called synapses. These sites display one of the best studied forms of plasticity, aptly called synaptic plasticity. Already in 1949, Hebb proposed that an axon that partakes in activating a certain neuron, and does so repeatedly, will change its metabolism or structure in such a way that it becomes more efficient in stimulating that particular neuron (Hebb, 1949). Since then, the Hebbian synapse has been found to play an essential role in learning and memory.

NMDA channels play an important role in establishing synaptic plasticity, since these channels provide a detection mechanism for coinciding pre-synaptic and post-synaptic activity. Upon opening of these channels, there is an influx of  $Ca^{2+}$  and induction of synaptic plasticity.  $Ca^{2+}$  is thought to act as a second messenger, activating the calcium dependent kinase CaMKII (Lisman et al., 2002),

which in turn phosphorylates membrane receptors and regulatory proteins. This results in altered trafficking and diffusional mobility of receptors (Ehlers et al., 2007), and to rearrangements of the actin cytoskeleton in the synapse.

## 1.4 Structural plasticity

If the inducing signals are strong enough or are prolonged, the changes to the cell and its synapse are confirmed in a process called structural plasticity. Many of the morphological changes depend on remodelling of the actin cytoskeleton in response to activation of Rho-GTPases, and can consist of an increase in the size of the synapse, perforation of the synapse, or the formation of additional boutons (Lamprecht et al., 2004). In addition to structural changes, plasticity can also lead to an increase in protein synthesis, in the soma of the neurons, but also locally in the neurite (Sutton & Schuman, 2006). Thus far it is not quite clear how the proteins are targeted to synapses that underwent plasticity, while neighbouring synapses are skipped. It is proposed that the locally produced proteins are preferentially captured by the synapses that are tagged by the inducing stimuli (Frey & Morris, 1997). Finally, plasticity results in an increase in gene transcription, both by activation of transcription factors, as well as by inducing epigenetic modifications (Guan et al. 2002, Levenson et al., 2005).

Together, synaptic and structural plasticity alter the excitability and connectivity of neurons, by modifying existing connections between neurons or by forming new connections (Lamprecht et al., 2004). This enables neuronal circuits to be formed that are beneficial to the organism, and conversely, non-beneficial circuits to be winnowed. This allows an organism to develop its mature behavioural repertoire, and store information for longer periods of time.

## 1.5 Correlating cellular responses to behaviour

Cellular plasticity is mostly studied in *in vitro* systems, such as cell cultures and brain slices. This has resulted in a wealth of information, as briefly summarised above. However, the manner in which plasticity is induced in these systems is fairly unphysiological. For instance the case in long term potentiation, synaptic plasticity is induced by high frequency electrical stimulation. This raises the question how and if these mechanisms are utilised *in vivo*. Therefore, many efforts have been undertaken to correlate *in vivo* behaviours to neuronal plasticity *in vitro*.

In order to gain insight into sensory perception, the rodent whisker system, the visual system and the olfactory system have been studied in considerable detail. The receptive fields of sensory systems are spatially organised in the central nervous system. Sensory deprivation resulted in changes in the receptive fields, suggesting that neuronal plasticity does play a role *in vivo*. However, the individual cellular components of the neuronal circuits remain poorly understood, not in the least because of the tremendous scale and complexity of the networks. To alleviate the problem of scale and complexity, several research groups have resorted to using simpler model organisms, such as the sea slug *Aplysia* and the fruit fly *Drosophila*. These organisms have been tested mostly in simple behavioural paradigms, by pairing neutral sensory stimuli with aversive cues (Kandel & Schwartz, 1982, Tully, 1999). These studies have offered a clear insight into the mechanisms of plasticity in clusters of neurons. However, the cellular aspects of this process are still difficult to establish. In order to be able to study plasticity in even finer detail, we have used the nematode *Caenorhabditis elegans*.

## 1.6 *C. elegans* in neurobiology

Because many biological processes have been conserved from worm to man, the nematode *Caenorhabditis elegans* has been used to study a wide variety of subjects in biology. In *C. elegans*, many genetic tools are available, enabling researchers to do forward and reverse genetic screens with relative ease. Besides its applicability in large scale screens, *C. elegans*' small size and simplicity are also an advantage. The nervous system of *C. elegans* consists of only 302 neurons, with reproducible morphologies, anatomical locations and connections. *C. elegans* is translucent, allowing every individual neuron to be identified within a living animal. The connectivity of all neurons has been described (for an example, see Figure 1.5D), which allows *C. elegans* to be used to study the role of cellular circuits that drive specific behaviours, and the function of single neurons herein. This is a major advantage compared to the other simple model organisms, whose nervous systems are often several orders of magnitude more complex.

The neurons in *C. elegans* have simple branching structures, which appear to be largely invariant between different animals and can be assigned to 118 neuronal classes based on their morphology and connectivity (White et al., 1986).

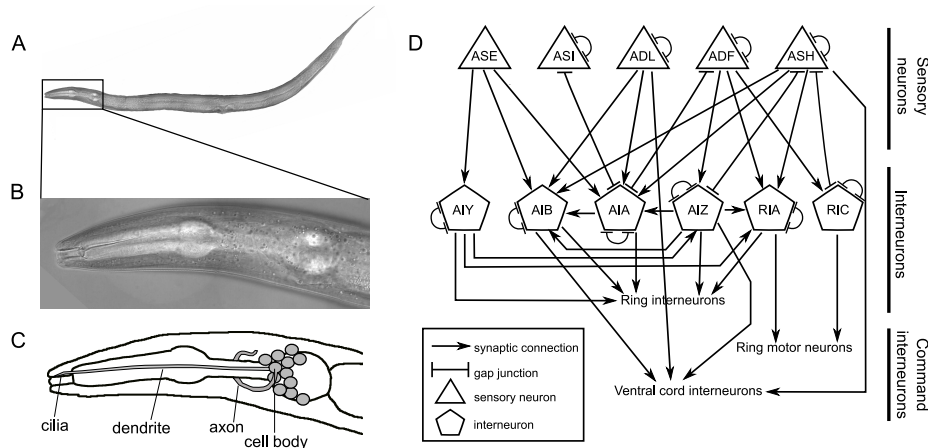


**Figure 1.1: Neuro-anatomy of *C. elegans*.** A. Differential interference contrast picture of an adult hermaphrodite. The animal is approximately 1 mm long. Anterior is left, dorsal is top. B. Blowup of the head. C. Schematic representation of B. The cell bodies of the amphid sensory neurons (gray circles) are located anterior of the second pharynx bulb. These neurons extend an axon to the nerve ring, and a dendrite towards the anterior tip of the animal. The dendrites terminate in a specialized ciliated structure. D. The connectivity data for the sensory neurons that were previously found to be involved in gustatory plasticity. Left and right neuron pairs are represented by a single symbol, and the number of connections is summed. Only connections consisting of more than six synaptic contacts or two gap junctions are shown. Connections between the left and right neuron pairs are indicated by self-connections. Information on the number of connections was extracted from White et al., 1986.

Most of the neurons in *C. elegans* are located around the pharynx, extending their processes to form the nerve ring (White et al., 1986). This structure is the central region of processing.

Many of the neurons have characteristic sensory or motor functions. In the head of the worm, a group of twelve pairs of neurons, called the amphid sensory neurons, form the primary chemosensory organ of *C. elegans* (Figure 1.5A, B and C). The cell bodies of these neurons are located anterior of the second pharyngeal bulb, and extend axons that project to the nerve ring (Figure 1.5C). The dendrites of the amphid neurons extend to the nose of the animal, and end in various specialized ciliated structures (Figure 1.5C). The AWA, AWB and AWC pairs of amphid neurons have a ciliated sheet-like terminus, and were shown to sense volatile chemicals (Bargmann & Horvitz, 1991). The dendrite

of the AFD neurons ends in a single cilium which is surrounded by approximately 50 villi. These neurons are involved in thermosensation. The ASE, ADF, ASG, ASH, ASI, ASJ, ASK and ADL neuron pairs have dendrites which end in a single (ASE, ASG, ASH, ASI, ASJ and ASK) or a pair (ADF and ADL) of rod-shaped cilia. These cilia are embedded in a sheath cell and end in a channel formed by the socket cell, directly exposing them to the environment. These eight pairs of neurons were found to respond to various stimuli, but mostly to water soluble compounds.

## 1.7 Cilia in signalling

The cilia of the amphid sensory neurons are indispensable for sensation. In addition, they provide a putative site for regulating neuronal sensitivity and signal strength. Cilia are specialized cellular compartments that are highly conserved in evolution and can be found in organisms as different as the unicellular *Chlamydomonas* or humans (Rosenbaum & Witman, 2002; Scholey 2003). These structures were long known for their role in motility, but are ever more implicated in sensory functions in development and normal physiology (Singla et al., 2006, Pan et al., 2005). Several receptors were found to localize to the cilia, such as TRP receptors (Teilmann & Christensen, 2005), the somatostatin 2 receptor (Händel et al., 1999), the angiopoietin receptor and the platelet derived growth factor receptor (Schneider et al., 2005). Moreover, cilia play an important role in Hedgehog signalling (Huangfu et al., 2002; Rohatgi et al., 2007).

For their proper function, cilia need to be maintained at a specific length, a process which is thought to be achieved by a continuous turnover of ciliary components (Pan & Snell, 2005), creating a balance of assembly and disassembly. Genetic approaches have thus far identified three proteins involved in the regulation of cilia length: two *Chlamydomonas reinhardtii* proteins with unknown function, LF1 and LF2 (Tam et al, 2003; Nguyen et al., 2005), and the *Chlamydomonas* MAP kinase LF4 (Berman et al., 2003) and its *Leishmania mexicana* homologue LmxMPK9 (Bengs et al., 05). These proteins were suggested to act on the specialized transport system in the cilia, called Intra Flagellar Transport (IFT) system, to regulate the length. IFT is responsible for bi-directional transport of proteins assembled on IFT particles, along the microtubular axonemal core. Recently, a kinesin that belongs to the kinesin 13 family with microtubule depolymerizing activity was identified as the first effector protein in this process, supporting the assembly/disassembly model (Blaineau et al., 2007).

If required, the length of cilia can also be changed. For instance at fertilization in *Chlamydomonas*, the tips of the cilia are modified and the singlet microtubules are extended (Mesland et al., 1980). Cilia can also be shortened when encountering environmental cues, or when entering in cell division. In *Chlamydomonas* it was shown that shortening of the cilia is the result of disassembly of the axoneme, an increase in IFT shuttling and blocking anterograde cargo loading (Pan & Snell, 2005). It was found that besides playing a role in the assembly of cilia, IFT also plays a role in organising signalling pathways (Wang et al., 2006).

## 1.8 Cilia in *C. elegans*

The cilia of *C. elegans* are very similar to those in mammals, with regard to their structure and function (Pan et al., 2005; Rosenbaum and Witman, 2002; Scholey, 2003). The nematode has 60 ciliated cells (White et al., 1986), including 12 pairs of sensory neurons in its head, the amphid neurons, which detect environmental cues. Since the cilia are the only parts of these neurons which are exposed to the environment, they are a potential site to regulate signalling strength, and thus to establish plasticity. Structurally, the cilia of *C. elegans* can be divided into a middle segment with nine doublet microtubules and a distal segment with nine singlet microtubules (Perkins et al., 1986). IFT is different in these two compartments: in the middle segment of the cilia anterograde transport is mediated by two kinesin complexes, heterotrimeric kinesin II, encoded by *klp-11*, *klp-20* and *kap-1*, and homodimeric OSM-3 kinesin (Signor et al., 1999; Snow et al., 2004). In the distal segments however, only OSM-3 kinesin mediates transport (Snow et al., 2004). The molecular mechanisms of this compartmentalization of transport have thus far remained elusive, as well as its functional significance.

Retrograde transport in the cilia is mediated by a dynein motor complex of which two subunits have been characterized, the dynein heavy chain *che-3* and the dynein light intermediate chain *xbx-1* (Schafer et al., 2003; Signor et al. 1999; Wicks et al., 2000). These molecular motors are proposed to dock onto a scaffold consisting of complex A and B proteins. Several complex A and B proteins have been identified in *C. elegans*, including the complex A proteins *daf-10* and *che-11* (Qin et al., 2001), and the complex B proteins *che-13*, *osm-1* and *osm-5* (Haycraft et al., 2001, 2002; Qin et al., 2001; Signor et al., 1999). In addition, three proteins have been identified with more regulatory roles. Two of these genes, *osm-12/bbs-7* and *bbs-8*, encode homologues of the mammalian BBS7 and BBS8 genes, which are associated with the Bardet-Biedl syndrome (Blacque et

al. 2004). In *C. elegans*, these proteins stabilize IFT complexes transported both by kinesin II and OSM-3 (Ou et al., 2005a). In *osm-12* and *bbs-8* animals complex A and B are no longer transported together, but are transported separately by kinesin II and OSM-3, respectively. In the same study, Ou et al. identified another gene, *dyf-1*, which is required for the activation of OSM-3 kinesin. Finally, there are several indications that IFT transports both structural components of the cilia and signaling molecules (Ou et al., 2005b; Qin et al., 2004; 2005).

## 1.9 Behavioural repertoire of *C. elegans*, and its plasticity

Despite its relative simplicity, *C. elegans* still shows various complex behaviours (Hobert, 2003). *C. elegans* has been shown to respond to a variety of sensory cues, representing a favourable environment, danger or the presence of other animals. The animals respond to volatile and water soluble compounds, oxygen levels, temperature and touch. Most of these responses are subject to attenuation based on previous experiences.

**Volatile attraction** *C. elegans* is attracted to members of at least seven distinct classes of volatile chemicals (Bargmann et al., 1993). It uses the AWA and the AWC pairs of neurons to detect these attractants. Remarkably, the animal is able to discriminate between all of these classes of chemicals, which indicates that it needs to utilize the limited number of cells to their fullest potential. *C. elegans* does this for instance by using functional asymmetry between the two AWC neurons, which allows discrimination between 2-butanone and benzaldehyde (Wes & Bargmann, 2001). In addition, it utilizes multiple signalling routes per cell (Lans et al., 2004). Prolonged exposure to odors leads to a reversible loss of sensitivity for that specific odour, while sparing the sensation of other odours that may be perceived by the same neuron (Colbert & Bargmann, 1995). This adaptation requires the absence of food (Colbert & Bargmann, 1995), and can be restored by exposing the animals to a different odorant (Nuttley et al., 2001). These results suggest that *C. elegans* can use odorants to predict nutrient deficient environments.

**Aerotaxis and foraging behaviour** In 2004, Gray and colleagues described that *C. elegans* is able to sense and respond to oxygen levels (Gray et al., 2004). For aerotaxis, four cells are needed, the URX pair of neurons and the AQR



and PQR neurons. In these neurons two specific soluble guanylate cyclases are expressed, *gcy-35* and *gcy-36*, of which the haem domain binds molecular oxygen (Gray et al., 2004; Cheung et al., 2005). This enables the worm to sense oxygen. When grown under standard laboratory conditions, the animals prefer an oxygen concentration of 5-11%. However, this preference can be altered in response to previous experiences and environmental conditions (Gray et al., 2004; Cheung et al., 2005; Chang et al., 2006). The avoidance of hyperoxic conditions has been suggested to represent a foraging behaviour, in which *C. elegans* moves to low-oxygen areas, corresponding to food (Chang et al., 2006; Gray et al., 2004). However, not all natural isolates of *C. elegans* display the same foraging behaviour: some strains are solitary feeders on plentiful food, while others form clumps at the borders of bacterial lawns (de Bono & Bargmann, 1998). These natural occurring differences were found to depend on the presence of one of two isoforms of the neuropeptide receptor NPR-1 (de Bono & Bargmann, 1998), altering the sensory landscape of the animals (de Bono & Bargmann, 1998; Gray et al., 2004; Cheung et al., 2005). Social feeding is induced by signals from the URX, AQP and PQR neurons (Coates & de Bono, 2002) as well as from the nociceptive neurons ASH and ADL, balanced by opposing signals from thus far unidentified neurons (de Bono et al., 2002).

**Thermotaxis** Already in 1975, Hedgecock and Russell described that *C. elegans* are able to sense temperature. If worms are cultivated at a certain temperature, they will move to that temperature if given a choice. However, this preference depends on whether the animals were fed at that temperature, indicating an association between food and temperature. Cryophilic behaviour is driven by the AFD neurons (Mori., 1999), while AWC has been suggested to drive thermophilic attraction (Okumura. personal communication). Signals from these neurons are relayed to the AIY, AIZ and RIA interneurons (Gray et al., 2005; Kodama et al., 2006), which are proposed to integrate food status and ambient temperature, driving the thermotactic behaviours. The integration of these signals was found to depend on insulin like signalling (Kodama et al., 2006).

**Mechanosensation** In the soil, *C. elegans* is exposed to a variety of external forces, which are perceived by in total 30 neurons in the hermaphrodite (Goodman, 2006). Gentle touch is perceived by a DEG/ENaC channel, linked to the extracellular matrix, and the intracellular microtubular cytoskeleton (as reviewed in Bounoutas et al., 2007). The response to mechanic stimulation



decreases after repeatedly touching the worm, a process which is referred to as touch habituation (Rankin et al., 1990). The speed with which *C. elegans* becomes habituated depends on the presence of food, and on dopamine signalling (Sanyal et al., 2004; Kindt et al., 2007), providing a way to integrate internal context and previous experiences to modulate mechanosensory attention.

**Gustatory attraction** As *C. elegans* lives at the air-water interface, it also needs to detect water-soluble compounds, such as NaCl, cAMP, biotin, NH<sub>4</sub>Ac and lysine (Bargmann & Horvitz, 1990). Attraction to these compounds is predominantly mediated by the ASE pair of neurons, but many other neurons also play a minor role in this form of chemoattraction. These include the ADF, ASG, ASI, and ASK neurons (Bargmann & Horvitz, 1990). The molecular mechanisms by which these ions are detected in *C. elegans* are not well understood. It is known that chemoattraction to NaCl requires cGMP and Ca<sup>2+</sup> signalling via the cGMP gated channels TAX-2/TAX-4, and the calcineurin subunit TAX-6. Recently, five additional molecules were shown to play a role in the detection of NaCl, that act via two distinct genetic pathways. One pathway involves *tax-4* and *tax-6*, together with the MAP kinases *nsy-1* and *sek-1*, while the second pathway contains *tax-2*, the TRPV channel *osm-9*, the G- $\alpha$  subunit *odr-3* and the guanylate cyclase *gcy-35*. (Hukema, 2006). The cellular correlates of these distinct pathways are unknown. However, the two ASE neurons are asymmetric, which is also reflected in their function. The left ASE cell senses Na<sup>+</sup> ions, whereas the right ASE cell perceives Cl<sup>-</sup> and K<sup>+</sup> ions (Pierce-Shimomura et al., 2001). It is tempting to speculate that the two genetic pathways correspond to the functionally different left and right ASE neurons, especially since *osm-9* mutants display ion-specific defects in plasticity (Jansen et al., 2002).

**Avoidance behaviours** Noxious stimuli are mostly perceived by the ASH neurons, and to a lesser extent by the ADL neurons. In addition, the AWB neurons function in the perception of volatile repellents. The ASH neurons are general nociceptive sensors, capable of sensing a broad palette of distinct sensory modalities. They sense touch, volatile compounds, high osmotic pressure, low pH, and water soluble compounds such as heavy metals, bitter compounds and detergents (Hart et al., 1999; Kaplan & Horvitz, 1993; Hilliard et al., 2005). The TRP channel OSM-9 as well as the G- $\alpha$  subunits ODR-3 and GPA-3 are essential for the function of ASH (Roayaie et al., 1998; Colbert et al., 1997). For touch and osmosensory stimuli it was shown that they are transmitted via distinct intracellular pathways, and that OSM-10 is required for osmosensation

(Hart et al., 1999; Hilliard et al., 2005). Interestingly, these neurons can differentially transmit several of these aversive stimuli to postsynaptic cells, a process that depends on the presence and the synaptic localisation of glutamate and NMDA receptors (Mellem et al., 2002).

## 1.10 Gustatory plasticity

*C. elegans* is attracted to concentrations of NaCl between 0.1 mM and 200 mM, and will avoid higher concentrations. However, if the animals have been exposed to an attractive concentration of NaCl for fifteen minutes directly prior to the assay, they will strongly avoid all concentrations of NaCl (Jansen et al., 2002; Hukema et al., 2006). This behavioural switch is called gustatory plasticity. It is specific for pre-exposure to  $\text{Na}^+$  and  $\text{Cl}^-$ , although it affects chemosensation of other watersoluble compounds as well, such as cAMP, biotin, ammonium acetate and lysine (Saeki et al., 2001; Jansen et al., 2002).

In a reverse genetic screen Hukema et al identified 85 genes that specifically affect this behavioural switch, without affecting normal attraction or avoidance (Hukema et al., 2006; Hukema, 2006). Several of these genes encode proteins that function in neurotransmitter production and release. Interestingly, genes specific for glutamate, dopamine, serotonin tyramine and tyrosine signalling were all found to affect gustatory plasticity (Hukema, 2006). Also many other proteins were found, such as ion channels, G-proteins and their regulatory proteins, transcription factors, indicating that gustatory plasticity is a tightly regulated process. Interestingly, many of the proteins known to be involved in synaptic plasticity also affect gustatory plasticity, arguing that these may be comparable or even related processes. For instance, of the proteins that are required for associative neuronal plasticity, the NMDA receptor homologue *nmr-1*, and the AMPA receptors *glr-1* and *glr-2* also affect gustatory plasticity. In addition, the CREB homologue *crh-1* and calcineurin subunits *tax-6* and *cnb-1* were also found to be defective in gustatory plasticity (Hukema, 2006). Of some key proteins in synaptic plasticity, the involvement in gustatory plasticity could not be confirmed by using behavioural assays. One example is the CaM kinase II homologue *unc-43*, which could not be tested because this mutant is severely impaired in its movement (Hukema, 2006).

## 1.11 Food signals are important for establishing gustatory plasticity

An alternative learning assay was described in several reports from the lab of Iino (Saeki et al., 2001; Tomioka et al., 2006). Here, the animals are pre-exposed to NaCl in the absence of food for a longer period of time, between 1-4 hours. This results in a strong activation of the insulin pathway and activation of the AIA interneuron. Interestingly, many components of the dauer pathway are activated. This pathway allows *C. elegans* to develop into an energy conserving dauer larva, in times of food shortage or high population density. Activation of the dauer pathway suggests that starvation during pre-exposure plays an important role in this form of plasticity. Previously it was found that the absence of food is required for establishing gustatory plasticity (Saeki et al., 2001; Jansen et al., 2002; Hukema et al., 2006, Hukema & Jansen, unpublished observations). However, many mutants that did not show gustatory plasticity upon pre-exposure to NaCl after 15 minutes, do show strong avoidance of NaCl when they are starved for a prolonged period of time (Hukema 2006, Hukema & Jansen unpublished observations). This suggests that plasticity after pre-exposure to NaCl is established via at least two different pathways, indicating that plasticity after prolonged starvation may either represent an advanced stage of gustatory plasticity, or an altogether different form of plasticity.

## 1.12 Dauer formation

*C. elegans* not only displays behavioural plasticity, it also displays a well studied form of developmental plasticity. The normal life cycle of *C. elegans* is comprised of an embryonic stage, four larval stages (L1 to L4) and adulthood. However, if L1 larvae of *C. elegans* are grown in adverse environmental conditions, such as food shortage, high population density or high temperature, they can develop into dauer larvae, rather than progress to the L2 larval stage (Riddle & Albert, 1997). Development into dauer larvae is accompanied by many morphological changes, including structural changes of the sheath cells and the cilia (Albert & Riddle, 1983). Of the amphid sensory neurons, the ASI and ASG neurons are displaced posteriorly in the amphid channel. (Albert & Riddle, 1983, Albert & Riddle, 1988).

One of the first factors of a complex network that regulates the decision between dauer formation versus reproductive growth is the guanylate cyclase DAF-11

(Birnby et al., 2000). DAF-11 stimulates the DAF-7 (TGF $\beta$ ) pathway, and to some extent the DAF-2 (insulin/IGF I receptor) pathway. The DAF-2 pathway is predominantly regulated by food/starvation signals (Gerisch et al. 2001; Li et al. 2003; Riddle & Albert, 1997). It has been suggested that these two signalling cascades funnel into a third endocrine pathway, which includes DAF-9 and DAF-12 (Albert & Riddle, 1988; Gerish et al., 2001).

A subset of the amphid sensory neurons can take up fluorescent dyes via their cilia, called dye filling. Most mutants with defects in the IFT machinery are dye filling defective, because their affected cilia are not exposed to the environment. Most of these mutants are also unable to develop into dauer larvae. However, *gpa-3QL* animals, which carry a dominant active sensory G-alpha protein *gpa-3*, are dye filling defective but also constitutively form dauers (Zwaal et al., 1997). This intriguing phenotype is suggestive of a dual role for GPA-3 in regulating accessibility of the cilia, and in dauer development.

### 1.13 Single cell studies & techniques

As mentioned before, one of the advantages of the use of *C. elegans* is the ability to correlate behaviours with the activity of single neurons. This was first studied by using laser ablation to inactivate individual neurons in the head of the worm. By testing the treated worms in several behavioural assays, the activating cues for many of the sensory neurons in the head of *C. elegans* were identified. (Bargmann & Horvitz, 1990; Bargmann et al., 1991).

Besides studies of the function of the sensory neurons, several efforts have been undertaken to determine the electrical properties of neurons in *C. elegans*. Goodman et al. extensively described the physiology of the ASER neuron in *C. elegans* (Goodman et al., 1998). This neuron failed to generate classical Na<sup>+</sup> action potentials, consistent with the lack of genes encoding voltage gated Na<sup>+</sup> channels in the genome of *C. elegans*. ASER displayed a high sensitivity to input currents over a wide dynamic range. In other neurons that were examined, similar electro-physiological properties were found, suggesting that *C. elegans* neurons share a common mechanism of sensitivity and dynamic range (Goodman et al., 1998).

However, electrophysiological studies of *C. elegans* have proven to be difficult, because of the pressurised cuticle that envelops the animal. Accessing the neurons requires dissecting the cuticle, which causes the neurons to burst out, potentially disrupting their connectivity. Alternatively calcium or voltage sensitive dyes can be used to probe the activity of the cells, however this also

requires some form of access to the cells to deliver the dye. The use of genetically encoded optical indicators has proven to be a particularly successful alternative (Miyawaki 2003; Miyawaki 2005; Bozza et al., 2004; Kerr et al., 2000; Nakai et al., 2002). One can observe changes in the cells, without having to open the cuticle. One of the first indicators that was used in *C. elegans* was the genetically encoded calcium probe Cameleon (Miyawaki et al., 1997; Kerr et al., 2000; Nagai et al., 2002). This chimeric protein consists of a Cyan Fluorescent Protein (CFP) and a Yellow Fluorescent Protein (YFP), which are linked by a Calmodulin protein (CaM) and a M13 linker protein. At low calcium concentrations the two fluorescent moieties are separated, so that at CFP excitation, only CFP emission can be observed. However, at high intracellular concentrations of calcium, for instance after activation of neurons in *C. elegans* (Goodman et al., 1998; Kerr et al., 2000), calcium ions bind to the calmodulin. This results in a conformational change, bringing the two fluorescent proteins close enough to allow Fluorescent Resonance Energy Transfer (FRET) to take place. In this process, energy from the CFP moiety is transferred to the YFP moiety. This results in decreased cyan emission and an increase in yellow emission after excitation of the CFP protein. The ratio between cyan and yellow emission provides a measure of activation of the cell. This technique has enabled confirmation of the presence of two signalling pathways in ASH (Kerr et al., 2000; Hilliard et al., 2005) and the remarkable asymmetrical behaviour of the ASE neurons to stimulation with NaCl (Hiroshi Suzuki, personal communication).

Another calcium indicator that is used is G-CaMP (Nakai et al., 2001). This reporter consists of a single Green Fluorescent Protein (GFP), linked to a CaM unit. When calcium binds to the CaM, the fluorescence of the GFP increases. This construct has been used to resolve the circuit for olfaction in *C. elegans*. (Chalasani et al 2007).

## 1.14 Conclusion

In this thesis I describe our efforts to elucidate several aspects of plasticity in *C. elegans*. First, we set out to identify the cellular correlates of gustatory plasticity. Previous studies showed that the ASE neurons are the principal NaCl sensing neurons, and that the ASH neurons mediate osmotic avoidance. These two pairs of neurons are also necessary for establishing gustatory plasticity. We hypothesised that the naïve biphasic behaviour in response to NaCl is the result of attraction driven by the ASE neurons which is overruled by osmotic avoidance signals from the ASH neurons. We sought to test this hypothesis,

and investigate whether pre-exposure affects the responses of the ASE and ASH neurons. We have used behavioural assays, and combined this with single cell imaging in these neurons, using the Cameleon construct.

We have also explored an alternative approach to assess the role of specific sensory neurons in gustatory plasticity. Besides the aforementioned ASE and ASH neurons, several other sensory neurons have been implicated in this behavioural switch: the ASI, ADF and ADL neurons. However, it is difficult to study the function of these cells, since they only play a minor role in NaCl perception. Other, more specific stimuli that activate these cells are not known, although the ASI neurons have been suggested to sense food. Introducing mammalian receptors, to whose specific ligands *C. elegans* does not show an endogenous response, would allow us to activate specific neurons. We have tested this by heterologously expressing two distinct types of receptors in a number of sensory neurons, and studying whether the receptors are integrated into endogenous signalling routes, and are able to drive novel sensory behaviours.

The cilia of the amphid sensory neurons in *C. elegans* have been found to be indispensable for sensory function. The cilia need to align and enter into a channel that is formed by the socket cell, in order to be exposed to the environment. This anatomical constraint suggests that cilia length and alignment are tightly regulated. We wondered whether DYF-5, a homologue of a protein that was previously found to regulate cilia length in *Chlamydomonas* and *Leishmania*, might play a role in this regulation. In addition, we wondered what the molecular mechanisms are of this process. Pan & Snell proposed that IFT plays a central role in the regulation of cilia length. In order to test this we have measured motility of fluorescently tagged components of the IFT machinery. The length of cilia is not constant over time. Rather, it is dynamically regulated, depending on developmental stage or by external cues. This provides a potential way to regulate sensitivity of sensory neurons. However, little is known about the molecular mechanisms that govern the plasticity of cilia, although it is likely that it involves IFT. Previous studies indicated that in dauer formation, the structure of specific cilia is altered. We wondered what role the  $G\alpha$  subunit GPA-3 plays in this process, as it was previously found to affect dauer formation, and also influences accessibility of the cilia. Given the role that G-proteins play in signalling, this might provide a link between environmental signals and regulation of cilia length.

*...while the wisdom of Man  
thinks it is working one thing,  
the wisdom of Nature con-  
strains it to work another, and  
quite a different and better  
thing.*

Edwin A. Abbott, 1884

# 2

## Altered sensitivity of ASE and ASH neurons explains gustatory plasticity in *C. elegans*

## 2.1 Abstract

Neuronal plasticity allows animals to alter their behaviour depending on previous experiences. Although many molecular and cellular aspects of neuronal plasticity have been characterized, the ultimate challenge has remained to directly correlate these processes to the behaviour of living animals. We study a behavioural switch in the response of *C. elegans* to NaCl, called gustatory plasticity. Naïve animals are attracted to low and avoid high concentrations of NaCl. However, after prolonged exposure to attractive NaCl concentrations, the animals strongly avoid all concentrations of NaCl. By using behavioural assays and cell specific  $\text{Ca}^{2+}$  imaging we show that in the naïve situation the ASE sensory neurons, which mediate attraction to NaCl, not only respond to low but also to high NaCl concentrations. The ASH nociceptive neurons only show  $\text{Ca}^{2+}$  responses to NaCl concentrations above 100 mM. After prolonged exposure to NaCl the responses of both sensory neuron pairs have changed. The dynamic range of the ASE neurons is shifted to higher concentrations, suggesting that they have become desensitised. In addition, the ASH neurons become sensitised and now respond to normally attractive NaCl concentrations. This induced avoidance pathway requires signals from the ASE neurons, but is independent of the osmotic avoidance pathway in the ASH neurons and also results in increased sensitivity to other ionic compounds. We propose that in *C. elegans* environmental NaCl is detected essentially by two pairs of sensory neurons, mediating attraction and avoidance, and that the strength of the response of these neurons can be modulated by other environmental signals. This model enables the detailed analysis of the molecular and cellular processes that govern this remarkable and tractable behavioural switch.

## 2.2 Results

*C. elegans* displays a biphasic behaviour in response to NaCl; it is attracted to concentrations up to 200 mM but will avoid higher concentrations (Bargmann & Horvitz, 1991, Hukema et al., 2006, Figure 2.1a and b). However, after prolonged exposure to 100 mM NaCl the animals will strongly avoid NaCl at all concentrations (Figure 2.1b). We call this behavioural switch gustatory plasticity and study it as a model to elucidate the molecular mechanisms of behavioural plasticity (Hukema et al., 2006, Jansen et al., 2002).



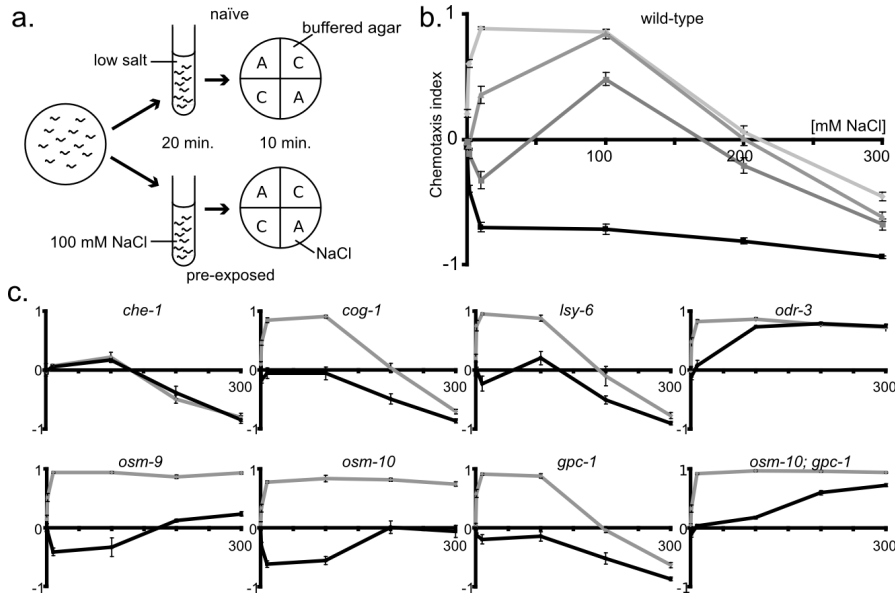


**Figure 2.1: Behavioural responses to NaCl.**

a. Flow scheme for the behavioural assays. Animals were washed with a buffer with or without 100 mM NaCl for 20 minutes, and placed on a plate where they are given the choice between two quadrants with buffered agar and NaCl (A), and two quadrants only containing buffered agar (C). b. Response of wild-type animals to NaCl. *C. elegans* shows attraction up to 200 mM NaCl, and avoid higher concentrations. After pre-exposure to 100 mM NaCl, the animals avoid all concentrations. The lines indicate from light to dark pre-exposure concentrations of 0 mM, 10 mM, 50 mM and 100 mM of NaCl. c. The responses of *che-1*(p679), *cog-1*(sy275), *lsy-6*(ot71), *odr-3*(n1605), *osm-9*(ky10), *osm-10*(n1602), *gpc-1*(pk298te) and *osm-10*(n1605);*gpc-1*(pk298te) animals. Gray lines indicate the naïve responses, and the black lines indicate the response after pre-exposure to 100 mM NaCl.

We hypothesised that the naïve response to different concentrations of NaCl results from two separable behavioural forces, attraction and avoidance, and that prolonged exposure to NaCl modulates these components to allow avoidance of all concentrations of NaCl.

We first confirmed the role of the individual components of the naïve response. Chemoattraction to NaCl is primarily mediated by one pair of neurons, the ASE neurons (Bargmann & Horvitz, 1991). These neurons are bilaterally asymmetric: the left ASE neuron (ASEL) predominantly senses  $\text{Na}^+$  ions, and the right one (ASER)  $\text{Cl}^-$  ions, and to a lesser extent  $\text{Na}^+$  (Pierce-Shimamura et al., 2001).

*che-1* mutant animals, which lack a Zn finger transcription factor essential for the specification of the ASE neurons (Uchida et al., 2003), have completely lost attraction to low concentrations of NaCl, but avoidance of high concentrations of NaCl is intact (Figure 2.1c; Hukema et al., 2006), indicating that while the ASE neurons are essential for attraction, they are not required for avoidance. Interestingly, we found that ASE asymmetry is dispensable for chemosensation under naïve assay conditions; the *lsy-6* and *cog-1* mutants, who have two left or two right ASE neurons, respectively (Johnston et al., 2005), behaved as wild type animals (Figure 2.1c). Avoidance of more than 200 mM NaCl is mediated by the ASH neurons, which are essential for responding to osmotic stimuli (Kaplan & Horvitz 1993, Hukema et al., 2006). Interestingly, the avoidance mutants *osm-9*, which lack a TRPV channel subunit (Colbert et al., 1997), *osm-10*, which lack a protein essential for osmotic avoidance in ASH (Hart et al., 1999), and *odr-3*, which lack a  $G\alpha$  subunit (Roayaie et al., 1998), all showed strong attraction to even lethal concentrations of NaCl (Figure 2.1c). Together, these data suggest that the naïve response of *C. elegans* to NaCl is indeed a balance between attraction mediated by the ASE neurons and avoidance mediated by ASH. Next we determined the dynamic range of the responses of the ASE and ASH neurons to NaCl, by using the genetically encoded  $Ca^{2+}$  reporter Yellow Cameleon (Nagai et al., 2002, Kerr et al., 2000), which can be used as a measure for neuronal activation. Suzuki et al. very recently demonstrated a striking difference in the response of the left and right ASE cell to NaCl. ASEL yields  $Ca^{2+}$  transients in response to an increase in NaCl concentration (upstep), whereas ASER responds to a decrease in NaCl (downstep; Suzuki, personal communication). We were able to reproduce these asymmetrical responses in ASE (Figure 2.2d, naïve, and data not shown). In agreement with our behavioural data, ASEL showed  $Ca^{2+}$  transients not only in response to low NaCl, but also to high NaCl concentrations (Figure 2.2b). Hilliard et al. have previously shown that stimulation of the ASH neurons with various nociceptive compounds, including osmotic stimuli, induces  $Ca^{2+}$  transients (Hilliard et al., 2005).

We found that the ASH neurons showed a gradual increase in  $Ca^{2+}$  transients at increasing concentrations of NaCl, starting at or just above 100 mM (Figure 2.2a). Thus, our imaging results are consistent with our behavioural data and fit a two factor model in which *C. elegans* is attracted to all NaCl concentrations, predominantly mediated by the ASE neurons, but that this attraction is overruled by osmotic avoidance, mediated by the ASH neurons, resulting in decreased attraction above 100 mM NaCl and avoidance of concentrations higher than 200 mM (Figure 2.4a, c).

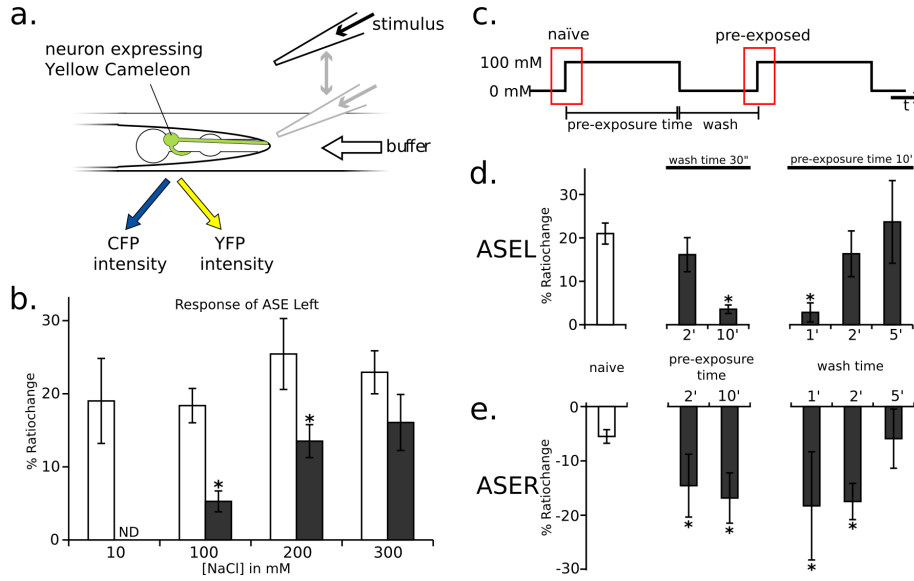


**Figure 2.2: Calcium imaging in the ASE gustatory neurons.** White bars are responses obtained in the naïve washbuffer, the black bars in the washbuffer containing 100 mM NaCl. Asterisks indicate a statistically significant difference between the naïve response and the corresponding pre-exposed response ( $P < 0.05$ ). **a.** Imaging setup for Yellow Cameleon imaging. The stimulus is applied by lowering a needle into a continuously flowing buffer, close to the nose of the immobilised animal. **b.** Responses of the left ASE neuron to a range of NaCl concentrations. Pre-exposure to 100 mM NaCl reduces the mean amplitude of the calcium transients in response to stimulation with 100 and 200 mM NaCl. **c.** Imaging protocol to mimic the plasticity response. All tested animals were mounted on the coverslip at least ten minutes prior to the pre-exposed recording. **d.** Responses in the left ASE after the pre-exposure imaging protocol. After ten minutes of pre-exposure to 100 mM NaCl, calcium transients in ASEL were completely abolished. If the wash time was 2 minutes or longer, this effect was lost. **e.** Responses in the right ASE neuron with the pre-exposure imaging protocol. Already after two minutes, the efflux of calcium from the right ASE cell was significantly increased. This effect was lost when the wash time was increased to 5 minutes.

What happens after prolonged exposure to NaCl? The observed avoidance could either be the result of desensitisation of attraction and sensitisation of avoidance, or of an alternative factor that overrules the naïve behaviour. To determine if the responses of the ASE and/or ASH neurons changes after pre-exposure to NaCl we tried to mimic the behavioural plasticity assay in our imaging set-up (Figure 2.2a, c). We exposed animals to NaCl for a period of

time ranging from 30 seconds to 10 minutes and after a brief wash ( 30 sec.) tested their response to an increase in NaCl concentration (Figure 2.2c).

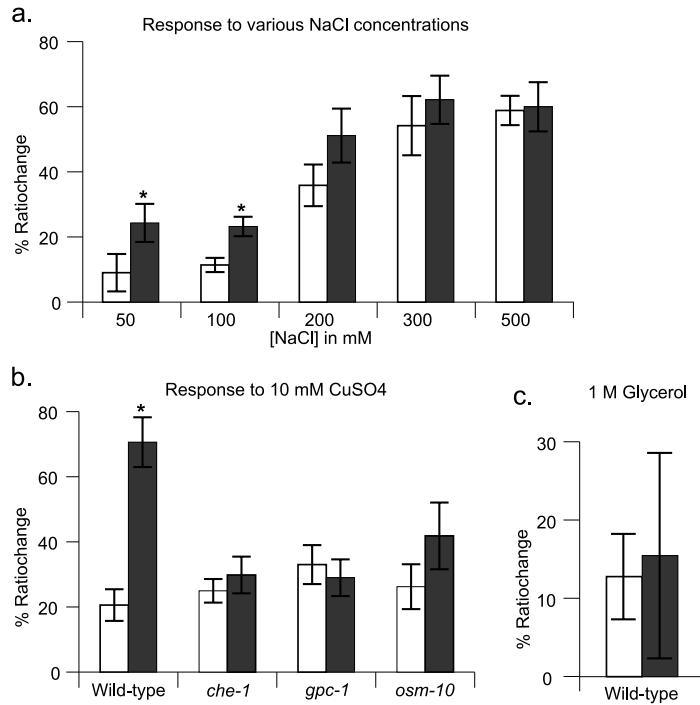


**Figure 2.3: Calcium imaging in the ASH nociceptive neurons.** White bars are responses obtained in the naïve washbuffer, the black bars in the washbuffer containing 100 mM NaCl. Asterisks indicate a statistically significant difference between the naïve response and the corresponding pre-exposed response ( $P < 0.05$ ). a. Mean amplitudes of the transients in ASH upon stimulation with NaCl concentrations ranging from 50 mM to 500 mM. b. Mean amplitudes of calcium transients in ASH of wild-type, *che-1*(p679), *gpc-1*(pk298te), *osm-10*(n1602) animals, after a stimulus with 10 mM CuSO<sub>4</sub>. c. Pre-exposure has no effect on the calcium transients upon osmotic stimulation with 1 M glycerol in wild-type animals.

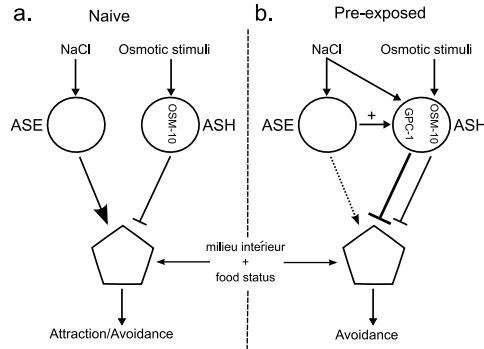
Consistent with our behavioural analyses, ten minutes pre-exposure to NaCl abolished Ca<sup>2+</sup> transients in the ASEL neuron and more than doubled the small efflux of Ca<sup>2+</sup> observed in ASER in response to stimuli up to 100 mM NaCl. Also

the dynamic range of responses of the ASH neurons changed after prolonged exposure: these neurons now showed  $\text{Ca}^{2+}$  transients in response to 50 mM NaCl, and the amplitudes of the responses to 100 mM NaCl were significantly increased compared to the naïve responses. The  $\text{Ca}^{2+}$  transients to higher concentrations were unaltered. Shorter pre-exposure times did not result in these effects and the plasticity effect was lost after increasing the wash time to two or five minutes. These results show that pre-exposure to NaCl results in altered responses of both the ASE and the ASH neurons, consistent with a model in which attraction of low NaCl concentrations mediated by the ASE neurons is desensitised, while avoidance mediated by ASH is sensitised.

The ASH nociceptive neurons are polymodal neurons: they respond to a variety of nociceptive stimuli, and can differentiate between some of them, including nose touch,  $\text{Cu}^{2+}$  and osmotic signals (Kaplan & Horvitz 1993, Hart et al., 1999, Mellem et al., 2002, Hilliard et al., 2005). To evaluate the contribution of the different ASH signalling routes we tested the behaviour of *osm-10* animals, which lack a protein of unknown function and show defects in osmotic avoidance but show wild type avoidance of  $\text{Cu}^{2+}$  (Hilliard et al., 2005). As expected, *osm-10* animals did not show avoidance of high concentrations of NaCl, but did avoid low NaCl concentrations after pre-exposure. This is in contrast to the behaviour of *gpc-1* animals, which lack a sensory specific  $\text{G}\gamma$  subunit and fail to avoid low concentrations of NaCl after pre-exposure but do avoid high NaCl concentrations (Jansen et al., 2002). Interestingly, *osm-10; gpc-1* double mutant animals showed no avoidance and strongly reduced attraction to NaCl after pre-exposure (Figure 2.1c). These results suggest that at least two avoidance routes exist, the osmotic avoidance route that requires *osm-10* and is mediated by ASH, and a second route that requires *gpc-1*. We think that attraction to high NaCl concentrations observed in *gpc-1; osm-10* animals reflects the response of the desensitised ASE neurons. Next, we wondered if the *osm-10* independent avoidance of low NaCl concentrations uses the same pathway that responds to  $\text{Cu}^{2+}$ . To test this we imaged the responses to 10 mM of  $\text{CuSO}_4$  in a buffer either containing or lacking 100 mM NaCl. Animals pre-exposed to 100 mM NaCl showed a slightly higher response to  $\text{Cu}^{2+}$  compared to naïve animals, but less than wild-type animals, and less than expected from the pre-exposed response in the behavioural assay (Figure 2.2b). This difference may reflect the fundamental differences between single cell/single event imaging and behavioural tests. The responses of wild-type animals to osmotic stimuli were unaltered after pre-exposure (Figure 2.2c).

We have previously reported that the ASE neurons are essential for establishing plasticity (Hukema et al., 2006), since *che-1* animals do not respond to low NaCl

Figure 2.4: **Model a.** Naïve situation: Chemosensation is the result of an attraction component from ASE and an osmotic avoidance signal from ASH. The outcome of these two inputs only depends on the concentration of NaCl, resulting in attraction to concentrations up to 200 mM and avoidance of higher concentrations b. After pre-exposure to attractive concentrations of NaCl in the absence of food, ASE is desensitised and in ASH a signalling route that senses ionic components is sensitised. The sensitisation of ASH depends on the presence of the ASE neurons. Thus far it is unclear where the modifying signals come from or interface with the core machinery.



concentrations after pre-exposure (Figure 2.1c). We found that the enhancement of the response to 10 mM  $\text{CuSO}_4$  depended also on *che-1*, and thus on the presence of the ASE neurons.

These experiments support the hypothesis that at least two independent sensory signalling routes exist in the ASH neurons, and strongly suggest that pre-exposition to 100 mM NaCl sensitises a signalling route in ASH that is also used for the perception of copper. To confirm that pre-exposure to NaCl leads to sensitisation of  $\text{Cu}^{2+}$  avoidance we tested the response to  $\text{CuSO}_4$  in our behavioural assay. In agreement with our imaging data, naïve *C. elegans* were not repelled by low  $\text{CuSO}_4$  concentrations, but even attracted, and strongly avoided  $\text{CuSO}_4$  after pre-exposure to 100 mM NaCl (data not shown). We hypothesise that this route senses other ionic compounds as well, which would be consistent with the finding that pre-exposure to NaCl also results in the avoidance of  $\text{NH}_4\text{Ac}$  and other ionic compounds (Jansen et al., 2002, Saeki et al., 2001).

Based on our results we propose that naïve chemosensation of NaCl is mediated by a core NaCl chemotaxis machinery, comprised of the ASE neurons that mediate attraction and the ASH neurons that mediate avoidance of osmotic stresses. Pre-exposure to 100 mM of NaCl in the absence of food results in signals that feed into this core circuit and modulate its outcome. The dynamic ranges in the ASE and ASH neurons are both affected, resulting in desensitisation of attraction and sensitisation of avoidance. Our data suggest that

signals from the ASE neurons, e.g. prolonged exposure to NaCl, are required for sensitisation of ASH. We expect that other inputs are required, since our previous studies have shown that the ASI and ADF neurons are involved as well (Hukema et al., 2006). Recently it was shown that the ASI neurons are involved in the sensation of food cues (Bishop & Guarente, 2007), suggesting that these neurons provide the link between food status and plasticity. We expect that this simple experimental system will allow a very detailed description of the molecular and cellular mechanisms of behavioural plasticity.

## 2.3 Materials & Methods

**Strains and germline transformation** Worm strains were maintained as described in Brenner 1974. Wild-type *C. elegans* were strain Bristol N2. The following alleles were used: *che-1(p679)*, *cog-1(sy275)*, *lsy-6(ot71)*, *odr-3(n1605)*, *osm-9(ky10)*, *osm-10(n1602)*, *gpc-1(pk298te)*. Germline transformation and transgene integration were performed as described (Mello et al., 1991). We used an *elt-2::GFP* construct (30 ng/ $\mu$ l) as coinjection marker (Fukushige et al., 1999). The promoters used for expressing the Yellow Cameleon (YC3.60) construct (Nagai et al., 2002) were *sra-6* for ASH (Troemel et al., 1995) and *flp-6* for ASE (Li et al., 1999).

**Behavioural assays** The behavioural assays were performed as previously described in Hukema et al., 2006, and depicted in figure 2.1a. In short, the worms were staged by bleaching and grown for three days at 25°C. Prior to the assay, worms were rinsed of the plate with CTX buffer (5 mM K<sub>2</sub>HPO<sub>4</sub>/KH<sub>2</sub>PO<sub>4</sub>, pH 6.6, 1 mM MgSO<sub>4</sub>, 1 mM CaCl<sub>2</sub>) for the naïve assays and CTX buffer plus 100 mM NaCl for the plasticity assays. After three washes of six minutes each, the worms were placed on the quadrant plate and allowed to explore the plate for ten minutes before being scored. The tested concentrations were 0.1 mM, 1 mM, 10 mM, 100 mM, 200 mM and 300 mM NaCl. A chemotaxis index was calculated: (AC)/(A+C), where A is the number of worms at the quadrants with NaCl and C is the number of worms at the quadrants without attractant.

**Cameleon imaging** Images were acquired with a Zeiss Axiovert 200M microscope, fitted with a Harvard apparatus MC-27 flowchamber. The naïve washbuffer contained 5 mM K<sub>2</sub>HPO<sub>4</sub>/KH<sub>2</sub>PO<sub>4</sub>, pH 6.6, 1 mM MgSO<sub>4</sub>, 1 mM CaCl<sub>2</sub>, the preexposition buffer contained an additional 100 mM NaCl. The

osmolarity of both buffers was set to 325 mosmol, using glycerol. The stimuli for the range tests were made by adding the required quantity of NaCl to either of the buffers. For the CuSO<sub>4</sub> assays, the 5 mM K<sub>2</sub>HPO<sub>4</sub>/KH<sub>2</sub>PO<sub>4</sub>, pH 6.6 was replaced by 10 mM HEPES.

The stimuli were applied by moving a capillary into the buffer close to the nose of the worm. The image was split into a CFP and YFP part with an Optical Insights Dualview beamsplitter (505 nm dichroic mirror, 465/30 nm and 535/30 nm emission filters). We used a custom automation in Improvise Openlab to control the movement of the capillary and to acquire the images. The resulting data files were processed using a custom Ruby script.

**Statistical analysis** Significance was determined using unpaired Students t-test, assuming equal variances. For all experiments, an  $\alpha$  level of 0.05 was used. All results are given as a mean +/- standard error of the mean.

**Acknowledgements** We thank Bill Schafer and Hiroshi Suzuki for their help in setting up the Cameleon imaging and for sharing unpublished results, and the Caenorhabditis Genetics Centre for strains. We also thank Renate Hukema and Suzanne Rademakers for helpful suggestions.



*Every sense hath been o'erstrung,  
and each frail fibre of the brain  
sent forth her thoughts all wild and  
wide*

Lord Byron

# 3

## Expression of mammalian receptors in *C. elegans* generates novel behavioural responses

Parts of this chapter have been published in:

Teng MS, Dekkers MPJ, Ng BL, Rademakers S, Jansen G, Fraser AW and McCafferty J (2006). BMC Biology, 2006 Jul 20;4:22

### 3.1 Abstract

Chemosensation in *C. elegans* is important for its interaction with the environment and is directed by gustatory and olfactory neurons driving repulsive and attractive behaviours. It uses many signalling components that are conserved in evolution, allowing the use of transgenic tools to both study chemosensory behaviour, and the characteristics of the transgenic proteins themselves.

Expression of the rat TRPV channel VR-1 in a number of sensory neurons imparts novel behaviours onto *C. elegans*. We show that activation of ASH results in avoidance, while activation of the ASI and ADF neurons leads to attraction. Expression of the mammalian GPCRs Sstr2 and CCR5 in ADL and ASH nociceptive neurons allow *C. elegans* to specifically detect and respond to somatostatin and MIP-1 $\alpha$  respectively in a robust avoidance assay. We demonstrate that mammalian heterologous GPCRs can signal via different endogenous G $\alpha$  subunits in *C. elegans*, depending on which cells it is expressed in. Furthermore, pre-exposure of GPCR transgenic animals to its ligand leads to behavioural adaptation to subsequent ligand exposure, most likely reflecting receptor desensitisation, providing further evidence of integration of the mammalian GPCRs into the *C. elegans* sensory signalling machinery.

Our results illustrate a remarkable evolutionary plasticity in interactions between mammalian receptors and *C. elegans* signalling machinery. Transgenic expression of signalling components in *C. elegans* provides a means to further dissect behavioural responses. In addition, it allows studying and screening interaction of GPCRs with extracellular agonists, antagonists and intracellular binding partners.

### 3.2 Introduction

The nematode *C. elegans* represents a simple and experimentally tractable multicellular organism. It is well suited for investigating many biological processes, including chemosensory behaviour (Bargmann & Mori, 1996). It uses only 11 pairs of amphid chemosensory neurons to detect environmental signals, and the complete neuronal circuit has been described (White et al., 1986). In addition, many components that mediate the detection of sensory signals are conserved across species. For instance, in *C. elegans* GPCRs also play an important role in the detection of sensory signals and these signals are relayed in the cell by heterotrimeric G proteins (Troemel et al., 1995; Jansen et al., 1999). However, the *C. elegans* sensory neurons express multiple GPCRs per sensory neuron and

use several *Ga* subunits per neuron for sensory transduction thus allowing the nematode to respond specifically to different environmental cues using only few sensory neurons (Troemel et al., 1995; Jansen et al., 1999; Lans et al., 2004). Previously, it was shown that expressing the mammalian TRPV-1 channel in the nociceptive ASH neurons of *C. elegans* results in a robust acquired avoidance behaviour of the ligand of this receptor, capsaicin (Tobin et al., 2002). Moreover, when the mammalian TRPV4 channel VR-OAC channel is expressed in the ASH neurons, the transgene partly rescued defects in *osm-9* mutant animals, which lack the *C. elegans* TRPV channel subunit OSM-9 (Liedtke et al., 2003). In addition, expression of the mammalian olfactory GPCR I7 in the AWA and AWB olfactory neurons, resulted in an altered responsiveness to octanal, the ligand of this receptor (Milani et al., 02). More recently, expression of several human and rodent T2R bitter GPCRs in the ASI neurons altered the innate avoidance responses of the bitter compounds. (Conte et al., 06). These results show that these mammalian TRP channels and GPCRs can be integrated into the endogenous sensory apparatus, suggesting that interaction domains of these signalling proteins are also conserved across widely diverged species. Transgenic expression of signalling components in specific neurons enables us to study the output of these cells and the neural networks in which they function, allowing us to further dissect behavioural responses. One such behaviour is chemosensation of NaCl in *C. elegans*. The nematode is attracted to low concentrations of NaCl, and avoids high concentrations (Bargmann et al., 1990; Jansen et al., 2002; Hukema et al., 2006). However, after prolonged exposure to attractive concentrations of NaCl, the animals will strongly avoid all concentrations of NaCl. We call this behavioural switch gustatory plasticity (Saeki et al., 2001; Jansen et al., 2002; Hukema et al., 2006). Previously, we found that the ASE, ASH, ASI and ADF neurons are essential for this switch. The ASE and ASH neurons are relatively well characterised. The ASE neurons mediate attraction to NaCl, and the ASH neurons have been shown to respond to a variety of nociceptive stimuli (Bargmann et al., 1990; Hart et al, 1995; Hilliard et al, 2004, 2005). However, the role of the ASI and ADF cells are less well understood. The ASI neurons are thought to mediate food signals (Bishop & Guarente, 2007), and the ASI and ADF neurons together with ASG are reported to mediate the residual attraction to NaCl after laser ablation of the ASE neurons (Bargmann & Horvitz, 1991). Thus far, for neither of these neurons a specific cue has been identified that strongly activates these cells, making it difficult to assess their contribution to the chemotactic behaviour, or their role in gustatory plasticity. Expressing mammalian receptors to whose ligands *C. elegans* does not show a native response, enables the study of the

function of these cells in this behaviour.

An interesting consequence of the ability to activate specific neurons by heterologous expression of signalling molecules is that it allows the study of GPCR receptor-ligand interactions. Current methods utilised for this purpose are mostly *in vitro* systems, which are not always an accurate reflection of *in vivo* interactions. Given that mammalian GPCRs are an important group of drug targets, it would be an advantage to have an alternative, preferably more *in vivo* system to investigate GPCR interactions with its respective agonists and antagonists. Hence, we set out to test whether we could elicit ligand-dependent behavioural responses of mammalian GPCRs in *C. elegans*. We aimed to express mammalian GPCRs in the ASH and ADL gustatory neurons as they are directly exposed to the environment allowing access of protein and peptide ligands to the heterologous receptors. In addition, the ASH and ADL neurons express a large variety of  $G\alpha$  subunits (Jansen et al., 1999), increasing the likelihood of GPCR- $G\alpha$  protein interaction. Finally, ASH and ADL neurons drive robust repulsive responses (Bargmann & Horvitz, 1991) and so receptor activation should be reflected in an avoidance response on ligand exposure, which can be analysed using behavioural assays (Wicks et al., 2000; Hilliard et al., 2002).

To investigate whether expression of mammalian receptors can be used to activate cells, and how well the characteristics of the receptors are retained after transgenic expression, we expressed the TRPV1 receptor in the ASE, ADF, ASH and ASI neurons, and Sstr2 and CCR5, two medically relevant GPCRs, in the ASH and ADL neurons. Somatostatin receptor (Sstr2) binds two isoforms of a tetradecapeptide, SST-14 and -28 (Brazeau et al., 1972; Padrayol et al., 1980). Both have broad regulatory functions, acting as neurotransmitters in the central and peripheral nervous system and inhibitors of hormone secretion (Brazeau et al., 1972; Padrayol et al., 1980). CCR5 is a chemokine receptor which binds MIP-1 $\alpha$  (CCL3), MIP-1 (CCL4) and RANTES and directs chemotactic responses in leucocytes. This receptor is also the route by which HIV-1 infection occurs, making this receptor a therapeutic target in AIDS treatment (Rossi & Zlotnik, 2000).

In this chapter we describe that transgenic *C. elegans* expressing mammalian GPCRs or TRP channel subunits show novel behavioural responses. Expression of the TRPV1 channel in the ASI and ADF gustatory neurons and the ASH nociceptive neurons allows the animals to respond to capsaicin, but we see no effects when it is expressed in the ASE neurons. In addition, we show that transgenic animals that express the Sstr-2 and CCR-5 receptor in the ASH and ADL nociceptive neurons display specific responses to their respective ligands. The avoidance behaviour in Sstr2 transgenic animals to somatostatin can be

inhibited using somatostatin antagonist, cyclosomatostatin. Furthermore, pre-exposure of the GPCR transgenic animals to its respective ligand abolishes this avoidance response without affecting its avoidance behaviour towards other repellents. Heterologously expressed GPCRs are able to signal via different endogenous  $G\alpha$  subunits depending on which cells they are expressed in, indicating that GPCRs and  $G\alpha$  proteins across highly diverged species are largely conserved in their interaction domains. Finally, we demonstrate the utility of this avoidance assay by identifying the key residues involved in interaction of somatostatin with its receptor.

### 3.3 Results

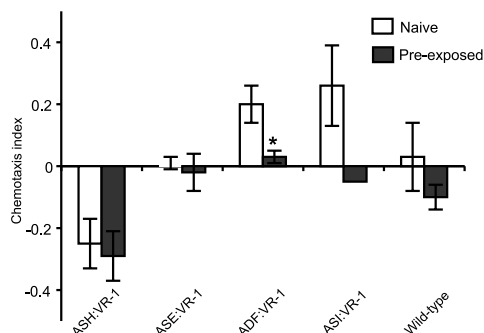
**Stimulation of TRPV1 expressing *C. elegans* with capsaicin results in attraction or avoidance behaviour.** We obtained the *sra-6::VR-1* construct that was originally published in 2002 (Tobin et al., 2002). Transgenic animals were created that expressed the TRPV1 channel subunit in the ASE, ADF, ASH and ASI pairs of neurons, using the promoters of *flp-6*, *srh-142*, *sra-6* and *gpa-4*, respectively.

The ASH::VR-1 worms were reported to display stops and reversals when tested in the drop assay and the dry drop assay (Tobin et al., 2002). In these assays, a single animal is allowed to explore an empty CTX agar plate, and tested by placing a drop containing the compound of interest near the tail of the worm or just in front of the animal, respectively (Hilliard et al., 2005). We repeated these experiments, and could confirm that the ASH expressing animals that we generated also displayed this behaviour (results not shown).

Drop assays are well suited for studying avoidance behaviours, but since we also want to study attraction, we used quadrant assays to test behavioural responses to capsaicin (Wicks et al., 2000; Jansen et al., 2002). In this assay, animals are given a choice between 2 quadrants filled with buffered agar containing capsaicin and 2% ethanol and 2 quadrants containing 2% ethanol. ASH::VR-1 transgenic animals showed avoidance of the quadrants containing capsaicin, as expected.

In contrast, animals that expressed the TRPV1 channel in the ADF and ASI neurons showed attraction towards capsaicin (Figure 3.1). This finding is in agreement with the previously suggested functions of these neurons (Bargmann & Horvitz, 1991; Conte et al., 2006), since both pairs of neurons were reported to be involved in the attraction to NaCl. Interestingly, the ASE::VR1 animals

**Figure 3.1: Expression of VR-1 in amphid sensory neurons in *C. elegans* induces novel behaviours.** Animals expressing VR-1 in the ASH neurons show avoidance of capsaicin in the quadrant assay, while ADF::VR-1 and ASI::VR-1 are attracted (white bars). Pre-exposition of these animals to 100 mM NaCl prior to the assay reduced attraction in the ADF::VR-1 and ASI::VR-1 animals. Each data point represents an average of at least two experiments, error bars denote standard error of the mean. Asterisk indicate a statistically significant difference between naive and pre-exposed transgenic animals. (black bars, \*  $P \leq 0.05$ ).



did not show any attraction towards capsaicin. Perhaps this absence of a response is due to the fact that ASE is a bilateral asymmetrical neuron pair, of which the left and right cell respond differently to a NaCl stimulus. The left cell responds primarily to an increase in NaCl, whereas the right cell responds to a decrease. This may indicate that concomitant stimulation of both neurons is not physiological, and hence does not result in attraction. However, we cannot exclude that the failure to respond is caused by another reason.

*C. elegans* displays a behavioural switch called gustatory plasticity. The nematode is attracted to low concentrations of NaCl, and avoids high concentrations. However, after prolonged exposure to an attractive concentration of NaCl, the animals will strongly avoid all concentrations of NaCl. We wondered whether preexposure to NaCl in these assays would alter the behaviour that we observe in the transgenic animals. This would suggest that the output of the cell that expresses the VR-1 receptor, or the circuit in which it functions is affected by pre-exposure

The ASE lines displayed neither attraction nor avoidance after pre-exposure, similar to the naive quadrant assay. The avoidance behaviour of the ASH lines was also unaffected by the pre-exposure to NaCl. However, the animals that express VR-1 in the ASI and ADF neurons did show an altered response: the attraction that these animals displayed in the naive assay setup was completely abolished after pre-exposure to 100 mM NaCl (Figure 3.1).

These results indicate that heterologous expression of TRPV1 channels can be used to study the contribution of cells to behavioural response. In these experiments we have confirmed that ASI and ADF function in attraction. Interestingly, the attraction mediated by these cells is subject to plasticity, suggestive of their

role in gustatory plasticity. However, this finding needs further analysis.

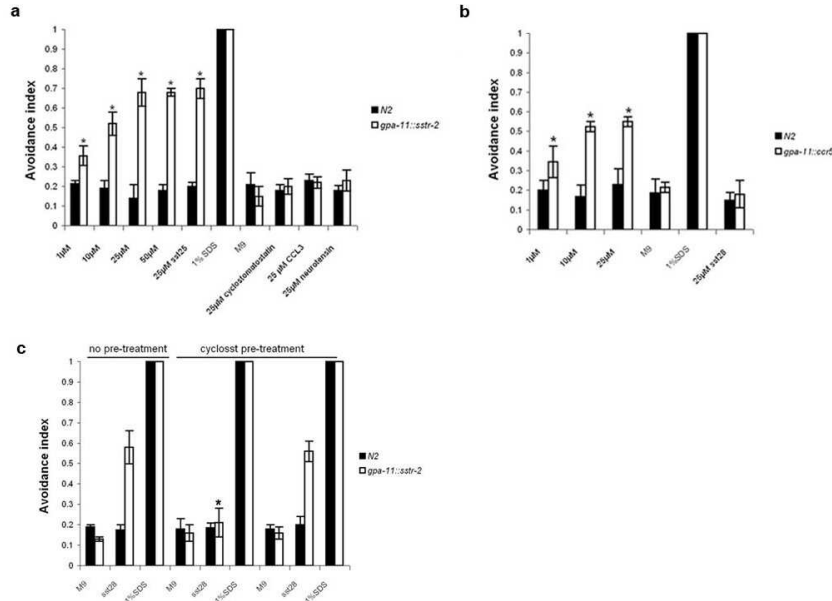


**Figure 3.2: Expression of mouse Sstr2 and human CCR5 in nociceptive neurons in *C. elegans* generates agonist specific avoidance behaviour.**

(A) Wild type and Sstr2 transgenic animals were tested with 1-50  $\mu$ M of SST-28. As controls, the responses to 1% SDS, M9 diluent, the unrelated neuropeptides, neurotensin and MIP-1 $\alpha$  were determined. Sstr2 transgenic animals did not avoid 25  $\mu$ M cyclosomatostatin. Both strains display a normal avoidance response to 1% SDS. Asterisks indicate a statistically significant difference between wild type and Sstr2 transgenic animals.

(B) Avoidance responses of wild type and CCR5 transgenic animals to various concentrations of MIP-1 $\alpha$ , M9 diluent, 1% SDS and 25  $\mu$ M SST-28. Asterisks indicate a statistically significant difference between wild type and CCR5 transgenic animals.

(C) Animals were either directly tested for their response to M9, SST-28 or 1% SDS or pre-incubated with 25  $\mu$ M cyclosomatostatin (denoted cyclosst in figure) for 3 minutes before the assays. Pre-treatment with 25  $\mu$ M cyclosomatostatin abolished the avoidance response of Sstr2 transgenic animals to 25  $\mu$ M SST-28. Avoidance responses can be recovered by an additional 5 minutes wash to remove cyclosomatostatin. Asterisks indicate a statistically significant difference between cyclosomatostatin treated and untreated transgenic animals. In all panels, each data point represents an average of at least 5 independent assays for wild type and each respective strain. Error bars denote the standard error of the mean. (\* $P \leq 0.05$ ). Avoidance Index = # worms behind barrier/ total # worms

**Transgenic animals expressing heterologous mammalian GPCRs are able to direct specific responses to its agonists.** The TRP channels are cation channels, some with high affinity for calcium (Minke & Cook, 2002). Therefore, they might bypass the endogenous pathways to activate cells, by allowing the entry of  $\text{Ca}^{2+}$  into the cell upon activation of the receptor. Previously it was shown that heterologous expression of GPCRs results in an altered behaviour, suggestive of integration into endogenous signalling cascades. To further investigate this, we generated transgenic *C. elegans* strains that express the mammalian Sstr2 and CCR5 GPCRs in the ASH and ADL nociceptive neurons, using the *gpa-11* promoter, which drives expression in these neuron pairs (Jansen et al., 1999).

Sorted populations of Sstr2 and CCR5 transgenic animals (denoted as *gpa-11::sstr2* and *gpa-11::ccr5* respectively in figures) were tested for their response to the native ligands using an adapted soluble compound avoidance assay (Wicks et al., 2000). Wild type and Sstr2 transgenic animals were tested for their response to varying concentrations of SST-28. In contrast to wild type animals, Sstr2 transgenic animals exhibited avoidance of SST-28 (Figure 3.3A). The strongest response was observed with 25  $\mu\text{M}$  SST-28. Ovine isolated SST-25 and human SST-28 have previously been found to have higher biological activity than SST-14 (Brazeau et al., 1982). The behaviour of the Sstr2 transgenic animals is consistent with this: SST-25 and SST-28 induced stronger avoidance responses than SST-14 (Figure 3.3A & 3.3). As a control, we tested the response of this strain to neurotensin and MIP-1 $\alpha$ . Neither compound elicited a response in the Sstr2 transgenic animals, confirming specificity of GPCR-ligand interaction (Figure 3.3A). Also *gpa-11::CCR5* transgenic animals showed specific avoidance of MIP-1 $\alpha$ , but not of the control ligands, SST-28 and neurotensin (Figure 3.3B). An optimal avoidance response was obtained with 10  $\mu\text{M}$  MIP-1 $\alpha$ . In addition, we also expressed CCR5 in the ASH neurons using the *sra-6* promoter, which also gave a robust avoidance response to 25  $\mu\text{M}$  MIP-1 $\alpha$  (Figure 3.3B). This demonstrates that mammalian GPCR expression in the ASH neurons is sufficient to generate avoidance behaviour to its ligands.

We also tested the response of the Sstr2 and CCR5 transgenic animals to SST-28 and MIP-1 $\alpha$  using the dry drop test (Hilliard et al., 2002). The average frequency of avoidance for each tested compound in this single animal assay was very similar to that in the population assay (Figure 3.3).

The ASH and ADL neurons of *C. elegans* normally direct avoidance responses to environmental agents such as low pH and SDS (Bargmann & Horvitz, 1991). When exposed to a barrier of 1% SDS, neither transgenic strain crossed the barrier, suggesting that normal avoidance behaviour is unaffected by expression



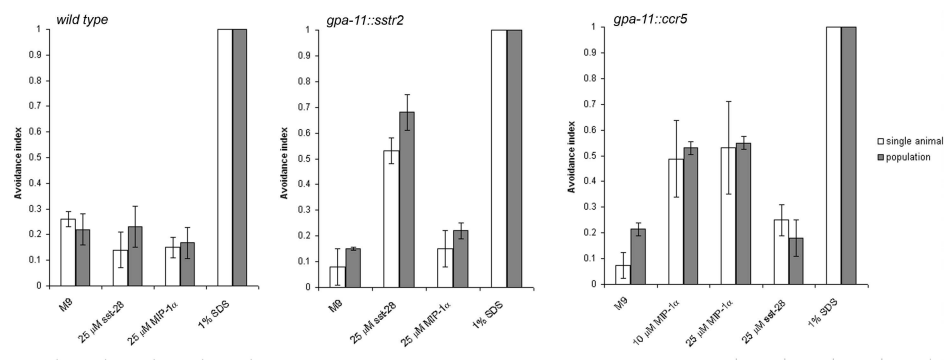


**Figure 3.3: Comparison of avoidance indices of population vs single animal avoidance assay (Dry drop test).** Wild-type, gpa-11::sstr2 and gpa-11::ccr5 animals were analysed for their response to 25  $\mu$ l, MIP-1 $\alpha$ , 1% SDS or control diluent (M9 buffer), using the dry drop assay or soluble compound avoidance assay. Both assays gave similar results. Error bars indicate standard error of the mean.

of heterologous GPCRs. We have thus shown that expression of mammalian GPCRs in transgenic animals generates a specific avoidance response towards its respective agonists.

**Pre-exposure to native agonists causes receptor desensitisation and adaptation behaviour in Sstr2 and CCR5 transgenic animals.** Activation of GPCRs in both worms and mammals eventually leads to receptor desensitisation through phosphorylation by GPCR kinases (GRKs) and arrestins (Palmitessa et al., 2005; Fergusson, 2004; Pitcher et al., 1998). To study whether the response of the Sstr2 and CCR5 transgenic animals to their respective ligands was subject to desensitisation (leading to adaptation), the animals were pre-exposed to either 1  $\mu$ M or 10  $\mu$ M of the respective peptides for 10 minutes in liquid before testing the avoidance responses.

The avoidance behaviour of Sstr2 transgenic animals in response to 25  $\mu$ M SST-28 was strongly reduced after pre-exposure to 1  $\mu$ M SST-28 whereas pre-exposure to 10  $\mu$ M SST-28 could fully abolish avoidance of SST-28 (Figure 3.3A). The avoidance behaviour to other repellents like 1% SDS was not affected by the pre-exposure to SST-28, suggesting that SST-28 adaptation is independent from the pathway that signals avoidance of 1% SDS. Similarly, CCR5 transgenic animals were pre-exposed to 1  $\mu$ M and 10  $\mu$ M of MIP-1 $\alpha$  and tested at three different MIP-1 $\alpha$  concentrations. Full adaptation to MIP-1 $\alpha$  was achieved with

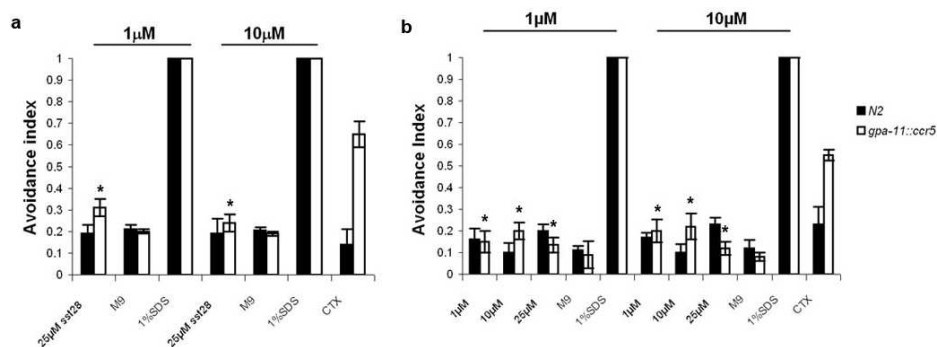


**Figure 3.4: Sstr2 and CCR5 transgenic animals mutants are desensitised by pre-exposure to agonists.**

(A) Pre-exposure of Sstr2 transgenic animals to 1  $\mu$ M and 10  $\mu$ M SST-28 prior to the assay strongly reduced or even abolished avoidance behaviour.

(B) Pre-exposure of CCR5 transgenic animals to 1  $\mu$ M and 10  $\mu$ M MIP-1 $\alpha$  fully abolished avoidance of 1  $\mu$ M, 10  $\mu$ M and 25  $\mu$ M MIP-1 $\alpha$ . In both cases, pre-exposure to the agonist did not affect the responses towards other repellents. Animals were washed in buffer as control. For each panel, each data point represents an average of at least 5 independent assays for wild type and each respective strain. Error bars denote the standard error of the mean. Asterisks indicate a statistically significant difference between transgenic animals pre-exposed to agonist or only to chemotaxis (CTX) buffer (\*P ≤ 0.05).

both pre-exposure concentrations; however pre-exposure did not affect other avoidance responses (Figure 3.3B). These results demonstrate that avoidance of SST-28 and MIP-1 $\alpha$  mediated by their respective mammalian GPCRs in *C. elegans* is subject to specific adaptation. We propose that the *C. elegans* signalling components involved in receptor desensitisation interact with the heterologous GPCRs.

**Sstr2 antagonist, cyclosomatostatin can inhibit response of Sstr2 transgenic animals to somatostatin.** To analyse the specificity of ligand-receptor interaction reflected in the avoidance response, Sstr2 transgenic animals were tested with a competitive somatostatin antagonist, cyclosomatostatin (cyclo(D-Trp-Lys-Thr-Ahep-Phe)), which blocks somatostatin binding to its receptors (Veber et al., 1981). Pre-exposure of Sstr2 transgenic animals to 10  $\mu$ M of cyclosomatostatin in liquid for 3 minutes eliminated most of the avoidance behaviour towards 25  $\mu$ M SST-28 (Figure 3.3C). Higher concentrations of cyclosomatostatin and longer incubation times tend to cause paralysis in both wild type and

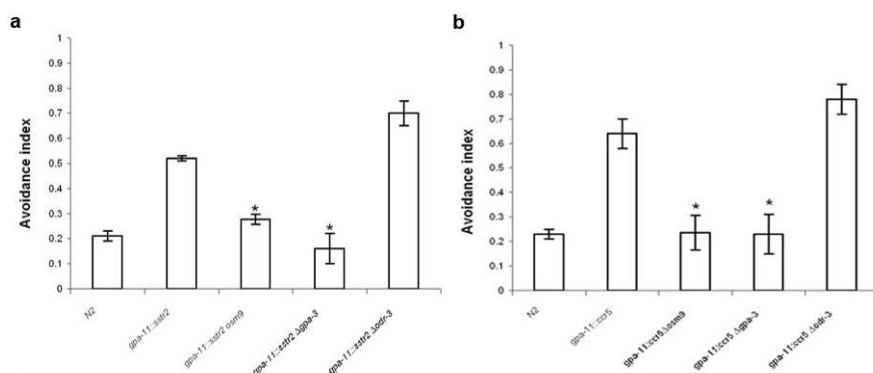


**Figure 3.5: Heterologously expressed GPCRs are integrated into an endogenous signalling pathway in *C. elegans*.** Mutation of the TRPV channel subunit *osm-9* and the  $G\alpha$  subunit *gpa-3* fully abolished avoidance of (A) 25  $\mu$ M SST-28 in Sstr2 transgenic animals and (B) 25  $\mu$ M MIP-1 $\alpha$  in CCR5 transgenic animals. Mutation of  $G\alpha$  subunit *odr-3* did not affect these responses. Each data point represents an average of at least 3 independent assays for wild type and each respective strain. Error bars denote the standard error of the mean. Asterisks indicate a statistically significant difference between *osm-9* or *gpa-3* mutant animals and wild type animals carrying the Sstr2 or CCR5 transgenes (\* $P \leq 0.05$ ).

transgenic animals (results not shown). We also tested for reversibility of this antagonistic effect by allowing the animals to recover for 5 minutes by washing the worms after the 3 minute pre-incubation step. The resulting effect was a recovery of the Sstr2 transgenic animals avoidance of SST-28 (Figure 3.3C). Hence, avoidance of SST-28 could be restored in 5 minutes after antagonist pre-exposure.

**Mammalian heterologous GPCRs can signal via different endogenous  $G\alpha$  subunits in *C. elegans*.** Our results confirm that the biological properties of the GPCRs can be translated into the altered sensory behaviour of the transgenic animals, suggesting that heterologous GPCRs use *C. elegans* signal transduction in nociceptive neurons. *gpa-11* is expressed predominantly in the ADL neurons, and to a lesser extent in the ASH neurons (Jansen et al., 1999). The ASH and ADL neurons express a variety of  $G\alpha$  proteins. Not much is known about the molecules used in the ADL cells. Nociceptive signalling in ASH involves the

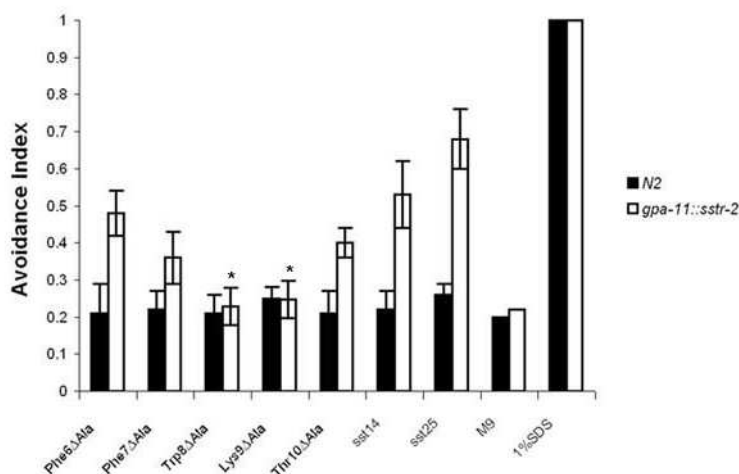


**Figure 3.6: Identification of SST-14 residues involved in Sstr2 activation.** Sstr-2 transgenic animals were tested for response to SST-14 and 5 variants with single alanine substitutions at residues 6-10. No avoidance behaviour was observed with 25  $\mu$ M of Trp8 $\delta$ Ala and Lys9 $\delta$ Ala SST-14 analogues while residual avoidance behaviour was found with Phe7 $\delta$ Ala and Thr10 $\delta$ Ala. Sstr2 transgenic animals were repelled by the Phe6 $\delta$ Ala analogue indicating that Phe6 is not essential for receptor:ligand interaction. Each data point represents an average of at least 5 independent assays for wild type and each respective strain. Error bars denote the standard error of the mean. Asterisks indicate a statistically significant difference between the avoidance index of the transgenic animals for the Trp8 $\delta$ Ala and Lys9 $\delta$ Ala analogues and native SST-14 agonist (\*  $P \leq 0.05$ ).

G $\alpha$  proteins ODR-3 (Roayaie et al., 1998) and GPA-3 (Hilliard et al., 2004).

These in turn lead to downstream activation of TRPV calcium channel OSM-9 or OCR-2 (Colbert et al., 1997; Tobin et al., 2002). To identify some of the molecules involved, we tested several mutants known to affect avoidance behaviour. Inactivation of *osm-9* or *gpa-3* fully abolished the response to SST-28 and MIP-1 $\alpha$  in Sstr2 and CCR5 transgenic animals respectively, whilst inactivation of *odr-3* did not (Figure 3.3A and 3.3B). These results indicate that the heterologous GPCRs, expressed predominantly in the ADL signals via GPA-3 to activate OSM-9. In contrast, avoidance of MIP-1 $\alpha$  of *sra-6::ccr5* animals expressing CCR5 in the ASH neurons were not affected by removal of *gpa-3* or *odr-3* (Figure 3.3C). Our results indicate that CCR5 can activate different *C. elegans* G $\alpha$  subunits, depending in which cells it is expressed. In the ASH

neurons, CCR5 could signal redundantly via GPA-3 or ODR-3 or any of the other  $G\alpha$  subunits present in these neurons. These results illustrate a level of promiscuity in the interactions between the heterologous GPCRs and the endogenous signalling components of *C. elegans*.

**Trp8 and Lys9 of SST-14 are essential for Sstr2 activation.** Given that heterologous GPCRs can be expressed functionally in nociceptive neurons, we sought to investigate the structure-function relationship by screening SST-14 analogues. Structure activity studies on SST-14 have suggested that amino acid residues Phe7, Trp8, Lys9 and Thr10 are important in receptor-ligand interaction, with Trp8 and Lys9 being essential, whereas Phe7 and Thr10 can undergo minor conserved substitutions (Veber et al., 1978). We investigated the role of these residues by testing the 5 peptide analogues, where residues 6-10 of SST-14 are individually substituted with Ala. The Sstr2 transgenic animals showed a completely attenuated response towards the Trp8 $\delta$ Ala and Lys9 $\delta$ Ala analogues whereas partial avoidance responses were observed to both Phe7 $\delta$ Ala and Thr10 $\delta$ Ala (Figure 3.3). No significant difference in avoidance response was observed with Phe6 $\delta$ Ala, indicating that this residue is not essential for receptor-ligand interaction.

### 3.4 Discussion

In order to gain insight into how the nervous system functions, it is important to study the individual signalling components as well as the cells and circuits in which they play their role. The *C. elegans* sensory system is exceptionally well suited for these purposes, since its neurons are easily identifiable and several networks have already been described (White et al., 1986; Gray et al., 2004; Chalasani et al., 2007; Hukema et al., 2006). Previous studies have shown that expression of TRPV (VR1 and VR-OAC) and of several GPCRs in various neurons of *C. elegans* resulted in functional changes, supporting the suitability of *C. elegans* as a heterologous expression system (Tobin et al., 2002; Liedtke et al., 2003; Milani et al., 2002; Conte et al., 2006).

In this chapter, we extend on these findings, by showing that introducing the TRPV1 receptor in the ASI, ADF generates attraction towards capsaicin, which can be modulated by pre-exposure to NaCl. This finding suggests that the output of the network that these cells function in is attenuated by the prolonged presence of NaCl. Previously, it was found that several cations such as  $Na^+$ ,  $Mg^{2+}$  and  $Ca^{2+}$  can modulate the sensitivity, or even directly activate TRPV1

channels (Ahern et al., 2005). Therefore, the altered response of the ASI::VR-1 and ADF::VR-1 animals may be the result of a direct effect of  $\text{Na}^+$  on the VR-1 receptors. However, we would expect that this effect would also be seen in the ASH::VR-1 animals, which would then result in a decreased avoidance of capsaicin. Rather, we find the avoidance of ASH::VR-1 animals after pre-exposure to be unaffected. Alternatively, the altered responses of the ASI::VR-1 and ADF::VR-1 animals may represent changes in excitability of the ASI and ADF neurons, or the networks they function in, by NaCl pre-exposure. It will be interesting to discriminate between these two possibilities, and further characterise the molecules and perhaps additional neurons that play a role in this alteration.

In this chapter we also show that expression of heterologous GPCRs in nociceptive neurons under the control of two different promoters, *gpa-11* (ADL and ASH expression) and *sra-6* (ASH expression), can drive repulsive responses to its respective ligands presented in its soluble pure form. The behavioural response to its ligands can be tested using robust avoidance assays, making this an useful system to study receptor-ligand interactions. Sstr2 and CCR5 transgenic animals were able to specifically avoid its respective agonists without affecting its avoidance behaviour towards other repellents. Similar responses were observed in multiple transgenic strains with different promoters using both the population and single animal avoidance assays. The fidelity of the system extends to antagonists since pre-exposure of Sstr2 transgenic animals to a somatostatin antagonist, cyclosomatostatin, inhibited its avoidance response to somatostatin. The antagonistic effect was reversible given that the avoidance behaviour can be recovered by washing the transgenic animals.

Attenuation of GPCR signalling by GRKs and arrestins is important for an organism to maintain a homeostatic cellular environment (Palmitessa et al., 2005; Fergusson, 2004; Pitcher et al., 1998). Desensitisation also ensures that receptors are ready for the next coming wave of stimuli. We found that pre-exposure to varying concentrations of the ligand leads to adaptation of the response to the ligand but not to other repellents. This suggests that the heterologously expressed mammalian GPCRs in *C. elegans* are subjected to desensitisation by the endogenous machinery, further supporting the fact that the heterologous GPCRs are integrated into the endogenous signalling pathway.

Our results demonstrate that mammalian GPCRs integrate into the normal endogenous  $\text{G}\alpha$  protein signalling pathway in the worm, and that several  $\text{G}\alpha$  proteins are involved in downstream signalling in the ASH neurons. Given the abundance of  $\text{G}\alpha$  proteins in these neurons, it would be interesting to examine the individual roles of  $\text{G}\alpha$  proteins involved in signalling with heterologous

GPCRs. It has previously been shown that widespread promiscuity occurs in the interactions of mammalian GPCRs with mammalian  $G\alpha$  proteins (Hermans, 2003; Guderman et al., 1996). In addition, rat Sstr2 has previously been demonstrated to interact with endogenous yeast  $G\alpha$  protein, Gpa1p, when the receptor was expressed in *Saccharomyces cerevisiae*. Together with our results, this provides further evidence that G proteins across highly diverged species are largely conserved in their interaction domains (Price et al., 1995).

G protein coupled receptors (GPCRs) represent the largest and most diverse family of proteins in the human genome (Hermans, 2003). Given that this family of proteins plays key roles in many biological processes, they constitute one of the principal targets for drug development. The *C. elegans* sensory system is exceptionally well suited for heterologous GPCR expression given that each neuron expresses multiple endogenous GPCRs (Troemel et al., 1995). Furthermore, multiple  $G\alpha$  subunits are expressed in each chemosensory neuron (Jansen et al., 1999) allowing cross talk between a single GPCR and potentially multiple  $G\alpha$  proteins. Moreover, the gustatory neurons are exposed to the external environment, making it accessible to water soluble ligands. The system for heterologous expression of functional GPCRs in *C. elegans* described here thus provides a novel means of screening for agonists and antagonists as well as carrying out structure function studies on GPCRs and their ligand. This potential is illustrated by our SST-14 analogue experiments. This work confirmed and extended the previous finding, based on activity of hexapeptide analogues, that residues 7-10 contain key elements necessary for its biological activity of somatostatin (Veber et al., 1981). This illustrates the practical utility of this system for identifying structure-function relationships in GPCR transgenic animals.

Using *C. elegans* can also be useful for screening of peptide banks, since the ligands do not need to be purified. Typically, the peptides are expressed in *E. coli*. These transgenic *E. coli* strains can be used as an alternative food source in a food preference assay for *C. elegans* (Stonda & Avery, 2006). When the peptide ligand expressed in *E. coli* is an agonist for the transgenic GPCR in *C. elegans*, the animals will display an altered food preference (Teng, unpublished observations), greatly facilitating the screening process.

Our work describes the generation of novel behavioural responses in *C. elegans* to exogenous ligands. By exploiting the sensory system of this nematode we have developed a powerful platform for exploring GPCR-ligand interactions in an animal model in vivo. Furthermore, the synthetic response holds potential in basic studies of neuronal circuitry, behaviour and higher learning in *C. elegans*.

### 3.5 Materials & Methods.

**Strains and plasmids** Nematodes were grown at 16 °C or 20 °C on E. Coli strain OP50 using standard methods (Brenner, 1974). Wild type animals were *C. elegans* variety Bristol strain N2. Strains used in this study are *odr-3(n1605)*, *gpa-3(pk35)* and *osm-9(ky10)*.

**Reagents.** SST-14, -28, -25 and its analogues were purchased from Bachem, UK. MIP-1 $\alpha$  was obtained from GeneFlow, UK. Peptides were dissolved in M9.

**Molecular Biology.** We obtained the *sra-6::VR-1* construct (Tobin et al., 2002) as a kind gift from C.I. Bargmann. The *sra-6* promoter region was exchanged for the promoters of the *gpa-4*, *flp-6* and *srh-142* genes, to drive expression in ASI (Jansen et al., 1999), ASE (Li et al., 1999) or ADF (Sagasti et al., 1999), respectively. Full length Sstr2 and CCR5 were cloned downstream of a 1.5 kb fragment of the *gpa-11* promoter into *pUC119*. The 3' UTR of *unc-54* was cloned downstream of both genes. The fragment containing CCR5 and the *unc-54* 3'UTR was subcloned into an *sra-6::GFP* construct.

**Transgenic strains.** Germ line transformation was carried out as described by Mello et al. (Mello et al., 1991) using 40 ng/  $\mu$ l of *gpa-11::sstr2*, *gpa-11::ccr5* with 100 ng/  $\mu$ l of *elt-2:gfp* plasmid, or 100 ng/  $\mu$ l of *sra-6::ccr5* with 25 ng/  $\mu$ l of *elt-2:gfp* (Fukushige et al., 1999). As the transgenic animals carry non-integrated arrays which could cause a degree of fluctuation in the assay, at least 3 transgenic strains were tested before picking out the best responding strain for repeating assays. For the mutant analysis, the best responding non-integrated strain was crossed with *osm-9(ky10)*, *gpa-3(pk35)*, *odr-3(n1605)* mutant. The mutant alleles were traced by PCR. At least 3 transgenic strains were tested before picking out the best responding strain for repeating assays.

**Sorting of transgenic animals.** Transgenic animals were sorted on fluorescence of the *elt-2:gfp* marker construct, using a COPAS Select sorter or a with a MoFlow sorter. Animals were washed with M9 and filtered through 100  $\mu$ m mesh filter (only for the MoFlow sorter). Appropriate sorting of each developmental stage was verified using epifluorescence microscopy. The animals were then grown for a day prior to testing in a quadrant assay or a soluble compound avoidance assay.



**Capsaicin quadrant assay.** The behavioural assays were performed as previously described in Hukema et al 2006. In short, the worms were staged by bleaching and grown for three days at 25° C. The animals were sorted the day before the assay with the Copas Select sorter. Prior to the assay, worms were rinsed of the plate with the CTX buffer for the nave assays and CTX buffer plus 100 mM NaCl for the plasticity assays. After three washes of six minutes each, the worms were placed on the quadrant plate and allowed ten minutes to explore the plate before being scored. A chemotaxis index was calculated:  $(AC)/(A+C)$ , where A is the number of worms at the quadrants with NaCl and C is the number of worms at the quadrants without attractant.

**Soluble compound avoidance assay.** Mutant avoidance behaviour was assessed on rectangular 4-well plates (Nunc, UK) using an assay adapted from (Wicks et al., 2000). This reduces the amount of avoidance compound used. Each compartment was filled with 12 ml CTX agar. A thin line of the soluble ligand was applied across one end of the well about 2.5 cm from the end of the plate. (Note that the ligand concentrations given here are the applied concentrations for the assay). Adult animals were washed 3 times in CTX buffer. When the test compound was absorbed into the agar, about 50 animals were placed 1 cm behind the line of the compound in about 5  $\mu$ l of CTX buffer. Volatile attractant of 1:10 benzaldehyde was added on the opposite end of the plate. The avoidance index was calculated by counting the number of worms that do not crawl past the boundary after 30 minutes, divided over the total number of worms applied. The assay was performed for 30 minutes as the avoidance index does not change significantly after 30-50 minutes into the assay. Avoidance Index = # worms behind barrier/ total # worms.

**Statistical analysis.** Statistical analysis of behavioural data was performed using the paired Students t test. If multiple groups were tested, statistical significance was determined by ANOVA. An  $\alpha$  level of 0.05 was used in all tests. All results are given as mean  $\pm$  s.e.m.



*Je hebt op het ogenblik al mensen  
die zijn niet gescheiden van tafel  
en bed, maar van Peugeot en Re-  
nault.*

Lucebert

# 4

## Mutation of the MAP kinase DYF-5 affects docking and undocking of kinesin-2 motors and reduces their speed in the cilia of *C. elegans*

Jan Burghoorn<sup>1,4</sup>, Martijn P.J. Dekkers<sup>1,4</sup>, Suzanne Rademakers<sup>1</sup>, Ton de Jong<sup>2</sup>, Rob Willemsen<sup>3</sup> and Gert Jansen<sup>1</sup>

Departments of <sup>1</sup> Cell Biology and Genetics and Center for Biomedical Genetics, <sup>2</sup> Pathology and <sup>3</sup> Clinical Genetics, Erasmus MC, P.O. Box 2040, 3000 CA Rotterdam, The Netherlands

<sup>4</sup> Contributed equally to this work

Proc. Natl. Acad. Sci. USA, 2007 Apr 24;104(17):7157-62

## 4.1 Abstract

In the cilia of the nematode *Caenorhabditis elegans* anterograde intraflagellar transport (IFT) is mediated by two kinesin-2 complexes, kinesin II and OSM-3 kinesin. These complexes function together in the cilia middle segments, while OSM-3 alone mediates transport in the distal segments. Not much is known about the mechanisms that compartmentalize the kinesin-2 complexes or how transport by both kinesins is coordinated. Here we identify DYF-5, a conserved MAP kinase that plays a role in these processes. Fluorescence and electron microscopy revealed that the cilia of *dyf-5* loss-of-function (*lf*) animals are elongated and not properly aligned into the amphid channel. Some cilia do enter the amphid channel but the distal ends of these cilia show accumulation of proteins. Consistent with these observations, we found that six IFT proteins accumulate in the cilia of *dyf-5(lf)* mutants. In addition, using genetic analyses and live imaging to measure the motility of IFT proteins, we show that *dyf-5* is required to restrict kinesin II to the cilia middle segments. Finally, we show that in *dyf-5(lf)* mutants OSM-3 moves at a reduced speed and is not attached to IFT particles. We propose that DYF-5 plays a role in the undocking of kinesin II from IFT particles and in the docking of OSM-3 onto IFT particles.

## 4.2 Introduction

Cilia are present on almost every vertebrate cell and have important functions in motility or sensation. Within cilia, structural components and signaling molecules are transported by a specialized system, called intraflagellar transport (IFT; Rosenbaum & Witman, 2002; Scholey, 2003; Qin et al., 2004; Qin et al., 2005; Ou et al., 2005). Transport from the base of the cilia to the tip (anterograde) is mediated by kinesin-2 motor complexes whereas dynein motor complexes mediate transport back to the base (retrograde). The nematode *C. elegans* has 60 ciliated neurons, including eight pairs of amphid neurons exposed to the environment (White et al., 1986). The cilia of these neurons can be divided into a middle segment with nine doublet microtubules and a distal segment with nine singlet microtubules (Perkins et al., 1986). In the middle segments two distinct kinesin-2 motor complexes mediate anterograde transport, heterotrimeric kinesin II, encoded by *klp-11*, *klp-20* and *kap-1*, and homodimeric OSM-3 kinesin (Snow et al., 2004). In the distal segments transport is only mediated by OSM-3 (Snow et al., 2004). Live imaging of the movement of these kinesins suggests that kinesin II alone moves at 0.5  $\mu\text{m/s}$  and OSM-3 alone moves at 1.3  $\mu\text{m/s}$ ,

while the two motor complexes together move at  $0.7 \mu\text{m/s}$  (Snow et al., 2004). Recently, Pan et al. (2006) have shown that these *in vivo* transport rates can be reconstituted *in vitro* using purified kinesin II and OSM-3 motors. Thus far, two proteins have been identified that are required to stabilize IFT complexes transported both by kinesin II and OSM-3, BBS-7 and BBS-8 (Ou et al., 2005). However, it remains unclear how kinesin II is restricted to the cilia middle segments while OSM-3 is allowed to enter the distal segments, and what the functional significance is of this compartmentalization.

Recently, Evans et al. (2006) have suggested that differences in the activities of the two kinesins contribute to morphological and functional differences between the cilia of individual neurons. Not much is known about the molecular mechanisms that control length and morphology of cilia, although it has been proposed that cilia length is controlled by a balance between cilia assembly and disassembly regulated by IFT (Marshall & Rosenbaum, 2001; Dentler, 2006; Pan & Snell 2005). Genetic approaches have thus far identified three proteins involved in the regulation of cilia length: two novel *Chlamydomonas reinhardtii* proteins, LF1 and LF2, and the *Chlamydomonas* MAP kinase LF4 and its *Leishmania mexicana* homologue LmxMPK9 (Tam et al., 2003; Nguyen et al., 2005; Bengs et al., 2005; Berman et al., 2003).

The identification of genes involved in IFT in *C. elegans* has profited significantly from the fact that a subset of *C. elegans*' amphid neurons exposed to the environment can take up fluorescent dyes via their cilia, called dye filling (Hedgecock et al., 1985). This phenomenon has allowed the identification of mutants with cilia defects, often caused by mutations in components of the IFT machinery (Rosenbaum & Witman, 2002; Scholey 2003; Perkins et al., 1986; Starich et al., 1995). Here we describe the identification of the gene mutated in *dyf-5* animals, a dye filling defective (Dyf) mutant isolated previously in a forward genetic screen (Starich et al., 1995). *dyf-5* encodes a predicted serine threonine kinase homologous to three human MAP kinases with unknown functions, *Chlamydomonas* LF4 and *Leishmania* LmxMPK9. We found that mutations in *dyf-5* affect cilia length and morphology. We also show that *dyf-5(lf)* affects the constitution and coordination of IFT particles. First, kinesin II can enter the distal segments in *dyf-5(lf)* mutants. Second, OSM-3 is separated from the IFT particles and moves at a reduced speed in *dyf-5(lf)* mutants. Third, *dyf-5(lf)* animals show accumulation of six different IFT proteins in the cilia.

### 4.3 Results

***dyf-5* encodes a conserved MAP kinase.** *dyf-5* has previously been mapped to a small region of chromosome I (Starich et al., 1995). We identified *dyf-5* as M04C9.5 using transgenic rescue and candidate gene sequencing (Figure 4.3a). Independently, others have also identified the *dyf-5* gene (Chen et al., 2006). *dyf-5(mn400)* contains a G to A transition in exon 3 (Figure 4.3a), which introduces a stop codon at amino acid position 49. In addition, we characterized two deletion alleles of *dyf-5*, *ok1170* and *ok1177*, generated by the *C. elegans* gene knock out consortium. Both deletion alleles remove most of the *dyf-5* coding region and are very likely null alleles (Figure 4.3a). All three *dyf-5(lf)* alleles show Dyf phenotypes (Figure 4.3b, c and results not shown). Dye filling could be restored by introducing low concentrations (5 ng/ $\mu$ l) of a 7.5 kb genomic fragment containing the M04C9.5 gene or a full length *dyf-5::gfp* fusion construct in *dyf-5(ok1170)* and *dyf-5(mn400)* animals (Figure 4.3d and results not shown), confirming that this gene indeed encodes *dyf-5*. Transgenic animals carrying high copy numbers of the *dyf-5* gene (*dyf-5XS*, injected with 75 ng/ $\mu$ l) or the full length *dyf-5::gfp* construct showed dye filling defects (Figure 4.3e and results not shown), suggesting that the levels of DYF-5 are important for its function. Characterization of the *dyf-5* gene structure using RT PCR identified an additional upstream exon, as well as some errors in the predicted M04C9.5 gene structure. We have communicated the confirmed *dyf-5* gene structure to Wormbase ([www.wormbase.org](http://www.wormbase.org)).

*dyf-5* encodes a protein of 471 amino acids, which shows extensive homology to three mammalian proteins that form a small subfamily of mitogen-activated protein (MAP) kinases. This subfamily consists of MAK (male germ cell associated kinase; Matsushime et al., 1990), ICK or MRK (intestinal cell kinase and MAK-related kinase, respectively; Togawa et al., 2000; Yang et al., 2002) and MOK (MAPK/MAK/MRK overlapping kinase; Miyata et al., 1999), with highly conserved N-terminal catalytic domains and more divergent C-terminal non-catalytic domains. Although the functions of these kinases in mammals are not known, studies in other organisms suggest a function in the cilia. Mutations in a DYF-5 homologue in *Leishmania mexicana*, LmxMPK9 (Bengs et al., 2005), and in one of the two homologues in *Chlamydomonas reinhardtii*, LF4 (Berman et al., 2003), affect the length of the flagella of these organisms. In addition, several genome-wide approaches have identified DYF-5 and its homologues as likely ciliary proteins (Chen et al., 2006; Blacque et al., 2005; Colosimo et al., 2004; Efimenko et al., 2005; Pazour et al., 2005; Stolc et al., 2005).

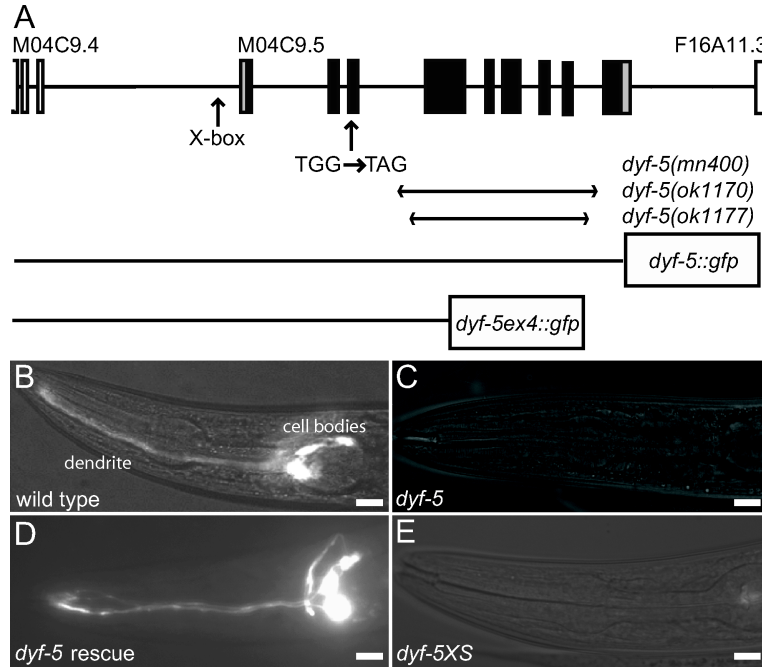
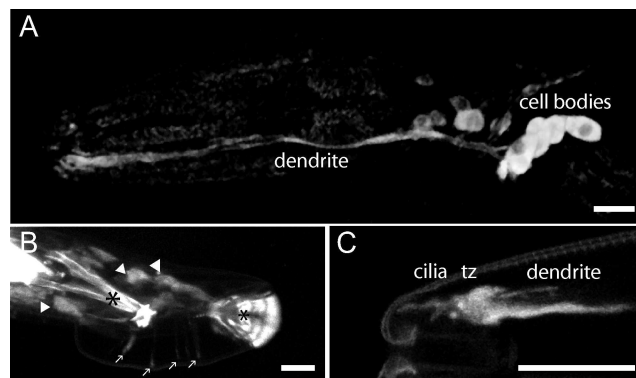


Figure 4.1: ***dyf-5* encodes a putative protein kinase.** (A) Schematic representation of the *dyf-5* gene structure (M04C9.5). Coding exons are indicated as black boxes; 5' and 3' UTR are depicted as gray boxes. Exons of the flanking genes are indicated as open boxes. The predicted X-box is indicated. Arrows indicate the position of the G to A substitution in *dyf-5(mn400)* animals, and the regions deleted in the *ok1170* and *ok1177* alleles. The two *dyf-5::gfp* fusion constructs have been indicated. (B-E) Dil dye filling of (B) wild-type, (C) *dyf-5(mn400)*, (D) *dyf-5(ok1170)* gjEx824(*dyf-5*) rescue strain, and (E) *dyf-5XS*(gjEx817) animals. Both *dyf-5(lf)* and *dyf-5(XS)* animals are dye filling defective. Scale bars represent 20 μm, anterior is to the left.

***dyf-5* functions in ciliated neurons.** We examined the expression pattern of *dyf-5* using two *dyf-5::gfp* fusion constructs: a full length, functional *dyf-5::gfp* fusion and a construct in which GFP is fused in frame to the fourth exon of *dyf-5* (*dyf-5ex4::gfp*) (Figure 4.3a). The full length *dyf-5::gfp* construct showed weak GFP expression in many neurons in the head, including amphid and labial sensory neurons (Fig. 2 a) and three pairs of neurons in the tail, including the phasmid sensory neurons. In addition, we observed expression in many



**Figure 4.2: *dyf-5::gfp* expression pattern.** (A) Expression of *dyf-5::gfp* in the dendrites and cell bodies of many neurons, including amphid sensory neurons in the head. (B) Strong *dyf-5::gfp* expression in many neurons in the male tail. Cell bodies are indicated with arrowheads, expression in the sensory rays is indicated with arrows, autofluorescence of the spicule and the posterior end of the fan is indicated with asterisks. (C) Strong *dyf-5::gfp* expression in the tip of the head in dendrites and transition zone (tz) and weakly in cilia. Scale bars represent 20  $\mu\text{m}$  (A and B) or 10  $\mu\text{m}$  (C), anterior is to the left.

cells in the male tail (Figure 4.3b). This DYF-5::GFP fusion could be detected uniformly in axons, cell bodies and dendrites. In addition, we observed strong fluorescence at the transition zones, which connect the cilia with the dendrites, and weak fluorescence uniformly in the cilia (Figure 4.3c). The *dyf-5ex4::gfp* fusion construct essentially showed the same *dyf-5* expression pattern, albeit stronger and more restricted to the cell bodies. In addition, DYF-5ex4::GFP could be detected in the CAN cells, neurons associated with the excretory canal (White et al., 1986) and in a pair of neurons in the posterior lateral ganglion (results not shown). Expression of many ciliary genes is regulated by the DAF-19 transcription factor (Swoboda et al., 2000). This regulation occurs through an X-box promoter element. The *dyf-5* promoter region contains a predicted X-box promoter element, 193 bp upstream of the SL1 trans splice site and 271 bp upstream of the translational start (Figure 4.3a).

Previous genomic analyses have identified many genes that contain X-box elements, including M04C9.5 (Chen et al., 2006; Blacque et al., 2005; Efimenko et al., 2005). Chen et al. have confirmed that expression of *dyf-5* is indeed regulated by *daf-19* (Chen et al., 2006).



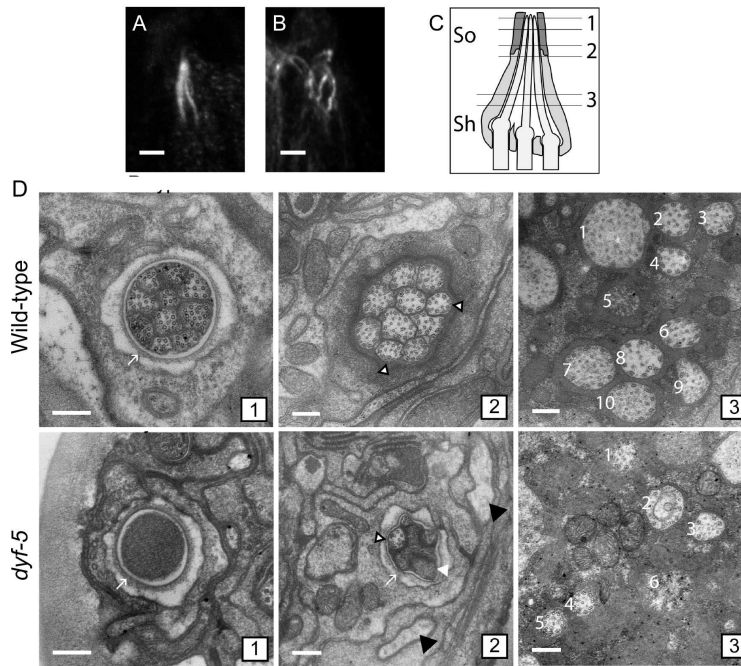


**Figure 4.3: Mutation of *dyf-5* affects cilia length and morphology.** (A, B) Anti-tubulin immunostaining of (A) wild-type and (B) *dyf-5(ok1177)* animals. Scale bar represents 2 μm, anterior is up. (C) Schematic representation of three of the amphid channel cilia embedded in the sheath cell (sh) and the socket cell (so). The approximate positions of the EM cross-sections in D have been indicated. (D) EM cross section of a (top panels 1-3) wild-type and (bottom panels 1-3) *dyf-5(lf)* animal. (1) Sections through the socket cell (arrow), showing the distal segments of the ten channel cilia which contain singlet microtubules in the wild-type animal and the channel filled with electron dense material in the *dyf-5(lf)* animal. (2) Ten channel cilia embedded in the sheath cell are present in the wild-type animal. Most cilia contain doublet microtubules, some contain singlets (open arrowheads). Section of a *dyf-5(lf)* animal through the socket cell (arrow), showing some cilia with singlet microtubules (open arrowhead) and some cilia filled with electron dense material (white arrowhead). Black arrowheads indicate oblique sections through cilia. (3) Sections through the middle segments close to the base of the cilia. In the wild-type animal ten channel cilia (numbered 1-10) embedded in the sheath cell are present, containing doublet microtubules. In the *dyf-5(lf)* animal six channel cilia (1-6) embedded in the sheath cell could be identified, containing doublet microtubules. The cilia are more dispersed than in wild-type animals. In all panels, scale bar represents 200 nm.

**Mutation of *dyf-5* affects cilia morphology and length.** We wondered whether mutations in *dyf-5* affect cilia morphology and length, as in *Chlamydomonas* and

*Leishmania* (Bengs et al., 2005; Berman et al., 2003). Visualization of the microtubular axonemes of the cilia using anti-tubulin antibodies revealed that the cilia of *dyf-5(lf)* animals were not properly aligned into the amphid pore. The cilia were more dispersed, misdirected and sometimes turned back towards the transition zone (Figure 4.3b). In contrast, in the two *dyf-5XS* strains, *gJls828* and *gJls831*, we observed very weak anti-tubulin staining and only very short or no cilia structures (results not shown).

To study the morphological defects in more detail, we examined cross-sections of wild-type and *dyf-5(lf)* animals with electron microscopy. In the wild-type animal the ten cilia were enveloped by the sheath cell, and projected to the tip of the animal, where the cilia ended in a channel lined by the socket cell (Figure 4.3c and d; Perkins et al., 1986; Ward et al., 1975; Ware et al., 1975). The microtubular axoneme in the middle segment consisted of a ring of nine doublet microtubules, and up to six singlet microtubules (Figure 4.3d; Perkins et al., 1986; Ward et al., 1975; Ware et al., 1975). In the tip of the cilium the nine microtubules were all singlets (Figure 4.3d; Perkins et al., 1986; Ward et al., 1975; Ware et al., 1975). In the *dyf-5(lf)* mutant the morphology of the cilia was severely affected. In the most proximal section the cilia were more dispersed, consistent with the anti-tubulin data (Figure 4.3d). We could not identify all ten cilia, perhaps because of their dispersion and their altered morphology. In the cilia, the microtubular axoneme consisted of an array of singlet and doublet microtubules (Figure 4.3d). More distally, we observed some cilia entering into the channel, indicating that the socket cell is present and open. At this level the microtubules were singlets. Not all cilia entered the channel. Next to the socket cell we observed two structures resembling oblique sections through cilia, which could be misdirected channel cilia (Figure 4.3d). In the most distal sections the channel was completely filled with electron dense matrix material, probably accumulated proteins (Figure 4.3d).

To study the effect of *dyf-5(lf)* on the morphology of individual amphid cilia we examined transgenic animals expressing *gpa-4::gfp* or *gpa-15::gfp*. The  $G\alpha$  subunits *gpa-4* and *gpa-15* are expressed in only the ASI amphid neurons or in the ADL, ASH and ASK neurons, respectively (Jansen et al., 1999) and localized along the length of the cilia in wild-type animals (Figure 4.3a and j). Again, we observed that the cilia were more dispersed and misdirected. In addition, the cilia of *dyf-5(lf)* animals were significantly longer than cilia of wild-type animals (Figure 4.3b and k and Table 1). In contrast, in *dyf-5XS* animals we observed very short cilia or, in 27% of the animals, no discernible cilia at all (Figure 4.3c, l and Table 4.3).

Genotype	<i>gpa-4::gfp</i>		<i>gpa-15::gfp</i>	
	Length $\mu\text{m}$	n	Length $\mu\text{m}$	n
wild type	4.94 $\pm$ 0.57	60	6.83 $\pm$ 0.40	40
<i>dyf-5</i>	5.66 $\pm$ 0.97 <sup>1</sup>	83	8.62 $\pm$ 0.86 <sup>1</sup>	30
<i>dyf-5XS(gjls828)</i>	1.89 $\pm$ 0.49 <sup>1</sup>	18	ND	
<i>dyf-5XS(gjls831)</i>	2.13 $\pm$ 0.66 <sup>1</sup>	15	4.56 $\pm$ 0.72 <sup>1</sup>	28
<i>kap-1</i>	4.78 $\pm$ 0.24	23	6.79 $\pm$ 0.40	31
<i>dyf-5; kap-1</i>	5.48 $\pm$ 1.11 <sup>2,3</sup>	54	8.32 $\pm$ 1.23 <sup>1,3</sup>	50
<i>osm-3</i>	3.77 $\pm$ 0.32 <sup>1</sup>	24	4.89 $\pm$ 0.47 <sup>1</sup>	41
<i>dyf-5; osm-3</i>	6.48 $\pm$ 0.86 <sup>1,4,6</sup>	43	8.70 $\pm$ 1.35 <sup>1,6</sup>	47
<i>kap-1; osm-3</i>	1.48 $\pm$ 0.31 <sup>1,3,6</sup>	26	ND	
<i>dyf-5; kap-1; osm-3</i>	1.86 $\pm$ 0.39 <sup>1,3,4,6</sup>	23	ND	
<i>dyf-5; gjEx312</i>	4.96 $\pm$ 0.97 <sup>5</sup>	24	ND	
<i>dyf-5; gjEx324</i>	4.83 $\pm$ 0.83 <sup>4</sup>	22	ND	

**Table 4.1: Cilia lengths of *dyf-5* mutant animals.** Indicated are the average lengths of GPA-4::GFP and GPA-15::GFP staining cilia  $\pm$  the standard deviation (in  $\mu\text{m}$ ), the significance tested using a 2-tailed paired T-test compared to wild type animals (1:  $P < 0.001$ , 2:  $p < 0.005$ ), *kap-1* (3:  $p < 0.001$ ), *dyf-5* (4:  $p < 0.001$ ; 5:  $p < 0.005$ ) and *osm-3* (6:  $p < 0.001$ ), and the number of animals (n). The *dyf-5XS* cilia lengths indicated represent the lengths of the cilia where cilia could be seen; in an additional 27% no cilia could be detected. *gjEx312* and *gjEx324* are two independent *gpa-4::dyf-5::gfp* strains that express *dyf-5* only in the ASI neurons.

The above described approaches all showed similar effects of *dyf-5(lf)* on the length and morphology of the cilia. To determine if *dyf-5* regulates cilia length in a cell autonomous fashion, we expressed the full length *dyf-5::gfp* construct specifically in the ASI neurons of *dyf-5(lf)* animals and determined the lengths of the ASI cilia of these animals using *gpa-4::gfp*. In two of the five transgenic lines that expressed *dyf-5::gfp* specifically in the ASI neurons, the cilia were significantly shortened, to approximately wild-type length (Table 4.3). These results indicate that *dyf-5* functions cell autonomously to regulate cilia length.

**Kinesin II localizes to the distal segments in *dyf-5(lf)* animals.** Next, we wondered whether elongation of the cilia in *dyf-5(lf)* animals requires the function of either of the two anterograde motors, kinesin II or OSM-3. To this end, we generated *dyf-5(lf); kap-1* and *dyf-5(lf); osm-3* double mutants. *osm-3* animals lack the cilia distal segments, because OSM-3 is essential for transport in these segments (Snow et al., 2004; Figure 4.3f and o). *kap-1* animals have lost an essential component of the heterotrimeric kinesin II complex, but have full length cilia since OSM-3 can mediate IFT by itself (Snow et al., 2004; Figure 4.3d and m).

Both *dyf-5(lf); osm-3* and *dyf-5(lf); kap-1* double mutant animals were dye filling

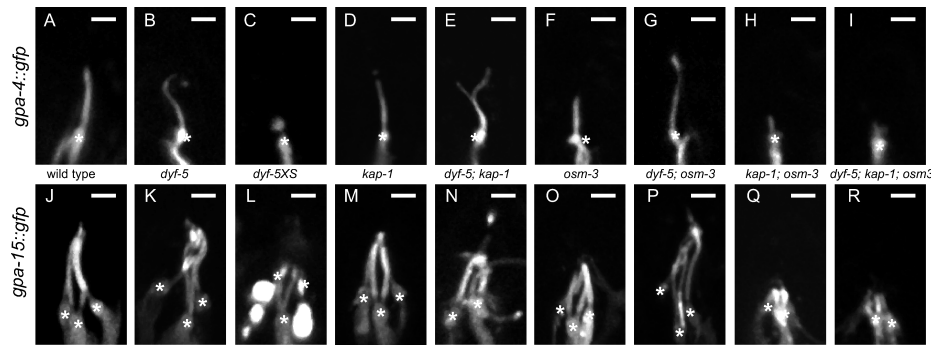


**Figure 4.4: Figure 4. Mutation of *dyf-5* affects cilia length.** Visualization of (A-I) ASI cilia structures using *gpa-4::gfp* and (J-R) ADL, ASH and ASK cilia morphology using *gpa-15::gfp* in (A, J) wild-type, (B, K) *dyf-5(ok1177)*, (C, L) *dyf-5XS(gjls828)*, (D, M) *kap-1(ok676)*, (E, N) *dyf-5; kap-1*, (F, O) *osm-3(p802)*, (G, P) *dyf-5; osm-3*, (H, Q) *kap-1; osm-3*, and (I, R) *dyf-5; kap-1; osm-3* animals. In *dyf-5*, *dyf-5; kap-1* and *dyf-5; osm-3* animals cilia were elongated and misdirected. In *dyf-5XS* animals cilia were very short or could not be detected. We observed branching of the cilia in 30% of *dyf-5; kap-1* animals. Transition zones are indicated with asterisks, scale bar represents 2  $\mu$ m, anterior is up.

defective (results not shown). Anti-tubulin antibody staining and *gpa-4::gfp* and *gpa-15::gfp* fluorescence showed that the cilia of both double mutants were as long as or even longer than the *dyf-5(lf)* cilia (Figure 4.3e, g, n and p and Table 4.3). This suggests that both motors can transport cargo along the full length of the cilia and thus that DYF-5 is required to restrict kinesin II to the middle segments. In addition, these results suggest that the elongation of the cilia in *dyf-5(lf)* does not solely depend on either of the two kinesin-2 motors. Interestingly, we observed an additional morphological defect of the cilia of *dyf-5(lf); kap-1* animals: in 30% of the animals the cilia were branched (Fig. 4 e), a defect that was observed in only 7% of *dyf-5(lf)* animals and never in wild-type or *kap-1* animals. In *dyf-5(lf); osm-3* animals branching was observed in only one animal of 33 analyzed. These results suggest that DYF-5 and kinesin II both play a role in cilium morphogenesis.

To determine if transport in the cilia of *dyf-5(lf)* animals can be mediated by a kinesin II and OSM-3 independent mechanism, we generated *dyf-5(lf); kap-1; osm-3* triple mutant animals. Visualization of the cilia using anti-tubulin antibodies and *gpa-4::gfp* and *gpa-15::gfp* showed that these triple mutants have no or only very short cilia, similar to *kap-1; osm-3* animals (Figure 4.3h, i, q and r and Table 4.3), indicating that either kinesin II or OSM-3 is required for

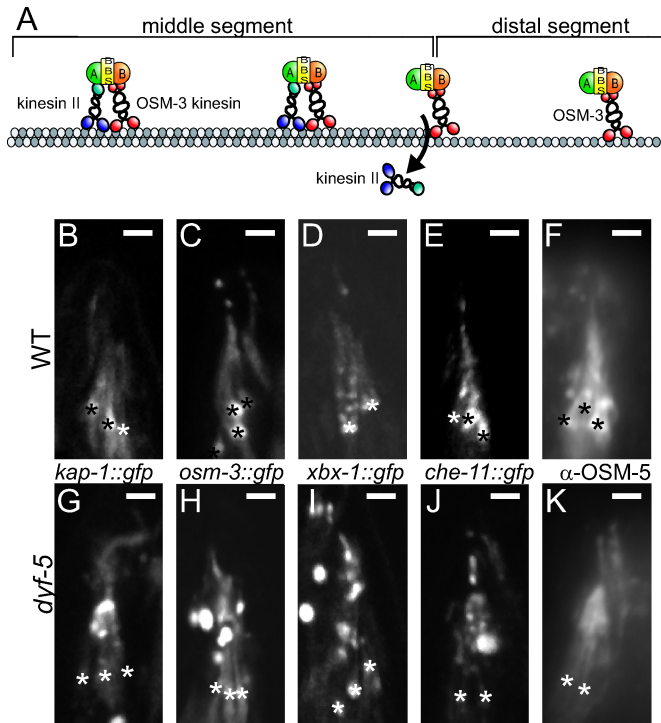


**Figure 4.5: DYF-5 is required to restrict kinesin II to cilia middle segments** (A) Model of anterograde IFT in *C. elegans* (based on model in ref. Ou et al., 2005). In the cilia middle segments cargo is transported by IFT particles that contain OSM-3 kinesin-2, kinesin II, complex A (A) and B (B) proteins and the BBS-7 and BBS-8 proteins (BBS). At the end of the middle segments kinesin II is probably released from the IFT particle. Transport in the distal segment is mediated by OSM-3. (B-K) Visualization of (B, G) OSM-3::GFP, (C, H) KAP-1::GFP, (D, I) XBX-1::GFP, (E, J) CHE-11::GFP and (F, K) OSM-5 in (B-F) wild-type and (G-K) *dyf-5(ok1170)* animals. All IFT proteins, including KAP-1::GFP, could be detected along the length of the cilia of *dyf-5* animals. We observed accumulation of all IFT proteins, approximately halfway the cilia, and in the distal segment. Since these GFP constructs are expressed in all channel cilia, it was impossible to determine the length of a specific cilium. Transition zones are indicated with asterisks, scale bar represents 2  $\mu$ m, anterior is up.

ciliogenesis.

Since both kinesin-2 motors are individually dispensable for cilia elongation in *dyf-5(lf)* animals, we analyzed the localization of OSM-3::GFP and KAP-1::GFP fusion constructs in *dyf-5(lf)* animals (Snow et al., 2004). In wild-type animals,

OSM-3::GFP could be detected along the length of the cilia, while KAP-1::GFP could only be detected in the cilia middle segment (Figure 4.3a, b and c), as reported previously (Snow et al., 2004). In *dyf-5(lf)* animals, OSM-3::GFP could be detected along the full length of the cilia. Additionally, we observed strong accumulation of OSM-3::GFP starting approximately two to three  $\mu\text{m}$  from the transition zone and in the distal region of the cilia (Figure 4.3h). Also KAP-1::GFP fluorescence could be seen along the full length of the cilia of *dyf-5(lf)* animals (Figure 4.3g), confirming that DYF-5 is required to restrict KAP-1::GFP to the middle segments. We also observed accumulation of KAP-1::GFP halfway of the cilia. *dyf-5XS* animals showed both OSM-3::GFP and KAP-1::GFP fluorescence at the transition zones, but not or only very weakly in the cilia of these animals (results not shown), confirming that *dyf-5* overexpression blocks cilia assembly.

To determine if the localization of other IFT proteins was affected we used a *che-11::gfp* fusion construct to visualize this complex A IFT protein (Qin et al., 2001), a *che-13::gfp* fusion construct and anti-OSM-5 antibodies to visualize these two complex B proteins (Qin et al., 2001; Haycraft et al., 2001; Haycraft et al., 2003), and *xbx-1::gfp* to visualize the dynein complex (Schafer et al., 2005). All these IFT proteins could be detected along the length of the cilia of *dyf-5(lf)* animals and they all showed accumulation starting approximately half way the cilia and into the distal segments (Fig. 5 d-f and i-k and results not shown). Also *dyf-5(lf); kap-1* and *dyf-5(lf); osm-3* double mutant animals showed accumulation of CHE-11 and OSM-5 in the cilia (results not shown), suggesting that these effects of *dyf-5(lf)* do not depend on either kinesin II or OSM-3.

***dyf-5(lf)* separates the OSM-3 motor from IFT particles** Since DYF-5 is required to restrict kinesin II to the cilia middle segments, we wondered whether *dyf-5(lf)* affects the transport rates of the two kinesin-2 motors. In the middle segments of wild-type animals, kinesin II and OSM-3 traveled jointly at 0.7  $\mu\text{m/s}$  (Table 2). In the absence of kinesin II OSM-3 moved faster (1.15  $\mu\text{m/s}$ ) and in the absence of OSM-3 kinesin II moved slower (0.5  $\mu\text{m/s}$ ; Table 2). In the distal segments, only OSM-3 is found, moving at a rate of 1.14  $\mu\text{m/s}$ . These speeds are in agreement with previous reports (Snow et al., 2004). Examples of live imaging of CHE-11::GFP in wild-type animals and corresponding kymographs are given in Figure 4.5.

We found that in the middle segments of *dyf-5(lf)* animals kinesin II traveled at a rate of 0.5  $\mu\text{m/s}$  and OSM-3 traveled at 0.59  $\mu\text{m/s}$  (Table 4.3). We found



IFT particle	genotype	Middle Segment		Distal Segment	
		speed $\mu\text{m/s}$	n	speed $\mu\text{m/s}$	n
KAP-1::GFP	wild type	0.70 $\pm$ 0.14	189		
	<i>osm-3</i>	0.49 $\pm$ 0.10 <sup>1</sup>	91		
	<i>dyf-5</i>	0.50 $\pm$ 0.12 <sup>1</sup>	110	0.51 $\pm$ 0.16	56
OSM-3::GFP	wild type	0.70 $\pm$ 0.19	117	1.14 $\pm$ 0.23	43
	<i>kap-1</i>	1.17 $\pm$ 0.24 <sup>1</sup>	124	1.23 $\pm$ 0.28	42
	<i>dyf-5</i>	0.59 $\pm$ 0.15 <sup>1,2</sup>	210	0.59 $\pm$ 0.17 <sup>1,3</sup>	84
	<i>dyf-5; kap-1</i>	0.58 $\pm$ 0.15 <sup>1</sup>	91		
CHE-11::GFP	wild type	0.69 $\pm$ 0.20	118	1.20 $\pm$ 0.27	49
	<i>osm-3</i>	0.50 $\pm$ 0.09 <sup>1</sup>	90		
	<i>dyf-5</i>	0.49 $\pm$ 0.11 <sup>1</sup>	170	0.49 $\pm$ 0.11 <sup>1</sup>	45
	<i>dyf-5; kap-1</i>	0.60 $\pm$ 0.16 <sup>1,4</sup>	118	0.61 $\pm$ 0.12 <sup>1,4</sup>	38
OSM-5::GFP	<i>dyf-5; osm-3</i>	0.49 $\pm$ 0.12 <sup>1</sup>	109	0.49 $\pm$ 0.11 <sup>1</sup>	31
	wild type	0.70 $\pm$ 0.17	136	1.13 $\pm$ 0.29	66
	<i>osm-3</i>	0.50 $\pm$ 0.11 <sup>1</sup>	88		
	<i>dyf-5</i>	0.51 $\pm$ 0.11 <sup>1</sup>	151	0.50 $\pm$ 0.11 <sup>1</sup>	42
	<i>dyf-5; kap-1</i>	0.59 $\pm$ 0.19 <sup>1,4</sup>	117	0.58 $\pm$ 0.12 <sup>1,4</sup>	45
XBX-1::GFP	<i>dyf-5; osm-3</i>	0.51 $\pm$ 0.13 <sup>1</sup>	103		
	wild type	0.70 $\pm$ 0.17	141	1.11 $\pm$ 0.19	55
	<i>dyf-5</i>	0.50 $\pm$ 0.11 <sup>1</sup>	139	0.47 $\pm$ 0.08 <sup>1</sup>	42

Table 4.2: ***dyf-5* separates the OSM-3 motor from IFT particles.** Indicated are average speeds  $\pm$  the standard deviation (in  $\mu\text{m/s}$ ) and the number of tracks (n). Asterisks indicated significant differences when comparing speeds of: 1 IFT protein in a mutant background to the same IFT protein in wild type ( $P < 0.001$ ), 2 & 3 OSM-3::GFP to the other IFT proteins in *dyf-5(lf)* animals (2  $p < 0.001$ ; 3  $p < 0.01$ ), and 4 CHE-11 and OSM-5 in *dyf-5; kap-1* to their speeds in *dyf-5* and *dyf-5; osm-3* animals. The speeds of all IFT proteins in *dyf-5* and *dyf-5; osm-3* animals, except OSM-3::GFP, were not significantly different from the speeds in *osm-3* animals. Speeds in *dyf-5; kap-1* animals were not significantly different from the speed of OSM-3::GFP in *dyf-5* animals.

very similar speeds in the distal segments, although imaging was very difficult in these segments due to the twisted appearance of the cilia, often only partly in focus, and accumulation of the GFP fusion proteins. These results suggest that kinesin II and OSM-3 move at least partly separately in the cilia. Ou et al. have recently described two mutants that cause separation of kinesin II and OSM-3 mediated transport: *osm-12/bbs-7* and *bbs-8* (Ou et al., 2005). In these animals, kinesin II transports the complex A proteins and OSM-3 the complex B proteins. To test if a similar separation occurs in *dyf-5(lf)* animals, we determined the anterograde speeds of the complex A protein CHE-11, the complex B protein OSM-5 and the dynein subunit XBX-1. Interestingly, all these proteins moved at 0.5  $\mu\text{m/s}$  in the middle and distal segments of the cilia of *dyf-5(lf)*

animals (Table 4.3), a rate very similar to kinesin II.

The difference in transport rates of kinesin II, CHE-11, OSM-5 and XBX-1 on the one hand and OSM-3 on the other hand, suggests that OSM-3 is no longer part of the joint IFT complex in *dyf-5(lf)* animals. However, the speed of OSM-3::GFP observed in *dyf-5(lf)* animals is lower than that of free traveling OSM-3 (Table 4.3; Snow et al., 2004; Ou et al., 2005). This effect can be explained by a reduction of the motility of OSM-3 itself. Alternatively, OSM-3 containing particles may be predominantly transported by the slower moving kinesin II, thereby reducing their average speed. To test the latter possibility, we measured transport rates of OSM-3::GFP, CHE-11::GFP and OSM-5::GFP in *dyf-5(lf); kap-1* and *dyf-5(lf); osm-3* double mutant animals. We found that in *dyf-5(lf); kap-1* animals OSM-3, CHE-11 and OSM-5 moved at 0.59 to 0.60  $\mu\text{m/s}$  (Table 4.3), while in *dyf-5(lf); osm-3* animals CHE-11 and OSM-5 moved at 0.5  $\mu\text{m/s}$ . These findings suggest that the speeds of OSM-3 and kinesin II in *dyf-5(lf)* animals are independent of each other and that these motors indeed move separately. Therefore, we favor the hypothesis that *dyf-5(lf)* reduces the speed of OSM-3 itself. In addition, these results confirm that in the absence of kinesin II IFT still can be mediated by OSM-3.

## 4.4 Discussion

In this paper we identify the gene mutated in *dyf-5* animals. DYF-5 encodes a putative MAP kinase that regulates the length of sensory cilia in *C. elegans*, similar to what has been reported for DYF-5 homologues in *Chlamydomonas*, LF4, and *Leishmania*, LmxMPK9 (Bengs et al., 2005; Berman et al., 2003): *dyf-5* loss-of-function results in cilia elongation, while overexpression results in shorter cilia. In addition, fluorescence and electron microscopy showed that in the absence of DYF-5 the cilia are more dispersed and that many cilia are not properly aligned into the amphid channel and sometimes turn back to the base, although some cilia do enter the channel.

Within the cilia we find three defects. First, six components of the IFT machinery are not properly localized in *dyf-5(lf)* animals. Interestingly, heterotrimeric kinesin II localizes to the distal segments of *dyf-5(lf)* animals. This is an intriguing finding, since this motor cannot enter this segment of the cilia in wild-type animals. In addition, all six IFT proteins tested accumulate approximately halfway and in the distal regions of the cilia, which correlates with the accumulation of protein seen in these regions using EM. Second, in *dyf-5(lf)* animals, OSM-3 containing particles travel at a different speed than particles containing



either kinesin II, complex A and B proteins or dynein, suggesting that OSM-3 travels separately. In addition, this suggests that DYF-5 functions in a different process than the BBS-7 and BBS-8 proteins, mutations of which result in separation of complex A and B particles (Ou et al., 2005). Interestingly, OSM-3 can still mediate IFT in *dyf-5(lf)* animals, but only in the absence of functional kinesin II. This suggests that inactivation of *dyf-5* does not fully block docking of OSM-3 onto IFT particles, but rather changes the affinity between either of the two kinesins and the IFT particles. Third, the speed of OSM-3 in *dyf-5(lf)* animals was markedly reduced, from 1.2  $\mu\text{m/s}$  to 0.6  $\mu\text{m/s}$ . Our results suggest that this reduced speed is not a result of a combined speed of kinesin II and OSM-3, but rather an effect on OSM-3 itself.

But how does mutation of *dyf-5* mediate these three effects on IFT and how do these effects correlate with cilia morphology and length? A possible explanation for the effects on the localization of IFT proteins is that DYF-5 functions at sites where the IFT particles switch between different motor complexes, such as the transition from the middle to the distal segment and at the distal tip. Failure in removing kinesin II from IFT particles would explain its entry into the distal segments in *dyf-5(lf)* animals. In addition, a failure in switching from antero- to retrograde transport would explain the aggregation of IFT proteins in the distal segments. However, such a model does not provide an explanation for the effects that *dyf-5(lf)* has on the speed of OSM-3.

The motility of kinesins can be modulated at several levels. For example, the processivity of these motors, and hence their speed, may be reduced by interference with the properties of the kinesin itself, such as ATP binding and hydrolysis, or allosteric inhibition of directional movement (Carter & Cross, 2005; Kwok et al., 2006). Also posttranslational modifications of the microtubules on which the kinesins walk have been reported to affect the motility of kinesins (Reed et al., 2006). Perhaps DYF-5 functions in a similar manner, changing the affinity of both kinesins for its normal targets, either the IFT particles, or the microtubules, resulting in the effects we observe. Interestingly, the entry of kinesin II in the distal segments or the presence of unattached OSM-3 by themselves do not cause the elongation of the cilia of *dyf-5(lf)* animals, since removal of kinesin II or OSM-3 in *dyf-5(lf); kap-1* or *dyf-5(lf); osm-3* animals did not suppress cilia elongation. It will be very interesting to further unravel the mechanisms by which DYF-5 regulates IFT, cilia morphology and length.

The DYF-5 kinase is conserved in evolution. Using BLAST searches we have identified putative DYF-5 homologues in various organisms that have cilia: in mammals, *Drosophila*, *Chlamydomonas*, *Leishmania* and *Trypanosoma* (results not shown). Interestingly, we could not find an obvious homologue in *Plasmodium*,

which has cilia, but the cilia are assembled in the cytoplasm in a process that does not require IFT (Witman et al., 2003). Mammals have three putative DYF-5 homologues that form a small subfamily of MAP kinases, the MAK kinases (Matsushime et al., 1990; Togawa et al., 2000; Yang et al., 2002; Miyata et al., 1999). The functions of these MAK, MOK and ICK/MRK proteins remain to be determined. However, given the evolutionary conservation of the IFT machinery, the DYF-5/MAK kinases and their functions in *C. elegans*, *Chlamydomonas* and *Leishmania*, we expect that one or more of the mammalian MAK kinases play a similar role as DYF-5 in the control of cilia length and the docking and undocking of kinesin-2 motors from IFT particles.

## 4.5 Materials and Methods

**Strains and constructs.** All strains were grown at 20°C. Strains used: Bristol N2 (wild type), *dyf-5(mn400)I*, *dyf-5(ok1170)I*, *dyf-5(ok1177)I*, *kap-1(ok676)III*, *osm-3(p802)IV*, *dyf-5XS(gjls828)* and *dyf-5XS(gjls831)*. *dyf-5(ok1170)* contains a 2058 bp deletion (deletion starts with 5' ATTCTGAAAATCCGTTCAAA, and ends with 5' TTTCTATTTCTTTCAATTTT) and a 583 bp insertion originating from the X chromosome; *dyf-5(ok1177)* contains a 1720 bp deletion (deletion starts with 5' GTTGTACAACAAATAAATAA, and ends with 5' ATTATTATTTCAGTAAAATG). *dyf-5* overexpressing animals (*dyf-5XS*) were generated by injecting 75 ng/μl of a 7.5 kb long range PCR fragment (primers: 5' ATTTCTCCTGATAACCTTCCATTTC, 5' CCACTTTCTTCCCATTTTCTTCTCCC). GFP reporters used: *gpa-15::gfp* (Jansen et al., 1999), *osm-3::gfp* and *kap-1::gfp* (Snow et al., 2004), *che-13::gfp* (Haycraft et al., 2003), *che-11::gfp* (Qin et al., 2001), *osm-5::gfp* (Haycraft et al., 2001; Qin et al., 2001) and *xbx-1::gfp* (Schafer et al., 2003). All GFP reporters were crossed into the *dyf-5(lf)* and *dyf-5XS* backgrounds. *dyf-5::gfp* reporter constructs were generated using a fusion PCR protocol (Hobert, 2002). *dyf-5ex4::gfp* contained 3 kb upstream region and the first four exons fused with GFP (primers: 5' ATTTCTCCTGATAACCTTCATTTC, 5' tggccaatcccggggatcctccgatcagatcttcattagctc). The full length GFP fusion was generated using the same forward primer and reverse primer 5' TGGCCAATCCCGGGGATCCTCACCACCCCAGAATATTGGGAAGAAAGGC. These fragments were fused with a PCR fragment containing the GFP open reading frame and the *unc-54* 3' UTR generated using plasmid pPD95.75 as a template (a gift from A. Fire, primers 5' GAGGATCCCCGGGATTGGCCA and 5' GCCGACTAGTAGGAAACAGT).

**Cloning and characterization of *dyf-5*.** *dyf-5(mn400)* or *dyf-5(ok1170)* mutant animals were injected with 5 ng/ $\mu$ l of the 7.5 kb long range PCR fragment containing M04C9.5, or the full length *dyf-5::GFP* construct. Rescue was analyzed using dye filling (Hedgecock et al., 1985). We performed RT-PCR to characterize the open reading frame of *dyf-5*.

**Microscopy.** The localization of GFP tagged proteins and cilia lengths were determined using a Zeiss confocal microscope CLSM510 or a Zeiss Imager Z1 microscope. Dye filling was performed using DiI (Molecular probes) (Hedgecock et al., 1985). Immunofluorescence using monoclonal rat antibody against tubulin (Abcam ab6160) and monoclonal mouse antibody against OSM-5 (a kind gift from B. Yoder and C. Haycraft) was performed as described (Finney & Ruvkun, 1990). Secondary antibodies were alexa-488-conjugated (Molecular Probes). Anti-tubulin antibodies stain many structures of *C. elegans*, including the microtubular axonemes of the simple cilia of the gustatory and nociceptive amphid neurons. We observed only weak staining of the wing-like cilia of the olfactory neurons.

**Electron microscopy.** Animals were rinsed off with M9 buffer from culture plates and immediately fixed in 3% glutaraldehyde for 16 hours, followed by post-fixation in 1% osmiumtetroxide for 2 hours. Subsequently, animals were orientated in special molds and embedded in Epon according to standard procedures. Ultrathin sections were cut with a Reichert ultramicrotome and sections were stained with uranylacetate and leadnitrate. Finally, sections were examined with a Philips CM100 at 80 kV.

**Life imaging of IFT particles.** Live imaging of the GFP tagged IFT particles was carried out as described previously (Snow et al., 2004). Images were acquired on a Zeiss LSM 510 confocal microscope. Animals were mounted on agarose pads and anaesthetized with 10 mM levamisole. Kymographs were generated in ImageJ with the Kymograph plugin, written by J. Rietdorf.

**Acknowledgments.** We thank E. Severijnen, T. de Vries Lentsch and R. Kopenol for technical assistance, M. Barr, A. Fire, C. Haycraft, B. Yoder, G. Ou, J. Scholey, the Caenorhabditis Genetics Center and the *C. elegans* Gene Knockout Consortium for *C. elegans* strains and constructs, M. Leroux for discussions and the members of the Jansen lab for critical reading of the manuscript. This work

was financially supported by the Center for Biomedical Genetics and the PKD Foundation. GJ is a Royal Netherlands Academy of Sciences fellow.

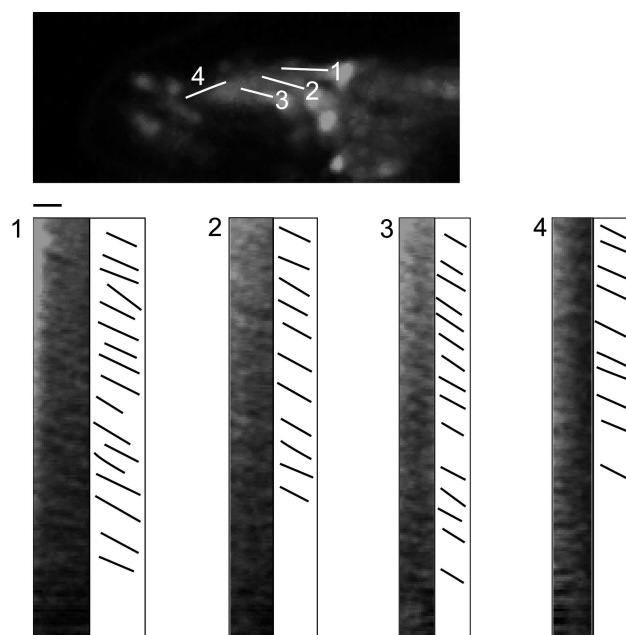


**Figure 4.6: CHE-11::GFP motility in the cilia of wild type animals.** Expression of CHE-11::GFP in the cilia of a wild type animal (see SI movie 1). Motility of CHE-11::GFP can be seen in middle segments (1-3) and a distal segment (4). Panels 1-4 show kymographs with corresponding cartoons of selected CHE-11::GFP particle trajectories along middle segments 1-3 and the distal segment 4. Kymograph Y-axis is 48 s, horizontal bar is 1  $\mu\text{m}$ .

*Quid custodiet ipsos custodes?*

Juvenalis

# 5

## Environmental cues and G protein signalling regulate intraflagellar transport and cilia length

Jan Burghoorn<sup>1</sup>, Martijn P.J. Dekkers<sup>1</sup>, Suzanne Rademakers<sup>1</sup>, Ton de Jong<sup>2</sup>, Rob Willemsen<sup>3</sup>, Peter Swoboda<sup>4</sup> and Gert Jansen<sup>1</sup>

Departments of <sup>1</sup> Cell Biology and Genetics and Center for Biomedical Genetics, <sup>2</sup> Pathology and <sup>3</sup> Clinical Genetics, Erasmus MC, P.O. Box 2040, 3000 CA Rotterdam, The Netherlands <sup>4</sup> Karolinska Institute, Department of Biosciences and Nutrition, Södertörn University College, School of Life Sciences, S14189 Huddinge, Sweden

## 5.1 Abstract

Cilia are cellular protrusions that function in several distinct processes, including in the regulation of signalling in cells. Despite increasing evidence that the length of cilia is dynamically regulated, depending on developmental stage or by external cues, the molecular mechanisms behind this are unknown. In this study we demonstrate that expression of a dominant active  $G\alpha$  protein, *gpa-3QL*, affects the morphology of amphid sensory cilia in *C. elegans* in a dose dependent and reversible way. The cilia are shorter and sometimes displaced posteriorly. Conversely, *gpa-3 loss-of-function (lf)* animals show no structural defects of the cilia. Components of the intra flagellar transport (IFT) complex localize normally in the cilia in *gpa-3(lf)* and in *gpa-3QL* animals. However, IFT is perturbed in both mutants: kinesin II speed is reduced and OSM-3 kinesin speed increased, while complex A/B proteins travel at approximately wild-type speeds. Previous studies have shown that GPA-3 functions in the developmental switch that regulates dauer formation. Interestingly, exposure to dauer pheromone induced alterations in cilia length, depending on GPA-3 and kinesin II, and affected OSM-3 speed, similar to mutation of *gpa-3*. We propose that environmental cues signal via G-proteins to regulate the constitution of IFT particles in the cilia, thereby altering its length and structure.

## 5.2 Introduction

All cells depend for their survival on the ability to perceive cues from their environment. Lately, it has become apparent that primary cilia play essential roles in perception of the environment (Pan et al., 2005; Pazour and Witman, 2003). For example, defects in cilia in the olfactory epithelium, in the retina and in the hair cells of the ear result in anosmia, blindness and hearing defects. Moreover, cilia in the renal tubules sense the fluid flow and malfunction results in Polycystic Kidney Disease. Many sensory signaling proteins, including receptors, channels and downstream molecules, are localized to cilia, and for some signaling pathways, such as the hedgehog pathway, it has been shown that ciliary localization is essential for signaling (Huangfu et al., 2003). Several observations indicate that mechanisms exist that allow plasticity of cilia. Cilia lengths are well known to be regulated during the cell cycle. In addition, during fertilization in *Chlamydomonas* the flagellar tip is modified and elongated and during *C. elegans* dauer development the structure of the cilia changes (Albert and Riddle, 1983; Mesland et al., 1980). A recent study sug-

gests that the organization of signaling pathways in *Chlamydomonas* flagella is regulated (Wang et al., 2006). However, little is known about the molecular mechanisms that regulate the plasticity of cilia, although it seems likely that these mechanisms involve a specialized transport machinery, called intraflagellar transport (IFT). We study this process in the nematode *Caenorhabditis elegans*. The structural and functional characteristics of the cilia of *C. elegans* are very similar to those in mammals (Pan et al., 2005; Rosenbaum and Witman, 2002; Scholey, 2003). *C. elegans* has 60 ciliated cells (White et al., 1986), including 12 pairs of sensory neurons, the amphid neurons, which it uses to detect environmental cues. A subset of the amphid neurons takes up fluorescent dyes, called dye filling (Perkins et al., 1986). The characterization of dye filling defective (Dyf) mutants has identified many genes that play important roles in IFT. IFT is responsible for bi-directional transport of cargo proteins assembled on IFT particles, along a microtubular axonemal core (Figure 5.3A and B). Kinesin II motors are responsible for anterograde transport from the transition zone, where the axoneme is anchored in the cell, to the tip of the cilium. Cytoplasmic dynein moves the particles back (retrograde). IFT particles can be separated in two complexes, A and B, and consist of at least 18 proteins. There are several indications that IFT transports both structural components of the cilia and signaling molecules (Ou et al., 2005b; Qin et al., 2004; 2005). Structurally, the cilia of *C. elegans* can be divided into a middle segment with nine doublet microtubules and a distal segment with nine singlet microtubules (Perkins et al., 1986). Anterograde transport in the middle segment is mediated by two kinesin complexes, homodimeric OSM-3 kinesin and heterotrimeric kinesin II, encoded by *klp-11*, *klp-20* and *kap-1* (Signor et al. 1999; Snow et al., 2004). Only OSM-3 mediates transport in the distal segments (Snow et al., 2004). Retrograde transport is mediated by a dynein motor complex of which two subunits have been characterized, the dynein heavy chain *che-3* and the dynein light intermediate chain *xbx-1* (Schafer et al., 2003; Signor et al. 1999; Wicks et al., 2000). Several complex A and B proteins have been identified in *C. elegans*, including the complex A proteins *daf-10* and *che-11* (Qin et al., 2001), and the complex B proteins *che-13*, *osm-1* and *osm-5* (Haycraft et al., 2001, 2002; Qin et al., 2001; Signor et al., 1999). In addition, four proteins have been identified with more regulatory roles. Mutation of three of them affects coordination of IFT by kinesin II and OSM-3 kinesin. In *osm-12/bbs-7* and *bbs-8* mutant animals, which lack homologues of the mammalian BBS7 and BBS8 genes (Blacque et al. 2004), complex A and B are no longer transported together, but are transported separately by kinesin II and OSM-3, respectively (Ou et al., 2005b). In *dyf-5* mutants, defective in a conserved MAP kinase, the A/B complexes are trans-

ported by kinesin II, while OSM-3 travels separately, and at a reduced speed (Burghoorn et al., 2007).

The bipartite cilium structure in *C. elegans* could provide a mechanism to regulate the length of the cilia, or even localization of signaling molecules in the two cilia segments, allowing plasticity of sensory signaling during environmental or developmental changes. An important developmental change of *C. elegans* in response to environmental cues is the dauer response. Under harsh environmental conditions such as starvation, high population density, or high temperatures *C. elegans* develops into a dauer larva (Riddle and Albert, 1997). This switch is accompanied by many morphological changes, including structural changes of the cilia (Albert and Riddle, 1983).

Most mutants with defects in the IFT machinery do not form dauers, because they lack the cilia to detect the environmental cues. However, *gpa-3QL* animals, which carry a dominant active sensory G $\alpha$  protein *gpa-3*, are dye filling defective but also constitutively form dauers (Zwaal et al., 1997). Since G-proteins play a key role in relaying environmental signals to intracellular responses, and mutation of *gpa-3* affects both cilia structure and dauer responses, we wondered whether *gpa-3* might play a role in regulating IFT.

Using EM and cilium specific GFP markers, we show that *gpa-3QL* affects the morphology of amphid sensory cilia in *C. elegans* in a dose dependent and reversible way. The cilia are shorter and sometimes displaced posteriorly. Conversely, *gpa-3(lf)* animals show no structural defects of the cilia. Although, the localization of components of the IFT complex is not affected in *gpa-3(lf)* and in *gpa-3QL* animals, IFT is perturbed in these animals: in both mutants kinesin II speed is reduced and OSM-3 kinesin speed increased, while complex A/B proteins travel at approximately wild-type speeds. Interestingly, exposure to dauer pheromone induced alterations in cilia length, depending on GPA-3 and kinesin II, and affected OSM-3 speed, which was very similar to that found in *gpa-3QL* and *gpa-3(lf)*. We propose that environmental cues signal via G-proteins to regulate the constitution of IFT particles in the cilia, thereby altering its length and structure.

### 5.3 Results

**GPA-3QL affects cilia structure.** The sensory G $\alpha$  protein *gpa-3* is expressed in almost all sensory neurons of *C. elegans* and functions in olfaction, nociception and dauer development (Jansen et al., 1999; Lans et al., 2004; Zwaal et al., 1997).



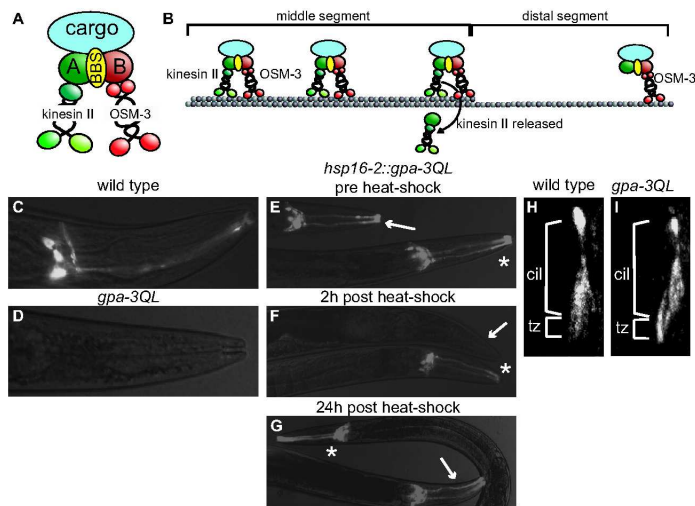


**Figure 5.1: *gpa-3QL* interferes with dye filling.** (A) Model of IFT particle for anterograde transport in *C. elegans* cilia, containing OSM-3 kinesin, kinesin II, complex A (A) and B (B) proteins and the BBS-7 and BBS-8 proteins (BBS) required to stabilize the IFT particle. Based on model presented in Ou et al. (2005a). (B) Model of anterograde IFT in *C. elegans* cilia. In the cilia middle segments cargo is transported by OSM-3 kinesin and kinesin II together. At the end of the middle segments kinesin II is released from the IFT particle, by an unknown mechanism, and transport in the distal segment is mediated by OSM-3. Based on Ou et al. (2005a). (C-D) DiO dye filling of wild type (C) and *gpa-3QL* (D) animals. In wild type animals staining can be seen in a subset of the amphid neurons. In *gpa-3QL* animals no dye filling can be seen. Anterior is to the right. (E-G) DiO dye filling of animals expressing *gpa-3QL* under control of the *hsp16-2* heat-shock promoter (marked with an arrow) before treatment (E), 2 hours after heat shock (F), and 24 hours after heat shock; also non-transgenic animals are shown (marked with \*). The Dyf phenotype can be induced by expression of *gpa-3QL* and is reversible. (H, I) Tubulin immunostaining of the cilia of wild type (H) and *gpa-3QL* animals revealed no obvious structural defects (cil, cilia; tz, transition zone).

The sensory  $G\alpha$  protein *gpa-3* is expressed in almost all sensory neurons of *C. elegans* and functions in olfaction, nociception and dauer development (Jansen et al., 1999; Lans et al., 2004; Zwaal et al., 1997). Animals that express a dominant active form of *gpa-3* (*gpa-3QL*) show a dye filling defective (Dyf) phenotype (Figure 5.3C and D; Zwaal et al., 1997). Most Dyf phenotypes are caused by mutations in components of the IFT machinery, resulting in severe defects of the microtubular axoneme (Perkins et al., 1986; Scholey, 2003). To determine if the Dyf phenotype of *gpa-3QL* animals is caused by a structural defect of the

cilia we visualized the morphology of the cilia using anti-tubulin antibodies. This staining of *gpa-3QL* animals revealed no apparent abnormalities of the cilia (Figure 5.3H and J). Alternatively, Dyf phenotypes can be caused by defects in the sheath cells (Perens and Shaham, 2005; Perkins et al., 1986), which support the cilia of the sensory neurons (White et al., 1986). However, expression of fluorescent proteins in the amphid sheath cells revealed no obvious morphological defects of these cells (results not shown).

To study the morphology in more detail, we examined cross-sections of the cilia of wild-type and *gpa-3(lf)* animals, as well as two independent alleles of *gpa-3QL* with EM. The cilia of wild-type animals looked as previously described (Figure 2). Their ten cilia project to the anterior tip of the animal, and are enveloped by the sheath cells proximally, and by the socket cells distally (Perkins et al., 1986; Ward et al., 1975; Ware et al., 1975). In the middle segment of the cilium, the microtubular axoneme consists of a ring of nine doublet microtubules, whereas in the distal segment the microtubules are singlets. The two *gpa-3QL* strains displayed a variety of morphological defects in the cilia. In the distal segments only four or five cilia could be distinguished, in which only few or even no microtubules could be seen (Figure 5.3). In the middle segments five to nine cilia could be identified, some of which were very small and contained only few microtubules. Closer to the transition zone ten cilia could be distinguished, some of which were very small. In contrast, EM analysis of *gpa-3(lf)* animals did not reveal any defects (results not shown).

**The effects of GPA-3QL are reversible.** The defects in the cilia of *gpa-3QL* animals could be developmental defects, or the result of deregulation of the mechanism that determines cilia length or structure. Therefore, we generated animals that carry a heat shock inducible *gpa-3QL* construct. Induction of *gpa-3QL* expression resulted in a dye filling defect, both in larvae and in adult animals (Figure 5.3E and F). The induced Dyf phenotype was reversible since dye filling was restored 24 hours after heat shock treatment (Figure 5.3G). These results suggest that the effect of *gpa-3QL* is not restricted to a specific developmental time-window, but affects a regulatory mechanism important for cilia function throughout *C. elegans* life.

**GPA-3QL affects the length of cilia.** To determine which neurons were affected, we expressed GFP in several amphid sensory neurons, using promoters that drive expression in a single or a restricted set of cells. The cilia of ASI neurons were visualized with *gpa-4::gfp*. In *gpa-3QL* animals the ASI neurons

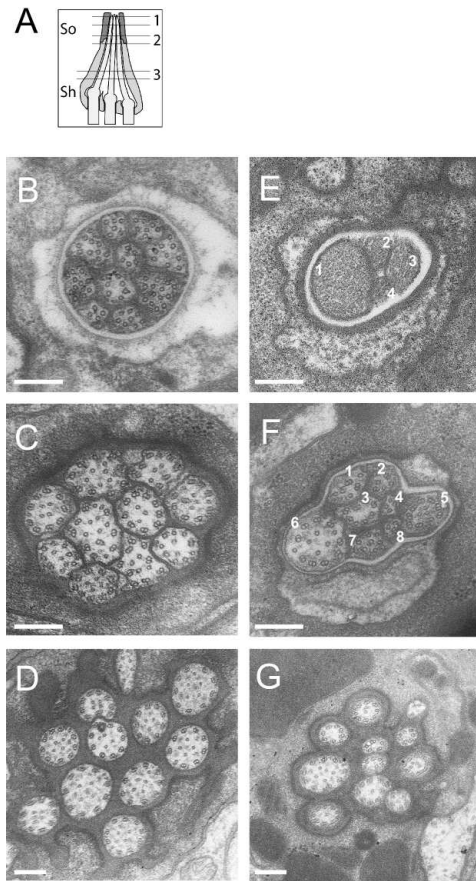


**Figure 5.2: *gpa-3QL* affects cilia length and morphology.** (A) Schematic representation of three of the amphid channel cilia embedded in the sheath cell (sh) and the socket cell (so). The approximate positions of the EM cross-sections in B have been indicated. (B-D) EM cross section of a wild-type and (E-G) *gpa-3QL(syls25)* animal. (B) Sections through the socket cell, showing the distal segments of the ten channel cilia, which contain singlet microtubules in the wild-type animal. (E) In *gpa-3QL* worms, less than ten cilia could be identified, and no microtubules could be discerned. (C) Ten channel cilia embedded in the sheath cell are present in the wild-type animal. Most cilia contain doublet microtubules, some contain singlets. (F) Section of a *gpa-3QL* animal through the socket cell, showing eight cilia. Some cilia have a normal appearance, others are small and contain singlet microtubules (cilium 4 and 7). (C, G) More posterior sections through the middle segments. In both the wild type (C) and the *gpa-3QL* (G) animal ten channel cilia embedded in the sheath cell are present.

In all panels, scale bar represents 200 nm.

Genotype	GPA-4::GFP				n	GPA-15::GFP				n
	Length in $\mu\text{m}$	SD	% Short			Length in $\mu\text{m}$	SD	% Short		
WT	4.76	$\pm$ 0.50	6		99	6.00	$\pm$ 1.00	3		118
<i>kap-1</i>	4.64	$\pm$ 0.47	9		64	6.56	$\pm$ 0.62	0		32
<i>osm-3</i>	3.68	$\pm$ 0.25	89		74	4.53	$\pm$ 0.34	98		81
<i>gpa-3QL(syIs25)</i>	3.60	$\pm$ 0.53 <sup>1</sup>	82		38	5.33	$\pm$ 1.09 <sup>1</sup>	56		57
<i>kap-1; gpa-3QL(syIs25)</i>	4.12	$\pm$ 0.46 <sup>2</sup>	37		46	5.35	$\pm$ 0.70	38		61
<i>osm-3; gpa-3QL(syIs25)</i>	3.10	$\pm$ 0.32 <sup>1,2</sup>	100		29	ND				
<i>gpa-3QL(syIs25)</i>	4.75	$\pm$ 0.66	14		36	4.89	$\pm$ 0.67 <sup>1</sup>	65		43
<i>kap-1; gpa-3QL(syIs25)</i>	4.43	$\pm$ 0.54	21		42	5.63	$\pm$ 0.59 <sup>2</sup>	20		50

**Table 5.1: GPA-3QL affects cilia length in *gpa-4::gfp* and *gpa-15::gfp* transgenic lines** Indicated are the average lengths of GPA-4::GFP and GPA-15::GFP staining cilia  $\pm$  the standard deviation (in  $\mu\text{m}$ ), the significance tested using a 2-tailed paired T-test compared to wild type animals (<sup>1</sup>:  $P < 0.001$ ), to *gpa-3QL(syIs25)* (<sup>2</sup>:  $P < 0.001$ ) or to *gpa-3QL(syIs24)* (<sup>3</sup>:  $P < 0.001$ ). Short cilia were determined as being smaller than the intersection between the distribution plots of cilia lengths in WT and *osm-3* animals. For GPA-4::GFP this length was 4.04  $\mu\text{m}$  and for GPA-15::GFP 5.18  $\mu\text{m}$ . n indicates the number of measurements.

showed increased fluorescence of the basal body, and a reduced length (Figure 5.3; Table 5.3). *gpa-15::gfp* was used to visualize the ASH, ASK and ADL neurons. In *gpa-3QL*, these cells showed a broad panel of defects. The cilia were more dispersed, compared to wild-type animals. In addition, the lengths of the cilia were reduced (Figure 5.3; Table 5.3), and the basal body of the ADL neurons was displaced posteriorly. Our attempts to assess the cilia of the ASJ neurons with *gpa-9::gfp*, ASH neurons with *sra-6::gfp* and the ASK neurons with *srg-8::gfp* were not successful, since expression of these constructs was severely reduced in the *gpa-3QL* background.

Interestingly, the length of the fluorescent area was found to be reduced in several cilia. This apparent shortening of the cilia can either be structural, or an exclusion of the fluorescent proteins from the distal segments. In the latter case a distal segment should still be present. In order to test this we expressed *gpa-4::tbb-4::mCherry* together with *gpa-4::gfp* in *gpa-3QL* animals. *tbb-4* encodes a  $\beta$ -tubulin that is found in the middle and distal segments of sensory cilia in *C. elegans* (Barr M, personal communication). In wild-type animals the average length of GFP fluorescence was 4.7  $\mu\text{m}$  (n=23), compared to 4.1  $\mu\text{m}$  for the mCherry fluorescence (n=23). In *gpa-3QL(syIs25)* animals, these lengths were 2.6  $\mu\text{m}$  for GFP versus 2.1  $\mu\text{m}$  for mCherry (n=26). These results, together with the EM data indicate that in *gpa-3QL* animals at least some cilia are shortened, among which the cilia of the ASI neurons.

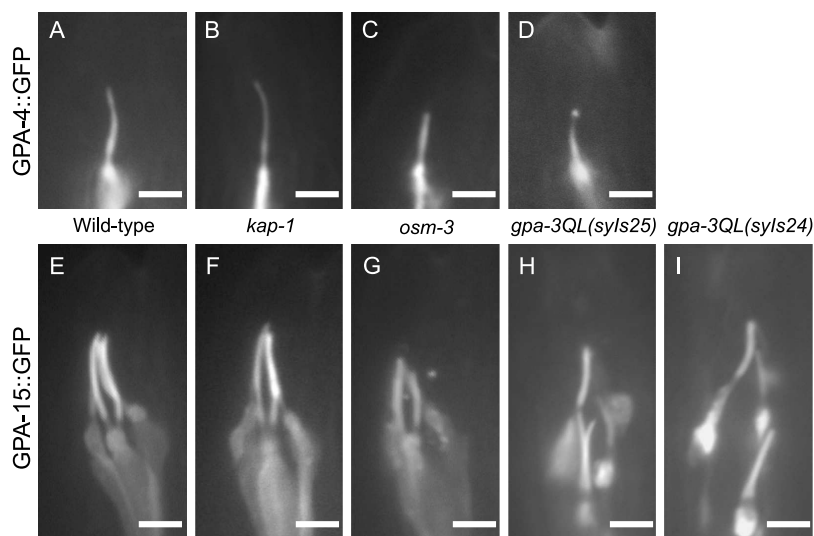


Figure 5.3: ***gpa-3QL* affects cilia lengths.** (A-D) Visualization of GPA-4::GFP in wild type animals (A), *kap-1* (B), *osm-3* (C) and *gpa-3QL(syIs25)* animals (D). GPA-4::GFP could not be detected in the distal segments of *gpa-3QL(syIs25)* animals, like in *osm-3* animals. (E-I) Visualization of GPA-15::GFP in wild type animals (E), *kap-1* (F), *osm-3* (G), *gpa-3QL(syIs25)* animals (H) and *gpa-3QL(syIs24)* animals (I). GPA-15::GFP could not be detected in the distal segments of the cilia of *gpa-3QL* animals, like in *osm-3* animals. In both *gpa-3QL* lines the basal bodies are dispersed, and the basal body of ADL is displaced posteriorly. In all panels, scale bar represents 2  $\mu$ m.

The two independent, integrated *gpa-3QL* strains tested showed phenotypic differences. The ASI marker *gpa-4::gfp* showed short cilia in the *gpa-3QL(syIs25)* background, whereas in the *gpa-3QL(syIs24)* the length of the ASI cilia was as in wild-type animals (Table 5.3). In contrast, *gpa-15::gfp* transgenic animals displayed shortened cilia in both alleles (Table 5.3). These differences may be caused by a variation in the expression of the *gpa-3QL* array in the two integrated strains, depending on the chromosomal context or the integrity and size of the array. To assess the effects of variations in expression levels, we injected a range of concentrations into wild-type animals and checked cilia length, morphology and posterior displacement of the basal bodies in *gpa-4::gfp* and *gpa-15::gfp* transgenic animals.

Already the lowest injected concentration of *gpa-3QL* induced some morphological differences compared to the wild-type animals (Table 5.3). At increasing

<i>gpa-3QL</i>	GPA-4::GFP			GPA-15::GFP			
	ASI morphology		% Dyf	Post. displ.		ADL cilia structure	
	% Accum	% No cilium		% One	% All	% Open	% Single
WT	0	0	0	0	0	0	0
20 ng	45	3	3	3	0	9	0
40 ng	78	0	35	30	3	21	29
85 ng	80	2	35	35	2	26	42
125 ng	81	8	81	45	8	56	43
170 ng	57	24	85	51	21	41	56

**Table 5.2: Injection of increasing concentrations of *gpa-3QL* results in an increase of cilia defects.** Indicated are the percentages of animals that were affected by a given phenotype. Accum. indicates accumulation of GFP at the Basal Body, Dyf indicates dye-filling defective, Post. Disp. signifies the percentage of animals in which one or all basal bodies were located posteriorly of the buccal cavity. In the ADL cilia defects, Open indicates that the two cilia of ADL did not join distally, and Single denotes the percentage of worms in which only one cilium was identifiable. Percentages were an average of at least 65 scored events in at least three independent transgenic strains.

concentrations the basal bodies became more pronounced and (as judged in the *gpa-15::gfp* animals) more dispersed. The basal bodies of the ADL neurons were consistently displaced posteriorly at 85 ng and higher concentrations. In addition, three of the six *gpa-4::gfp* strains injected with 170 ng *gpa-3QL* and several *gpa-15::gfp* strains injected with *gpa-3QL* (one out of three injected with 40 ng, two out of three injected with 125 ng and one out of three injected with 170 ng *gpa-3QL*) showed significantly reduced cilia lengths (results not shown). The severity of all defects varied considerably between the different injection lines. Together these results confirmed the ciliary defects observed in *gpa-3QL(syIs25)* and *gpa-3QL(syIs24)* and suggest that the variation in phenotypes is caused by differences in *gpa-3QL* expression levels.

**GPA-3 affects transport in the cilia of *C. elegans*.** Previously, Pan and Snell proposed that cilia length is regulated by controlling transport into the cilia (Pan & Snell, 2005). In addition, many of the proteins that were identified in dye filling and dauer formation screens are part of the IFT machinery. Hence we set out to see if GPA-3 affects IFT. First, we determined if the effects of *gpa-3QL* on the length of the cilia require either of the two kinesin 2 motors, OSM-3 or kinesin II. Interestingly, *gpa-3QL(syIs25); kap-1* double mutants showed significantly longer ASI cilia than *gpa-3QL(syIs25)* animals and also *gpa-3QL(syIs24); kap-1* double mutants showed longer ADL, ASH and ASK cilia than *gpa-3QL(syIs24)* animals (Table 5.3). Loss-of-function of OSM-3 did not restore the length of



the cilia in *gpa-3QL* animals to wild-type lengths. These results suggest that the reduction of cilia length in *gpa-3QL* animals is at least partially mediated by kinesin II.

Secondly, we determined the localization of several components of the IFT machinery: KAP-1::GFP and OSM-3::GFP to visualize the two kinesin 2 motors (Signor et al 1999; Snow et al., 2004), the dynein light intermediate chain XBX-1::GFP, the complex A protein CHE-11::GFP (Qin et al., 2001) and the complex B proteins CHE-13::GFP (Haycraft et al., 2003) and OSM-1::GFP (Signor et al., 1999). All these proteins showed wild-type localization in the cilia of *gpa-3QL* animals (results not shown).

Scholey and co-workers have previously reported that transport in the cilia of *C. elegans* is mediated by kinesin II and OSM-3 kinesin in the middle segment, and by OSM-3 kinesin alone in the distal segment. In the middle segments of wild-type animals, kinesin II and OSM-3 traveled both at  $0.7 \mu\text{m/s}$  (Table 5.3). In the absence of kinesin II, OSM-3 moved faster ( $1.15 \mu\text{m/s}$ ) and in the absence of OSM-3, kinesin II moved slower ( $0.5 \mu\text{m/s}$ ; Table 5.3). In the distal segments, only OSM-3 is found, moving at a rate of  $1.14 \mu\text{m/s}$ . These speeds are in agreement with previous reports (Snow et al., 2004; Ou et al., 2005a).

Next we measured the transport rates in *gpa-3QL* and *gpa-3(lf)* animals. In both mutants OSM-3::GFP containing particles moved at a speed of approximately  $1 \mu\text{m/s}$ , whereas IFT particles that contained KAP-1::GFP traveled at a speed of approximately  $0.55 \mu\text{m/s}$ , indicating that the two kinesin motors do not travel together in the same IFT particles (Table 5.3). Such a separation of OSM-3 and kinesin II can be due to a separation of the complex A and B proteins (Ou et al, 2005a), or a failure of one of the motors to link to the complex A/B scaffold (Burghoorn et al, 2007), or by a third, thus far unknown mechanism.

To discriminate between these possibilities we measured the speeds of fluorescently tagged complex A protein CHE-11, complex B protein OSM-1 and dynein light intermediate chain XBX-1. The velocities in the middle segments of wild-type animals were  $0.70 \mu\text{m/s}$  for these proteins, as expected. In *gpa-3(lf)* animals the speeds of these three proteins were slightly increased compared to the wild-type speeds (Table 5.3). In *gpa-3QL* animals, CHE-11, OSM-1 and XBX-1 travelled at wild-type speeds or slightly faster. These results suggest that the separation of the kinesin motors is not caused by the previously described mechanisms (Ou et al., 2005a; Burghoorn et al., 2007). We propose that in the *gpa-3* and *gpa-3QL* animals, the complex A/B scaffolds are loaded with either kinesin II or OSM-3 kinesin, but rarely both, resulting in the two kinesin motors travelling at different rates. However, since the complex A and B proteins are

IFT particle	genotype	Middle Segment		Distal Segment	
		speed $\mu\text{m/s}$	n	speed $\mu\text{m/s}$	n
OSM-3::GFP	wild type	0.70 $\pm$ 0.18	192	1.07 $\pm$ 0.23	87
	<i>gpa-3(pk35)</i>	1.04 $\pm$ 0.24 <sup>1,4,9</sup>	152	1.16 $\pm$ 0.24 <sup>2</sup>	74
	<i>gpa-3QL(syIs25)</i>	0.84 $\pm$ 0.22 <sup>1,3,4,9</sup>	178	1.12 $\pm$ 0.18	49
	<i>gpa-3QL(syIs24)</i>	1.09 $\pm$ 0.19 <sup>1,5,9</sup>	123	1.04 $\pm$ 0.18 <sup>3,4</sup>	46
	<i>kap-1</i>	1.17 $\pm$ 0.24 <sup>1,9</sup>	130	1.23 $\pm$ 0.28 <sup>1</sup>	42
	<i>L2</i>	0.72 $\pm$ 0.25	146	1.10 $\pm$ 0.29	50
	<i>L2d</i>	0.89 $\pm$ 0.26 <sup>7</sup>	154	0.98 $\pm$ 0.34	43
KAP-1::GFP	wild type	0.70 $\pm$ 0.14	194		
	<i>gpa-3(pk35)</i>	0.57 $\pm$ 0.14 <sup>1,6,8</sup>			
	<i>gpa-3QL(syIs25)</i>	0.56 $\pm$ 0.12 <sup>1,6,8</sup>			
	<i>gpa-3QL(syIs24)</i>	0.57 $\pm$ 0.15 <sup>1,6,8</sup>			
	<i>kap-1</i>	0.49 $\pm$ 0.10 <sup>1</sup>	91		
XBX-1::GFP	wild type	0.70 $\pm$ 0.17	141	1.11 $\pm$ 0.19	55
	<i>gpa-3(pk35)</i>	0.77 $\pm$ 0.23 <sup>2,8,9</sup>	202	1.14 $\pm$ 0.23	86
	<i>gpa-3QL(syIs25)</i>	0.73 $\pm$ 0.23 <sup>8,9</sup>	183	1.13 $\pm$ 0.27	76
	<i>gpa-3QL(syIs24)</i>	0.73 $\pm$ 0.18 <sup>8,9</sup>	159	1.12 $\pm$ 0.28	41
CHE-11::GFP	wild type	0.69 $\pm$ 0.21	118	1.20 $\pm$ 0.27	49
	<i>gpa-3(pk35)</i>	0.78 $\pm$ 0.16 <sup>1,8,9</sup>	190	1.22 $\pm$ 0.33	46
	<i>gpa-3QL(syIs25)</i>	0.73 $\pm$ 0.23 <sup>8,9</sup>	222	1.11 $\pm$ 0.22	65
	<i>gpa-3QL(syIs24)</i>	0.70 $\pm$ 0.17 <sup>3,8,9</sup>	282	1.17 $\pm$ 0.20 <sup>8</sup>	65
OSM-1::GFP	wild type	0.70 $\pm$ 0.26	224	1.10 $\pm$ 0.30	76
	<i>gpa-3(pk35)</i>	0.80 $\pm$ 0.20 <sup>1,8,9</sup>	196	1.17 $\pm$ 0.26	51
	<i>gpa-3QL(syIs25)</i>	0.77 $\pm$ 0.27 <sup>2,8,9</sup>	217	1.09 $\pm$ 0.18 <sup>1,3</sup>	65
	<i>gpa-3QL(syIs24)</i>	0.79 $\pm$ 0.21 <sup>1,9</sup>	233	1.12 $\pm$ 0.23 <sup>1,3</sup>	63

**Table 5.3: Table 3: *gpa-3(lf)* and *gpa-3QL* affect transport rates in the cilia.** Indicated are average speeds  $\pm$  the standard deviation (in  $\mu\text{m/s}$ ) and the number of tracks (n). Asterisks indicate significant differences when comparing speeds of: <sup>1</sup> & <sup>2</sup> IFT protein in a mutant background to the same IFT protein in Wild type (<sup>1</sup>: P<0.001, <sup>2</sup>: P<0.005), <sup>3</sup> IFT protein in the *gpa-3(lf)* to the same IFT proteins in *gpa-3QL(syIs24)* and *gpa-3QL(syIs25)* animals (p<0.001), <sup>4</sup> & <sup>5</sup> OSM-3::GFP in *textitkap-1* to its speeds in *gpa-3(lf)*, *gpa-3QL(syIs24)* and *gpa-3QL(syIs25)* animals (<sup>4</sup>: P<0.001, <sup>5</sup>: P<0.005), <sup>6</sup> KAP-1::GFP in *textitkosm-3* to its speeds in *gpa-3(lf)*, *gpa-3QL(syIs24)* and *gpa-3QL(syIs25)* animals (<sup>6</sup>: P<0.001), <sup>7</sup> OSM-3::GFP in L2 larvae compared to L2d larvae (P<0.001), <sup>8</sup> IFT protein compared to OSM-3::GFP in the same mutant background (P<0.001) and <sup>9</sup> IFT protein compared to KAP-1::GFP in the same mutant background (P<0.001).



transported by both kinesins, their speeds are intermediate compared to the kinesin speeds.

**Mutation of *gpa-3* affects dauer development by changing *daf-7* expression levels.** It was previously demonstrated that cilia length is dynamically regulated, depending on cell cycle, developmental stage and reproductive cycle, and can be influenced by environmental signals (Pugacheva et al., 2007; Pan & Snell, 2005). An important developmental change in *C. elegans* is the dauer response (Riddle and Albert, 1997), which was shown to involve alterations in the position and structure of several cilia. Since *gpa-3QL* animals show a dauer constitutive phenotype, while *gpa-3 (lf)* animals are dauer defective (Zwaal et al., 1997), we wondered whether the cilia defects in *gpa-3QL* were the results of activation of the dauer pathway.

One of the first factors of a complex network that regulates the decision between dauer formation versus reproductive growth in response to the dauer pheromone is the guanylate cyclase DAF-11 (Birnby et al., 2000). DAF-11 stimulates the DAF-7 (TGF $\beta$ ) pathway, and to some extent the DAF-2 (insulin/IGF I receptor) pathway. The DAF-2 pathway is predominantly regulated by food/starvation signals (Gerisch et al. 2001; Li et al. 2003; Riddle & Albert, 1997). It has been suggested that these two processes funnel into a third endocrine pathway, which includes DAF-12 (Riddle & Albert, 1988; Gerish et al., 2001).

Zwaal and colleagues (1997) have shown that mutation of *daf-5* suppresses constitutive dauer formation of *gpa-3QL* animals, suggesting that *gpa-3QL* functions upstream of DAF-5 in the *daf-7/TGF $\beta$*  pathway. We examined the expression of GFP tagged DAF-7 in *gpa-3* and *gpa-3QL* animals. *gpa-3* animals showed wild type levels of *daf-7::gfp* expression under normal growth condition (Figure 5.3A, B and D). However, no or only very little expression of *daf-7::gfp* could be detected in *gpa-3QL* animals (Figure 5.3C and D). Expression of *daf-7* under control of the dauer-independent promoter of *kin-8* in *gpa-3QL* animals completely suppressed the Daf-c phenotype (results not shown). Together these results confirm that GPA-3 regulates dauer formation by modulating *daf-7* expression.

Murakami and colleagues (2001) have shown that the transmembrane guanylyl cyclase DAF-11 is required for normal *daf-7* expression. Birnby et al. (2000) have shown that the Daf-c phenotype of *daf-11* animals can be rescued by supplementing these animals with the membrane permeable cGMP analogue 8-bromo-cGMP. When *gpa-3QL* animals were grown in the presence of 8-Bromo-

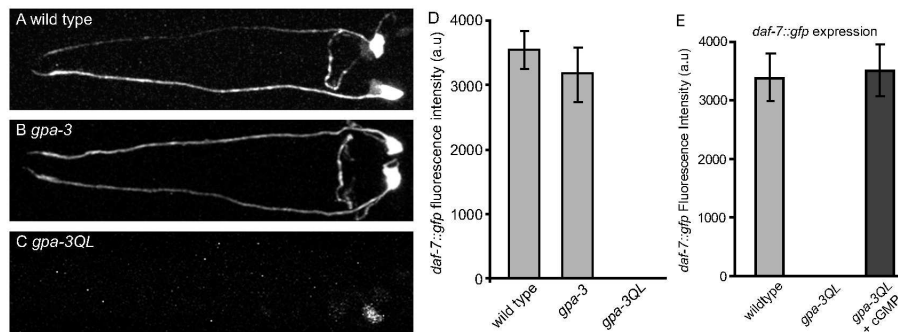


**Figure 5.4: *gpa-3* functions in the *daf-7*/TGF $\beta$  pathway in dauer development.** (A-C) Visualization of DAF-7::GFP expression in (A) wild type, (B) *gpa-3* and (C) *gpa-3QL* animals under normal growth conditions. *daf-7::gfp* expression is not affected by l.o.f. of *gpa-3*, but strongly reduced in *gpa-3QL* animals. Anterior is to the left. (D) Quantification of *daf-7::gfp* fluorescence intensity (a.u.) in wild type, *gpa-3* and *gpa-3QL* animals under normal growth conditions ( $n \geq 20$ ). *daf-7::gfp* expression is not affected by l.o.f. of *gpa-3*, but strongly reduced in *gpa-3QL* animals. (E) Quantification of *daf-7::gfp* fluorescence intensity (a.u.) in wild type and *gpa-3QL* animals cultured in the presence or absence of 8-Bromo-cGMP. Presence of 8-Bromo-cGMP completely restored *daf-7::gfp* expression in *gpa-3QL* animals, suggesting that *gpa-3QL* inhibits *daf-7* expression by reducing cGMP levels, probably by inhibiting *daf-11*.

cGMP, they displayed similar *daf-7::gfp* fluorescence intensity as wild type animals (Figure 5.3E), suggesting that the Daf-c phenotype of *gpa-3QL* animals is caused by inhibition of *daf-11*.

If the shortening of the cilia in *gpa-3QL* or dauer pheromone exposed animals would be caused by inhibition of the DAF-11/DAF-7 pathway, then loss-of-function of either of these signaling molecules would affect the length of the cilia as well. However, the cilia of both *daf-7* and *daf-11* mutant animals are similar in length to wild type (data not shown). Furthermore, expression of *daf-7* under control of the *kin-8* promoter in *gpa-3QL* animals, which restores normal dauer development, did not restore the reduced lengths in ASI, ASH, ASK and ADL (data not shown). This indicates that the reduction in cilia length is not the result of the activity of the DAF-11/DAF-7 signaling pathway.

**Exposure to dauer pheromone reduces cilia length, a process mediated by GPA-3 and KAP-1.** The previous experiments indicate that GPA-3 acts via *daf-11* and *daf-7* to induce dauer formation, and through a *daf-11* and *daf-7* inde-

pendent pathway to regulate the length of the cilia of *C. elegans*. We wondered whether the environmental cues that induce development into dauer larvae also result in cilia alterations similar to those found in *gpa-3QL* animals. Dauer development can be induced by exposing larvae to dauer pheromone, a continuously secreted compound that probably serves as a measure of the population density (Riddle and Albert, 1997). We exposed larvae to dauer pheromone and measured the length of GPA-4::GFP and GPA-15::GFP fluorescence in L2 or L2d animals, a preparatory stage for dauer arrest, and in L4 or dauer animals. First, we determined whether the cilia of the L2d larvae were still exposed to the environment by dye filling. Interestingly, the cilia of these animals did take up dye, suggesting that they are full length. However, in L2d larvae the length of GPA-4::GFP fluorescence was significantly shorter than in wild type animals, grown in the absence of dauer pheromone, comparable to the length of the cilia of *osm-3* animals (Figure 5.3J). GPA-15::GFP fluorescence was not changed in L2d animals. These results suggest that while most cilia of L2d animals are still full length, exposure to dauer pheromone reduces the length of the ASI cilia. We wondered whether *gpa-3* and kinesin II were involved in this process, by exposing *gpa-3* and *kap-1* mutant animals to dauer pheromone. Interestingly, strong GPA-4::GFP fluorescence could be observed along the normal length of the cilia of *gpa-3* and *kap-1* L2d animals (Figure 5.3D-G and 5.3J), indicating that the effect of dauer pheromone on the length of the ASI cilia requires *gpa-3* and *kap-1*.

After prolonged exposure to dauer pheromone for 50 hours, the cilia of dauer animals are no longer exposed to the environment (Albert and Riddle, 1983) and do not take up fluorescent dyes (results not shown). Interestingly, in dauer animals the length of the GPA-4::GFP fluorescence was restored to normal. Given the similarities between the *gpa-3QL* and the dauer-pheromone induced length reduction of the cilia, and the requirement for GPA-3 and KAP-1 for the latter, we wondered whether dauer pheromone exposition affects IFT motility in a similar way as *gpa-3QL* and *gpa-3*. For this purpose we measured transport rates of OSM-3::GFP in L2 and L2d animals. In the middle segments of untreated wild-type L2 larvae OSM-3 travels at a speed of 0.7  $\mu\text{m}/\text{sec}$ , which is comparable to the speeds in young adult animals. Exposure of larvae to dauer-pheromone during the 24 hours prior to imaging increased the speed to 0.89  $\mu\text{m}/\text{sec}$  ( $p < 0.001$ ). This speed is very similar to the OSM-3::GFP speed measured in *gpa-3* mutant animals. We hypothesize that exposure to dauer pheromone affects the coordination of IFT by the two kinesins, by activating GPA-3.

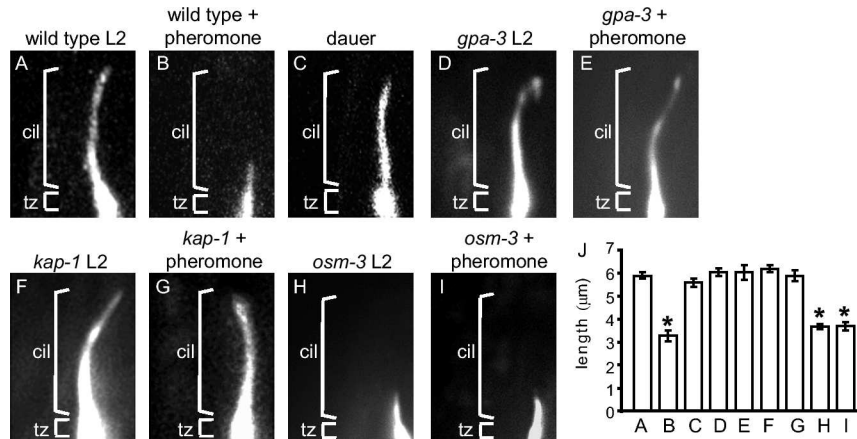


**Figure 5.5: Dauer pheromone affects ASI cilium length.** (A-I) GPA-4::GFP localization in cilia of L2 larvae, not exposed to dauer pheromone (A), L2d larvae (B), dauer larvae (C), *gpa-3* L2 larvae, not exposed to dauer pheromone (D), *gpa-3* L2d larvae (E), *kap-1* L2 larvae, not exposed to dauer pheromone (F), *kap-1* L2d larvae (G), *osm-3* L2 larvae, not exposed to dauer pheromone (H) and *osm-3* L2d larvae (I). Exposure to dauer pheromone results in GPA-4::GFP localization only in the middle segments, but not in the distal segments in L2d animals, a process that requires *gpa-3* and *kap-1* (cil, cilia; tz, transition zone). (J) Lengths of GPA-4::GFP staining in the cilia, in μm in (A) wild type L2 not exposed to dauer pheromone (n=21), (B) wild type L2d exposed to dauer pheromone (n=32), (C) dauer animals (n=26), (D) *gpa-3* L2 (n=20), (E) *gpa-3* L2d (n=28), (F) *kap-1* L2 (n=20), (G) *kap-1* L2d (n=20), (H) *osm-3* L2 (n=20) and (I) *osm-3* L2d animals (n=22).

## 5.4 Discussion

Using EM and cilium specific GFP markers, we show that *gpa-3<sup>QL</sup>* affects the morphology of amphid sensory cilia in *C. elegans* in a dose dependent and reversible way. The cilia are shorter and sometimes displaced posteriorly. Conversely, *gpa-3(lf)* animals show no structural defects of the cilia. The localization of components of the IFT complex is not affected in *gpa-3(lf)* and in *gpa-3<sup>QL</sup>* animals. However, IFT is perturbed in these animals: in both mutants kinesin II speed is reduced and OSM-3 kinesin speed increased, while complex A/B proteins travel at approximately wild-type speeds.

How could such a change in IFT cause a shortening of the cilia in *gpa-3<sup>QL</sup>*, while in *gpa-3* the cilia appear normal? In *Chlamydomonas* it has been shown that shortening of the cilia is the result of disassembly of the axoneme, an increase in IFT shuttling and blocking anterograde cargo loading (Pan & Snell, 2005). One

intriguing possibility is that in *gpa-3QL* animals a certain subset of particles is transported by OSM-3, instead of being transported by both kinesin II and OSM-3. If the OSM-3 transported IFT particles are empty or carry proteins that promote cilia shortening, while the kinesin II particles contain molecules that maintain the integrity of the cilia, the cilia distal segments would be shortened, while the middle segments remain intact. In *gpa-3(lf)* animals, the loading of kinesins could be the other way around, thus leaving the cilia intact and full length. However, this implies that at least two types of cargo particles exist. This model could be tested by measuring speeds of cargo molecules, which might be differentially transported by either one of the IFT motors. At present only few IFT cargo molecules have been identified. Most cargo proteins identified thus far are structural components of the cilia (Qin et al., 2004), although, some signalling molecules have been shown to be IFT cargo (Ou et al., 2005b; Qin et al., 2005). Thus, further analysis of many putative cargo molecules is required. Recently, Aurora A kinase, together with HEF-1 were proposed to play a key role in relaying external growth hormone signals to cilia resorption. Essential for this process was phosphorylation of histone deacetylase HDAC6, which destabilises the microtubular axoneme of the cilium (Pugacheva et al., 2007). The closest homologue of HDAC6 is F41H10.6 (results not shown) and it would be interesting to assess its role in this process.

Previously, it was found that GPA-3 plays a role in the dauer pathway, upstream of *daf-5*. We found that GPA-3 functions by regulating *daf-7* levels to activate the dauer pathway. Interestingly, exposure to dauer pheromone induced shortening of the cilia of ASI neurons, which depends on GPA-3 and kinesin II. In addition, it resulted in an increase in OSM-3 kinesin speeds in the middle segments of the cilia, very similar to what we found in *gpa-3QL* and *gpa-3(lf)*. However, GPA-3 is not required for dauer formation - *gpa-3(lf)* is only mildly defective in dauer formation-, which may be due to functional redundancy of  $\alpha$  subunits in the amphid sensory neurons (Jansen et al., 1999). In addition, the effects of *gpa-3QL* on the cilia are *daf-7* independent, and not required for dauer formation, as *kap-1* animals are not Daf-d (JB and GJ, unpublished results).

The regulation of cilia length by localization of molecules in the cilia segments in *C. elegans* involves a choice between transport mediated by kinesin II and OSM-3 kinesin. Until recently, it was unclear if also in other organisms OSM-3 kinesin motors function in cilia transport, although homologues had been identified in several other organisms, such as *Chlamydomonas*, *Tetrahymena* and in mice (Awan et al., 2004; Cole, 2003; Setou et al., 2000). Recently, Jenkins et al. (2006) have shown that the mouse homologue of OSM-3, KIF17, is required

for the proper localization of cyclic nucleotide gated channels in the cilia of olfactory sensory neurons, suggesting that perhaps also in other organisms mechanisms exist that regulate the localization of specific signaling molecules by modulating transport by either of the two ciliary kinesins. In addition, a recent study by Peden and Barr (2006) has identified yet another kinesin motor, KLP-6, which was found to function in localizing signaling proteins to the cilia. Given the evolutionary conservation of the IFT machinery and the signalling proteins involved, we expect that future studies will uncover that similar mechanisms are used to respond to other environmental changes, both in worms and perhaps also in other organisms including mammals.

## 5.5 Materials & Methods

**Strains and constructs used.** All strains were grown at 20°C and cultured according to standard procedures (Brenner, 1974). Strains and alleles used: wild type Bristol N2, *gpa-3QL(syIs25)X*, *gpa-3QL(syIs24)IV*, *kap-1(ok676)II* and *textitism-3(p802)IV*. GFP reporters used: *gpa-4::gfp*, *gpa-9::gfp* and *gpa-15::gfp* (Jansen et al., 1999), *vap-1::rfp* (a gift from B. Westlund), *che-11::gfp* (Qin et al., 2001), *osm-1::gfp* (Signor et al., 1999), *textitism-3::gfp* and *kap-1::gfp* (Orozco et al., 1999), *che-13::gfp* (Haycraft et al., 2003), *osm-5::gfp* (Haycraft et al., 2001) and *xbx-1::gfp* (Schafer et al., 2003). All GFP reporters were crossed into the *gpa-3QL(syIs25)* background. A heat shock inducible *gpa-3QL* construct (*hsp16-2::gpa-3QL*) was generated by subcloning *gpa-3QL* into the pPD49.78 vector (Mello and Fire, 1995).

**Immunofluorescence and microscopy.** Animals were fixed, permeabilized and stained with anti GPA-3, GPA-13, ODR-3 and tubulin antibodies as described previously (Finney and Ruvkun, 1990; Lans et al., 2004). Monoclonal rat antibody against tubulin was purchased from Abcam (ab6160). Secondary antibodies were goat-anti-rabbit alexa-594-conjugated and goat-anti-rat alexa-488-conjugated (Molecular Probes). The localization of fluorescent proteins and cilia morphology was examined using a Zeiss confocal microscope CLSM510. Dye filling (Perkins et al., 1986) was performed using DiI (Molecular probes). Cilia lengths were measured using a Zeiss Imager Z1 microscope.

**Life imaging of IFT particles.** Live imaging of the GFP tagged IFT particles was carried out as described previously (Orozco et al., 1999; Snow et al., 2004).

Images were acquired on a Zeiss LSM 510 confocal microscope with a 63x (NA 1.4) objective. The worms were mounted on an agarose pad, were anaesthetized with 10 mM tetrazizole. Kymographs were generated in ImageJ with the Kymograph plugin, written by J. Rietdorf.

**Dauer analysis.** Dauer pheromone was isolated as described previously (Golden and Riddle, 1984). Adult animals were allowed to lay eggs on plates with inducing concentrations of dauer pheromone, and removed after three hours. The localization of GPA-4::GFP en GPA-15::GFP was determined in L2d larvae after 24 to 28 hours at 25°C or after 52 to 58 hours in dauer animals. To analyze whether the ASI cilia were still in contact with the environment the worms were subjected to dye filling.

**Statistics.** Significance was determined using an unpaired, two-tailed Student's T-test, assuming equal variance. For all experiments an  $\alpha$ -level of 0.05 was used.

**Acknowledgements.** We thank T. Stiernagle and the Caenorhabditis Genetics Center, P. Sternberg, M. Barr, A. Fire, C. Haycraft, B. Yoder, G. Ou, J. Scholey and B. Westlund for *C. elegans* strains, antibodies and constructs. We thank the members of the Jansen lab for comments on the manuscript. This work was supported by the Centre for Biomedical Genetics and the PKD Foundation.





*et puis, et puis encore?*  
Baudelaire, la Mort

# 6

## Discussion

## 6.1 Plasticity in *C. elegans*

In this thesis I describe several aspects of plasticity in *C. elegans*. We have used gustatory plasticity as a model for studying the capacity of animals to respond differentially to environmental cues. *C. elegans* is normally attracted to low and avoids high concentrations of NaCl. However, after prolonged exposure to attractive NaCl concentrations, the animals strongly avoid all concentrations of NaCl. This is called gustatory plasticity. Previously it was found that this behavioural switch is a tightly regulated process in which many different signalling pathways are involved (Hukema, 2006). This process requires a number of cells, the ASE, ASH, ASI and ADF amphid sensory neurons, and the URX, AQR and PQR neurons which are exposed to the body fluid. How these neurons interact to bring about the switch from attraction to avoidance is not well understood. In order to gain insight into the neuronal network that drives this behavioural switch, we have used a reductionist approach. We started by studying naive chemosensation of NaCl, and found that it is mainly the result of attraction signals from the ASE neurons, and, at hyperosmotic concentrations, of signals from the ASH nociceptive neurons, explaining the biphasic appearance of NaCl chemosensation behaviour. The involvement of these particular neurons was expected, since the ASE neurons were previously found to be the prime NaCl sensing cells (Bargmann et al., 1990), and the ASH neurons have been described to drive avoidance of hyperosmotic stimuli (Bargmann et al., 1990; Kaplan & Horvitz, 1993).

We hypothesised that gustatory plasticity is the result of a modification of the naive response. Using *in vivo* imaging (Miyawaki et al., 1997; Kerr et al., 2000; Nagai et al., 2002), we demonstrated that after prolonged exposure to NaCl, the ASE neurons are desensitized, and the ASH neurons become sensitized. In addition, we found that the ASE neurons provide a signal that induces sensitisation of the ASH neurons (Hukema et al., 2006 and this thesis), suggesting a dual role for the ASE neurons in gustatory plasticity.

The molecular mechanisms that mediate the desensitisation of attraction remain to be determined. Unfortunately, the signalling pathway used for the sensation of NaCl in the ASE neurons is poorly understood, requiring further characterization before regulatory mechanisms can be understood.

It is very likely that additional non-cell-autonomous factors are involved in mediating desensitization of NaCl attraction. A first indication comes from studies using mutants that affect ASE L/R asymmetry. It was previously found that the ASE pair of neurons is functionally asymmetrical (Pierce-Shimomura et al., 2001). This asymmetry is dispensable for naive attraction to NaCl, but we

found it to be required for proper establishment of gustatory plasticity. This may shed some light on the role of the ASE neurons in gustatory plasticity. Interestingly, both the mutant that has two right ASEs and in the mutant with two left ASEs show attraction nor avoidance to low concentrations of NaCl. Since chemotaxis to NaCl is determined by a balance of attraction and avoidance, these results can be interpreted as a partial effect of pre-exposure, resulting in reduced attraction and increased avoidance or a partial combination of both. It would be interesting to study which is the case in the ASER/R and ASEL/L mutants, and, even more interesting, if it is the same in these two asymmetry mutants.

A second indication for non-cell-autonomous factors to play a role in the desensitization of the ASE neurons is provided by the behaviour of the *odr-3* mutants. These mutants are defective in avoidance signalling in ASH (Roayaie et al., 1998; Hukema et al., 2006; Hilliard et al., 2005). However, after pre-exposure, *odr-3* animals only show very limited desensitisation of attraction to low concentrations of NaCl. The gustatory plasticity phenotype can be rescued by expressing ODR-3 in the ADF neurons (Hukema et al., 2006), suggesting that these neurons aid desensitization of the ASE neurons.

We found that preexposure to NaCl sensitizes the ASH nociceptive neurons, enabling these cells to respond to low concentrations of NaCl. The ASH neurons can sense several different sensory modalities, such as touch, volatile and water-soluble stimuli. Furthermore, they can transmit a number of these stimuli differentially. Currently it is thought that two main signalling routes exist in the ASH neurons: an OSM-10 dependent route that senses high osmotic stresses and an OSM-10 independent route that is used after stimulation with nose touch or copper (Hart et al., 1999; Hilliard et al., 2005). Previously it was described that maximal induction of gustatory plasticity requires NaCl (Saeki et al., 2001; Jansen et al., 2002; Hukema et al., 2006; Hukema, 2006). However, pre-exposure to NaCl affects chemosensation of other chemicals as well, such as biotin, cyclic AMP, lysine and ammonium acetate (Saeki et al., 2001; Jansen et al., 2002). We hypothesised that the sensitized route in ASH that perceives NaCl after pre-exposure is a general ion sensing pathway. We indeed found that the amplitudes of the FRET responses to stimulation with copper were significantly increased after pre-exposure to NaCl, supporting the model that the sensitized pathway is non NaCl specific and that this pathway also mediates avoidance of other ionic compounds.

## 6.2 Constructing circuits for behaviour

The EM studies conducted by Ward, Ware, White and Perkins have been instrumental in launching *C. elegans* into the field of neurobiology (Ward et al., 1975; Ware et al., 1975; White et al., 1986; Perkins et al., 1986). It has allowed researchers to utilize the simplicity of the nervous system of *C. elegans* to correlate behaviour with the action of a defined neuronal network, and analyse the function of individual neurons in it. However, from these extensive EM studies it could not be inferred whether the connections between the different cells are excitatory or inhibitory.

In order to understand how *C. elegans* can chemotax to a point source of an attractant, the group of Lockery has created a theoretical model of this behaviour. It was known that *C. elegans* moves in a biased random fashion: periods of sinusoidal forward movement (runs) are interspersed by stops and turns (pirouettes) (Dusenbury et al., 1980). Pierce-Shimomura proposed that chemotaxis is the result of altering the latency of the pirouettes (Pierce-Shimomura et al., 1999). Elongation of the run times when moving up a gradient of an attractive compound effectively results in chemotaxis towards the source. Conversely, by shortening the run times when encountering a noxious substance, animals move away and avoid the repellent (Pierce-Shimomura et al., 1999). Dunn et al. searched for theoretical network patterns that enable *C. elegans*' chemotaxis (Dunn et al., 2004). One type of network that was able to simulate chemotaxis was a three neuron differentiator network with extensive inhibitory feedback. Especially the latter characteristic was interesting, because the inhibitory feedback allows the animals to regulate the latency of the systems output relative to its input, which would support the Pierce-Shimomura model for chemotaxis. Differentiator networks are suggested to play a role *in vivo* as well, as several of them can be identified between the ASE neurons and the AVA/AVB locomotory command neurons in the connectivity data by White (White et al., 1986; Dunn et al., 2004).

This theoretical framework for chemotactic behaviour in *C. elegans* can be very useful in understanding what happens in gustatory plasticity, as it predicts that the response to a stimulus can be modulated by altering the strengths of the inhibitory connections in the network. For this purpose it would be useful to construct a map with synaptic connections of the cells that are involved in plasticity. However, this will undoubtedly result in a very complex picture, since this behavioural switch involves many sensory neurons. The ASE, ASH, ASI and ADF amphid sensory neurons and the URX, AQR and PQR proprioceptive neurons were already identified to play a role, and other, yet unidentified

neurons still may be involved. Of these neurons it is not known whether they function as input neurons or as interneurons in the circuit that establishes plasticity.

Our data suggest that the ASE and ASH neurons drive attraction and avoidance, and that their input or outputs are modulated by signals from other cells. It is well established that plasticity depends on the absence of food (Saeki et al., 2001; Jansen et al., 2002; Hukema et al., 2006; Tomioka et al., 2006). The ASI neurons were recently reported to perceive food inputs (Bishop & Guarente, 2007), perhaps these cells perform a similar role in gustatory plasticity. The involvement of the AQR/PQR and URX neurons is striking, and may suggest that the constitution of fluid in the pseudocoelomic space serves as short term record of previous experiences. What the recorded signal is, be it the NaCl concentration in the body cavity fluid or perhaps a hormonal compound, is unknown, but its identity would be interesting to further pursue.

The integration site of these inputs is unclear. However, based on the connectivity data by White, the interneurons that are most likely to be involved are the AIA, AIB, AIY and AIZ (White et al., 1986). The AIA neurons were recently identified in a potentially related form of plasticity (Tomioka et al., 2006), and *txx-3* mutants, which lack a transcription factor essential for AIY function (Hobert et al., 1997; Altun-Gultekin et al., 2001), are defective in plasticity (Hukema 2006), supporting the involvement of these interneurons.

### 6.3 Technical opportunities and challenges

There are several ways to study the role that a specific neuron plays in a certain behaviour. In brief one can inactivate the neuron of interest, express a transgene that allows exogenous stimulation or inhibition, or track the activation of the neuron.

Laser ablation of cells is the best known method to inactivate cells in *C. elegans*, and has extensively been used to study the function of specific neurons in behaviour. By ablating single or small groups of neurons, Bargmann has been able to identify the neurons that drive attraction to volatile chemicals or water soluble compounds, the neurons that drive repulsive behaviours and the cells that are involved in dauer formation or recovery (Bargmann et al, 1990; Bargmann & Horvitz, 1991). Later, Gray et al deciphered the circuit for navigation in *C. elegans*, by studying the effect of ablation of specific interneurons (Gray et al., 2005). Laser ablations are a sure-fire way to inactivate cells. However, this technique is labour intensive, limiting its application to single

animal experiments. In addition, it is not well understood how the physical absence of the ablated cell influences signalling from neighbouring cells, and if the networks they were involved in exhibit some sort of corrective adaptation to it.

Another well known way to inactivate cells is to study mutants for proteins that have differentiation or functional defects in single or small groups of neurons. In chapter two, I have described the usage of several mutants from this category. The *che-1*, *cog-1* and *lsy-6* animals lack factors essential for the proper development of the asymmetrical ASE neurons (Ushida et al., 2003; Chang et al., 2003; Johnston 2003), and the *osm-9*, *odr-3*, *gpc-1* and *osm-10* mutants lack components of signalling pathways needed for function of ASH (Colbert et al., 2007; Bargmann et al., 1993; Jansen et al., 2002; Hart et al., 1999). Using mutant animals provides the possibility to use large numbers of animals with a fairly uniform phenotypic background. However, many of these genes and proteins function in multiple cells, making it important to confirm results by testing additional mutants, double mutants and cell specific rescues.

A complementary approach is to study the effect of activating specific neurons. Previously, it was shown that expressing the mammalian TRPV1 channel subunit in the nociceptive ASH neurons of *C. elegans* results in a robust acquired avoidance behaviour of the ligand of this receptor, capsaicin (Tobin et al., 2002; Liedtke et al., 2003). In addition, it was found that GPCRs integrate into the endogenous signalling machinery in *C. elegans* as well (Milani et al., 2002; Conte et al., 2006). In chapter three we corroborated these findings and extended their utilization. By expressing the TRPV1 receptor in the ASI and ADF neurons we confirmed that these cells drive attractive behaviours, but that this capacity is lost after pre-exposure to NaCl. Thus far, we have not taken the heterologous expression of the GPCRs to the same level, however this technique holds great potential to study network connectivity. Introducing different receptors into a number of cells would allow the study of concomitant activation of multiple cells, enabling assessment of interactions between these cells.

Although expressing transgenic channels into cells allows one to study the effects of stimulation of sensory neurons, it is very difficult if not impossible (depending on the receptor that is used) to study neurons that are not exposed to the external environment. Recently, the advent of optogenetics has opened the possibility to activate all neurons regardless whether they are exposed or not. In this technique, the cDNA of a light activatable sodium or chloride channel is introduced into cells to allow for either evoking or blocking of action potentials, respectively (Li et al., 2005; Zhang et al., 2007). These channels have already successfully been applied in *C. elegans*, and were found to be capable to

drive novel behaviours. (Nagel et al., 2005; Zhang et al., 2007). These channels may prove invaluable in unravelling the mechanisms of gustatory plasticity. Finally one can learn about the function of cells by studying their activation. In principle one can probe for the activation of a cell at all levels of the signalling cascade. In the canonical pathway of G-protein signalling, binding of a ligand to a GPCR enables the G-protein to bind to it. This results in a conformational change, allowing the  $\alpha$  subunit to exchange GDP for GTP, and dissociate from the  $\beta/\gamma$  subunits. By constructing fluorescently tagged versions of the G-protein  $\alpha$  subunit and of  $\beta/\gamma$  subunits one can follow the activation of the cell (Janetopoulos et al., 2001).

Activation of G-proteins results in amplification of the signal, which also increases the fidelity of the read-out of probes that one might use. One of the known downstream pathways that are activated after G-protein activation is the PIP2 signalling pathway. G-proteins can activate phospholipase C  $\beta$ , which cleaves PIP2 to produce IP3 and diacylglycerol, which in turn can activate a range of downstream targets. By tagging CFP and YFP with a pleckstrin homology domain, which can only bind to PIP2, one can track the receptor mediated breakdown of PIP2. (van der Wal et al., 2001; van Rheenen et al., 2002).

Typically, neurons will change their membrane potential after activation. This can be tracked by using voltage sensitive dyes or by using a molecular probe that reports voltage changes (Sakai et al., 2001; Knöpfel et al., 2003). As mentioned before, neurons in *C. elegans* use calcium extensively as a potentiogenic ion and as a second messenger. Probes that detect changes in intracellular calcium concentrations have been successfully applied to study the activation of specific neurons. Examples of genetically encoded probes are the Cameleon construct (Miyawaki et al., 1997, Nagai et al., 2002), which has been used to track activation of the ASE and ASH neurons in chapter one and in studies from the Schafer lab (Kerr et al., 2000; Hilliard et al., 2005), and G-CaMP (Nakai et al., 2001), which has been used in dissecting the circuit for olfaction (Chalisani et al., 2007). The final step in transmitting signals through a cell is the release of neurotransmitters that can activate downstream targets. This step can be traced by synapto-pHluorin, a permutated GFP of which the fluorescence intensity depends strongly on the pH (Miesenböck et al., 1998). It is targeted to excretory synaptic vesicles (Ng et al., 2002), which have a low pH, leading to a quenching of GFP emission. After fusion, the pH rises and fluorescence intensity increases about 20-fold. Together, these techniques allow a fine grained analysis of cellular function, especially when several approaches are combined.

## 6.4 Are all forms of plasticity equal?

How does gustatory plasticity compare to other forms of plasticity? One of the best studied forms of plasticity is synaptic plasticity. Here, a specific pattern of stimulation of a synapse results in an enhanced or, conversely, decreased ability of that synapse to be activated. In this process, NMDA receptors were found to play a central role, as well as AMPA type receptors. Activation of these channels leads to the influx of calcium, which is thought to act as a second messenger, binding to Calcium/Calmodulin dependent kinases (CaMKs), and thereby phosphorylating a range of downstream effector proteins. This finally results in an altered excitability of the neuron via that synapse.

As already mentioned in Chapter 1, several of the proteins known to be involved in synaptic plasticity also affect gustatory plasticity, arguing that these may be comparable processes. For instance, the NMDA receptor homologue *nmr-1*, and the AMPA receptors *glr-1* and *glr-2* also affect gustatory plasticity. In addition, the CREB homologue *crh-1* and calcineurin subunits *tax-6* and *cnb-1* were also found to be defective in gustatory plasticity (Hukema, 2006). Of some key proteins in synaptic plasticity, the involvement in gustatory plasticity could not be confirmed by using behavioural assays. One example is the CaM kinase II homologue *unc-43*, which could not be tested because this mutant is severely impaired in its movement (Hukema, 2006). The aforementioned single cell imaging techniques may be useful in assessing the role of this protein in gustatory plasticity.

Of course there are differences too: *C. elegans* is not known to have long term memory, not in the least because of its average lifespan of nearly three weeks. The effects of pre-exposure to NaCl in gustatory plasticity are already lost after 5 minutes (Jansen, unpublished observations), and in thermotaxis assays, the temperature preference of the animals is maintained for up to four hours (Mori, 1999). The only recorded preference that lasts beyond this four hour period is in olfactory imprinting. In this process, exposure to a volatile compound during a critical period in development leads to lasting enhanced chemotaxis to that substance. (Remy & Hobert, 2005).

It would be interesting to further study similarities and differences between these two processes. One of the key characteristics of synaptic plasticity is, as the name already implies, a changed constitution of the synapse. The amphid neurons are essentially bipolar neurons, extending their axon to the nerve-ring, where they form synaptic connections to other neurons. Thus far it is unknown if and how the different forms of plasticity in *C. elegans* influence the constitution, size or number of synapses. This is testable by expressing fluorescently



tagged proteins that are targeted to pre- or post-synaptic sites. The pre-synapse can be tagged with SNB-1, the *C. elegans* homologue of SynaptoBrevin (Nonet, 1999), and postsynaptic sites can be visualised by using *glr-1* or *lin-10* (Shen & Bargmann, 2003; Rongo et al., 1998). Moreover, many components that comprise the synaptic complexes in *C. elegans* have been identified (Jin, 2006; Sieburth et al., 2005), allowing an even more detailed analysis of potential changes in the synapse.

It is remarkable how many proteins are shared between these forms of plasticity, given the distinct electrophysiological properties of *C. elegans*' neurons compared to neurons in other organisms. *C. elegans* lacks voltage gated sodium channels, and therefore does not exhibit typical  $\text{Na}^+$  action-potentials. Calcium and potassium are thought to be the prime potentiogenic ions in *C. elegans*. Despite the differences, that still need further scrutiny, the regulatory elements that modulate sensitivity and excitability of the neurons may very well be conserved.

## 6.5 Structural plasticity of the cilia

Cilia are present on almost every vertebrate cell and have important functions in motility or sensation. Within cilia, structural components and signalling molecules are transported by a specialized transport system called IFT. IFT particles consist of motor proteins, cargo, and the scaffold to which they bind. The molecular motors that mediate anterograde movement in the cilia of *C. elegans* are heterotrimeric kinesin II and OSM-3 kinesin, while retrograde movement is mediated by dynein. These proteins are proposed to be docked to a scaffold that consists of the complex A and B proteins. Finally, the cargo is expected to be bound to this complex.

It is important that cilia are maintained at a certain length for their proper function (Pan & Snell, 2005), but the molecular mechanisms that control length and morphology of cilia are largely unknown. It has been proposed that cilia length is regulated by a balance between cilia assembly and disassembly mediated by IFT (Pan & Snell, 2005). In chapter four we describe the identification and functional analysis of DYF-5, a homologue of the *Chlamydomonas reinhardtii* MAP kinase protein LF4 and the *Leishmania mexicana* homologue LmxMPK9. All these proteins were found to play a role in the maintenance of cilia length. Mutation of *dyf-5* affects cilia length and morphology. We also found that *dyf-5(lf)* affects the constitution and coordination of IFT particles. First, kinesin II can enter the distal segments in *dyf-5(lf)* mutants. Second, OSM-3 is separated

from the IFT particles and moves at a reduced speed in *dyf-5(lf)* mutants. Third, *dyf-5(lf)* animals show accumulation of six different IFT proteins in the cilia. In chapter five, we analyzed the phenotypes of *gpa-3QL* animals, which carry a dominant active form of GPA-3. In these animals defects in cilia length and structure also coincided with defects in IFT. Motility measurements suggest that kinesin II and OSM-3 kinesin no longer dock to the same IFT particles. Together, these results provide at least circumstantial evidence that IFT indeed affects length and morphology of the cilia.

Structurally, cilia of *C. elegans* can be divided into two parts: the middle segment and the distal segment. In the middle segment, the microtubular axoneme consists of a ring of nine doublet microtubules, while the distal segment has nine singlet microtubules. IFT in the middle segments is mediated by both kinesin II and OSM-3 kinesin, whereas OSM-3 kinesin only mediates transport in the distal segments. However, the functional consequence of this bipartite cilium structure is unclear. It is tempting to speculate that the distal segment of the cilia in *C. elegans* serves as a probe that can be exposed to the environment, or retracted if specific sensory inputs are undesirable. The results described in chapter four provide some support for such a model. We find that GPA-3QL affects IFT in *C. elegans*, and leads to a shortening of the cilia. Also in other organisms cilia have been reported to be able to be extended or shortened in a regulated fashion. For cell division it is required that primary cilia are dissociated. Conversely, the cilia of the biflagellate alga *Chlamydomonas* are extended when these organisms engage in fertilisation, a process that depends on IFT and CrPKG (Wang et al., 2006), and has been suggested to involve a *Chlamydomonas* homologue of OSM-3 kinesin (Ou et al., 2005).

But what is the function of this *gpa-3* dependent shortening? Previously it was found that GPA-3QL induces *C. elegans* to develop into dauer arrested larvae (Zwaal et al., 1997). This is an energy conserving stage in times of food shortage or high population densities, allowing the animals to survive for up to two months. When dauer larvae perceive a favourable environment, they exit the dauer stage and develop into adult nematodes. We found that a similar shortening of the cilia could be induced by exposing wild-type larvae to dauer-pheromone, a continuously excreted compound that may serve as a measure for population density (Albert & Riddle, 1983). We found that this shortening was dependent on GPA-3 and on KAP-1. It was known that *gpa-3* animals are mildly defective in dauer-formation (*daf-d*) (Zwaal et al., 1997). However, *kap-1* animals are not *daf-d*, indicating that the shortening of the cilia is not essential in dauer formation. Rather, we propose that it may serve as a means to consolidate the choice to develop into dauer larvae, by preventing contradicting

signals from the environment from reaching the cilia.

The ultrastructure of cilia and many proteins that function in it are conserved in many species. This suggests that similar mechanisms of IFT and regulating cilia length exist in these organisms, including mammals. Heterotrimeric kinesin II is known to function in mammalian cilia (Marzulek et al., 2000), and recently, the mammalian homologue of OSM-3 kinesin, KIF17 was shown to transport cyclic nucleotide gated channels in the cilia (Jenkins et al., 2006). However, in mammals it has not (yet) been found that the cilia are compartmentalized into a middle and distal segment, nor that the length can be regulated in a different way than the all-or-none fashion required for entering into mitosis.

Recently, a number of studies identified an additional function of KIF17. This kinesin was found to transport NR2B subunits of NMDA channels to and in the dendrites of neurons (Guillaud et al., 2003). It was also found that, after CaMKII dependent phosphorylation, KIF17 releases from the scaffolding protein Mint1, and consequently of its cargo (Guillaud et al., 2008). These results provide an attractive mechanism by which cargo is delivered at a specific site. It will be interesting to see if a similar mechanism of cargo release exists in cilia of *C. elegans*, and if so, whether it functions in plasticity.

## 6.6 Conclusion

The ability of *C. elegans* to flexibly cope with its environment has taken many guises, making it a fascinating subject to study. It alters the structures within the cells of this organism, and affects its development and behaviour. The accessibility of the nervous system of *C. elegans* and the recently developed molecular probes have allowed us to study these processes in considerable detail, providing new insights into the generation of plasticity. But at the end of it all, *C. elegans* remains, that capricious little creature....



# 7

## References

- Agrawal A (2001).** Phenotypic Plasticity in the Interactions and Evolution of Species. *Science* Vol. 294:321-326.
- Ahern GP, Brooks IM, Miyares RL and Wang XB (2005).** Extracellular cations sensitize and gate capsaicin receptor TRPV1 modulating pain signaling. *J Neurosci* 25(21):5109-16.
- Albert PS and Riddle DL (1983).** Developmental alterations in sensory neuroanatomy of the *Caenorhabditis elegans* dauer larva. *J Comp Neurol* 219:461-481.
- Albert PS and Riddle DL (1988).** Mutants of *Caenorhabditis elegans* that form dauer-like larvae. *Dev Biol* 126(2):270-93.
- Altun-Gultekin Z, Andachi Y, Tsalik EL, Pilgrim D, Kohara Y, Hobert O (2001).** A regulatory cascade of three homeobox genes, *ceh-10*, *ttx-3* and *ceh-23*, controls cell fate specification of a defined interneuron class in *C. elegans*. *Development* 128(11):1951-69.
- Awan A, Bernstein M, Hamasaki T and Satir P (2004).** Cloning and characterization of Kin5, a novel *Tetrahymena* ciliary kinesin II. *Cell Motil Cytoskeleton* 58:1-9.
- Bargmann CI, Thomas JH and Horvitz HR (1990).** Chemosensory cell function in the behavior and development of *Caenorhabditis elegans*. *Cold Spring Harb Symp Quant Biol* 55:529-38.
- Bargmann CI and Horvitz HR (1991).** Chemosensory neurons with overlapping functions direct chemotaxis to multiple chemicals in *C. elegans*. *Neuron* 7:729-742.
- Bargmann CI, Hartwig E and Horvitz HR (1993).** Odorant-selective genes and neurons mediate olfaction in *C. elegans*. *Cell* 74(3):515-27.
- Bargmann CI and Mori I (1997).** Chemotaxis and thermotaxis In *C. elegans* II. Edited by Riddle DL, Blumenthal T, Meyer BJ & Priess, JR Cold Spring Harbour, NY: Cold Spring Harbour Laboratory Press; 1997, 25: 717-737.
- Bargmann, C.I.** Chemosensation in *C. elegans* (October 25, 2006), WormBook, ed. The *C. elegans* Research Community, WormBook, doi/10.1895/wormbook.1.123.1, <http://www.wormbook.org>.
- Bengs F, Scholz A, Kuhn D and Wiese M (2005).** LmxMPK9, a mitogen-activated protein kinase homologue affects flagellar length in *Leishmania mexicana*. *Mol Microbiol* 55:1606-1615.
- Benton MJ and Ayala FJ (2003).** Dating the tree of life. *Science* 300:1698-1700.
- Berman SA, Wilson NF, Haas NA and Lefebvre PA (2003).** A novel MAP kinase regulates flagellar length in *Chlamydomonas*. *Curr Biol* 13:1145-1149.
- Birnby DA, Link EM, Vowels JJ, Tian H, Colacurcio PL, and Thomas JH (2000).** A transmembrane guanylyl cyclase (DAF-11) and Hsp90 (DAF-21) regulate a common set of chemosensory behaviors in *Caenorhabditis elegans*. *Genetics* 155:85-104.
- Bishop NA and Guarente L (2007).** Two neurons mediate diet-restriction-induced longevity in *C. elegans*. *Nature* 447:545-9.
- Blacque OE, Reardon MJ, Li C, McCarthy J, Mahjoub MR, Ansley SJ, Badano JL, Mah AK, Beales PL, Davidson WS, Johnsen RC, Audeh M, Plasterk RH, Baillie DL, Katsanis N, Quarmby LM, Wicks SR and Leroux MR (2004).** Loss of *C. elegans* BBS-7 and BBS-8 protein function results in cilia defects and compromised intraflagellar transport. *Genes Dev.* 18:1630-1642.
- Blacque OE, Perens EA, Boroevich KA, Inglis PN, Li C, Warner A, Khattri J, Holt RA, Ou G, Mah**

**AK, et al. (2005).** Functional genomics of the cilium, a sensory organelle. *Curr Biol* 15: 935-941.

**Blaineau C, Tessier M, Dubessay P, Tasse L, Crobu L, Pages M and Bastien P (2007).** A novel microtubule-depolymerizing kinesin involved in length control of a eukaryotic flagellum. *Curr Biol* 17(9):778-82.

**Bounoutas A and Chalfie M (2007).** Touch sensitivity in *Caenorhabditis elegans*. *Pflugers Arch* 454(5):691-702

**Bozza T, McGann JP, Mombaerts P and Wachowiak M (2004).** In vivo imaging of neuronal activity by targeted expression of a genetically encoded probe in the mouse. *Neuron* 42(1):9-21.

**Brazeau P, Vale W, Burgus R, Ling N, Rivier J and Guillemin R (1972).** Hypothalamic polypeptide that inhibits the secretion of immunoreactive pituitary growth hormone. *Science* 129:77-79.

**Brazeau P, Ling N, Esch F, Bohlen P, Benoit R and Guillemin R (1981).** High biological activity of the synthetic replicates of somatostatin-28 and somatostatin-25. *Regul Peptides* 1: 255-264.

**Brenner S (1974).** The genetics of *Caenorhabditis elegans*. *Genetics* 77:71-94.

**Carter NJ, Cross RA (2005).** Mechanics of the kinesin step. *Nature* 435: 308-312.

**Chalasani SH, Chronis N, Tsunozaki M, Gray JM, Ramot, Goodman MB and Bargmann CI (2007).** Dissecting a circuit for olfactory behaviour in *Caenorhabditis elegans*. *Nature* 450:63-70.

**Chang AJ, Chronis N, Karow DS, Marletta MA and Bargmann CI (2006).** A distributed chemosensory circuit for oxygen preference in *C. elegans*. *PLoS Biol* 4(9):e274.

**Chang S, Johnston RJ Jr and Hobert O (2003).** A transcriptional regulatory cascade that controls left/right asymmetry in chemosensory neurons of *C. elegans*. *Genes Dev* 17(17):2123-37.

**Chang S, Johnston RJ Jr, Froekjaer-Jensen C, Lockery S and Hobert O (2004).** MicroRNAs act sequentially and asymmetrically to control chemosensory laterality in the nematode. *Nature* 430:785-9.

**Chen N, Mah A, Blacque OE, Chu J, Phgora K, Bakhoum MW, Newbury CRH, Khattra J, Chan S, Go A, et al. (2006).** Identification of ciliary and ciliopathy genes in *Caenorhabditis elegans* through comparative genomics. *Genome Biol* 7: R126.

**Cheung BHH, Arellano-Carbajal F, Rybicki I and de Bono M. (2005).** Soluble guanylate cyclases act in neurons exposed to the body fluid to promote *C. elegans* aggregation behaviour. *Curr Biol* 15(10):905-17

**Coates JC and de Bono M (2002).** Antagonistic pathways in neurons exposed to body fluid regulate social feeding in *Caenorhabditis elegans*. *Nature* 419:925-9

**Colbert HA and Bargmann CI (1995).** Odorant-specific adaptation pathways generate olfactory plasticity in *C. elegans*. *Neuron* 14(4):803-12.

**Colbert HA, Smith TL and Bargmann CI (1997).** OSM-9, a novel protein with structural similarity to channels, is required for olfaction, mechanosensation, and olfactory adaptation in *Caenorhabditis elegans*. *J Neurosci* 17(21):8259-69

**Cole DG (2003).** The intraflagellar transport machinery of *Chlamydomonas reinhardtii*. *Traffic* 4: 435-442.

**Colosimo M, Brown A, Mukhopadhyay S, Gabel C, Lanjuin A, Samuel A, Sengupta P (2004).**

Identification of thermosensory and olfactory neuron-specific genes via expression profiling of single neuron types. *Curr Biol* 14: 2245-2251.

**Conte C, Guarin E, Marcuz A and Andres-Barquin PJ (2006).** Functional expression of mammalian taste receptors in *Caenorhabditis elegans*. *Biochimie* 88(7):801-6.

**Davenport JR, Watts AJ, Roper VC, Croyle MJ, Groen van T, Wyss JM, Nagy TR, Kesterson RA and Yoder BK (2007).** Disruption of Intraflagellar Transport in Adult Mice Leads to Obesity and Slow-Onset Cystic Kidney Disease *Curr Biol*, 17(18):1586-94.

**de Bono M, and Bargmann C I (1998).** Natural variation in a neuropeptide Y receptor homolog modifies social behavior and food response in *C. elegans*. *Cell* 94:679-689.

**de Bono M, Tobin DM, Davis MW, Avery L and Bargmann CI (2002).** Social feeding in *Caenorhabditis elegans* is induced by neurons that detect aversive stimuli. *Nature* 419:899-903.

**Dentler W (2005).** Intraflagellar transport (IFT) during assembly and disassembly of *Chlamydomonas* flagella. *J Cell Biol* 170:649-659.

**Dunn NA, Lockery SR, Pierce-Shimomura JT, Conery JS (2004).** A neural network model of chemotaxis predicts functions of synaptic connections in the nematode *Caenorhabditis elegans*. *J Comput Neurosci* 17(2):137-47.

**Dusenbery DB (1980).** Responses of the nematode *Caenorhabditis elegans* to controlled chemical stimulation. *J Comp Physiol [A]* 136:327-331.

**Efimenko E, Bubb K, Mak HY, Holzman T, Leroux MR, Ruvkun G, Thomas JH, Swoboda P (2005).** Analysis of *xbx* genes in *C. elegans*. *Development* 132: 1923-1934.

**Ehlers MD, Heine M, Groc L, Lee M-C and Choquet D (2007).** Diffusional trapping of GluR1 AMPA receptors by input-specific synaptic activity. *Neuron* 54(3):447-60.

**Evans JE, Snow JJ, Gunnarson AL, Ou G, Stahlberg H, McDonald KL and Scholey JM (2006).** Functional modulation of IFT kinesins extends the sensory repertoire of ciliated neurons in *Caenorhabditis elegans*. *J Cell Biol* 172:663-669.

**Feldman DE and Brecht M (2005).** Map Plasticity in Somatosensory Cortex. *Science* 310:810-815

**Ferguson SS (2004).** Evolving concepts in G protein-coupled receptor endocytosis: the role in receptor desensitisation and signalling. *Pharmacol Rev* 53:1-24.

**Ferkey DM, Hyde R, Haspel G, Dionne HM, Hess HA, Suzuki H, Schafer WR, Koelle MR and Hart AC (2007).** *C. elegans* G Protein Regulator RGS-3 Controls Sensitivity to Sensory Stimuli. *Neuron* 53:39-52.

**Finney M and Ruvkun G (1990).** The *unc-86* gene product couples cell lineage and cell identity in *C. elegans*. *Cell* 63:895-905.

**Frey U and Morris RG (1997).** Synaptic tagging and longterm potentiation. *Nature* 385:533-536

**Fujiwara M, Ishihara T and Katsura I (1999).** A novel WD40 protein, CHE-2, acts cell-autonomously in the formation of *C. elegans* sensory cilia. *Development* 126:4839-4848.

**Fukushige T, Hendzel MJ, Bazett-Jones DP and McGhee JD (1999).** Direct visualisation of the *elt-2* gut-specific GATA factor binding to a target promoter inside the living *Caenorhabditis elegans* embryo. *Proc Natl Acad Sci USA* 96: 11883-11888.



**Gainetdinov RR, Premont RT, Bohn LM, Lefkowitz RJ and Caron MG (2004).** Desensitization of G protein-coupled receptors and neuronal functions. *Annu Rev Neurosci* 27:107-44.

**Gerisch B, Weitzel C, Kober-Eisermann C, Rottiers V and Antebi A (2001).** A hormonal signaling pathway influencing *C. elegans* metabolism, reproductive development, and life span. *Dev Cell* 1:841-851.

**Golden JW, and Riddle DL (1982).** A pheromone influences larval development in the nematode *Caenorhabditis elegans*. *Science* 218:578-580.

**Goodman MB, Hall DH, Avery L and Lockery SR (1998).** Active Currents Regulate Sensitivity and Dynamic Range in *C. elegans* Neurons. *Neuron* 20:763-772.

**Goodman MB.** Mechanosensation (January 06, 2006), WormBook, ed. The *C. elegans* Research Community, WormBook, doi/10.1895/wormbook.1.62.1, <http://www.wormbook.org>.

**Gray JM, Hill JJ, Bargmann CI (2005).** A circuit for navigation in *Caenorhabditis elegans*. *Proc Natl Acad Sci USA* 102(9):3184-91.

**Gray JM, Karow DS, Lu H, Chang AJ, Chang JS, Ellis RE, Marletta MA and Bargmann CI (2004).** Oxygen sensation and social feeding mediated by a *C. elegans* guanylate cyclase homologue. *Nature* 430:317-22.

**Guan Z, Giustetto M, Lomvardas S, Kim JH, Miniaci MC, Schwartz JH, Thanos D and Kandel ER.(2002).** Integration of long-term-memory-related synaptic plasticity involves bidirectional regulation of gene expression and chromatin structure. *Cell* 111(4):483-93.

**Gudermann T, Kalkbrenner F and Schultz G (1996).** Diversity and selectivity of receptor-G protein interaction. *Annu Rev Pharmacol Toxicol* 36:429-459.

**Guillaud L, Setou M and Hirokawa N (2003).** KIF17 dynamics and regulation of NR2B trafficking in hippocampal neurons. *J Neurosci* 23(1):131-40.

**Guillaud L, Wong R and Hirokawa N (2008).** Disruption of KIF17-Mint1 interaction by CaMKII-dependent phosphorylation: a molecular model of kinesin-cargo release. *Nat Cell Biol* 10(1):19-29.

**Händel M, Schulz S, Stanarius A, Schreff M, Erdtmann-Vourliotis M, Schmidt H, Wolf G and Hähl V (1999).** Selective targeting of somatostatin receptor 3 to neuronal cilia. *Neuroscience* 89(3):909-26.

**Hart AC, Kass J, Shapiro JE, Kaplan JM (1999).** Distinct signaling pathways mediate touch and osmosensory responses in a polymodal sensory neuron. *J Neurosci* 19:1952-1958.

**Hart AC, Sims S and Kaplan JM (1995).** Synaptic code for sensory modalities revealed by *C. elegans* GLR-1 glutamate receptor. *Nature* 378:82-85.

**Hausdorff WP, Caron MG and Lefkowitz RJ (1990).** Turning off the signal: desensitization of beta-adrenergic receptor function. *FASEB J* 4:2881-2889.

**Haycraft CJ, Schafer JC, Zhang Q, Taulman PD and Yoder BK (2003).** Identification of CHE-13, a novel intraflagellar transport protein required for cilia formation. *Exp Cell Res* 284: 251-263.

**Haycraft CJ, Swoboda P, Taulman PD, Thomas JH and Yoder BK (2001).** The *C. elegans* homolog of the murine cystic kidney disease gene *Tg737* functions in a ciliogenic pathway and is disrupted in *osm-5* mutant worms. *Development* 128:1493-1505.

- Hebb DO. (1949)** The Organization of Behavior; a Neuropsychological Theory (Wiley, New York, 1949)
- Hedgecock EM, and Russell RL (1975).** Normal and mutant thermotaxis in the nematode *Caenorhabditis elegans*. *Proc Natl Acad Sci USA* 72:4061-4065.
- Hedgecock EM, Culotti JG, Thomson JN, Perkins LA (1985).** Axonal guidance mutants of *Caenorhabditis elegans* identified by filling sensory neurons with fluorescein dyes. *Dev Biol* 111: 158-170.
- Hermans E (2003).** Biochemical and pharmacological control of multiplicity of coupling at G-protein-coupled receptors. *Pharmacol Therap* 99:25-44.
- Hilliard MA, Bargmann CI and Bazzicalupo P (2002).** *C. elegans* responds to chemical repellents by integrating sensory inputs from the head and the tail. *Curr Biol* 12(9):730-4.
- Hilliard MA, Bergamasco C, Arbucci S, Plasterk RH and Bazzicalupo P (2004).** Worms taste bitter: ASH neurons, QUI-1, GPA-3 and ODR-3 mediate quinine avoidance in *Caenorhabditis elegans*. *EMBO J* 23(5):1101-11
- Hilliard MA, Apicella AJ, Kerr R, Suzuki H, Bazzicalupo P and Schafer WR (2005).** In vivo imaging of *C. elegans* ASH neurons: cellular response and adaptation to chemical repellents. *EMBO J* 24(1):63-72
- Hobert O, Mori I, Yamashita Y, Honda H, Ohshima Y, Liu Y and Ruvkun G (1997).** Regulation of interneuron function in the *C. elegans* thermoregulatory pathway by the *ttx-3* LIM homeobox gene. *Neuron* 19(2):345-57.
- Hobert O (2002).** PCR fusion-based approach to create reporter gene constructs for expression analysis in transgenic *C. elegans*. *Biotechniques* 32: 728-730.
- Hobert O (2003).** Behavioral plasticity in *C. elegans*: paradigms, circuits, genes. *J Neurobiol* 54(1):203-23.
- Huangfu D, Liu A, Rakeman AS, Murcia NS, Niswander L and Anderson KV (2003).** Hedgehog signalling in the mouse requires intraflagellar transport proteins. *Nature* 426:83-87.
- Hucho T and Levine JD (2007).** Signaling pathways in sensitization: toward a nociceptor cell biology. *Neuron* 55(3), 365-76
- Hukema RK, Rademakers S, Dekkers MPJ, Burghoorn J and Jansen G (2006).** Antagonistic sensory cues generate gustatory plasticity in *Caenorhabditis elegans*. *EMBO J* 25(2):312-22.
- Hukema RK (2006).** Gustatory behaviour in *Caenorhabditis elegans*, Doctoral thesis
- Ishihara T, Iino Y, Mohri A, Mori I, Gengyo-Ando K, Mitani S and Katsura I (2002).** HEN-1, a secretory protein with an LDL receptor motif, regulates sensory integration and learning in *Caenorhabditis elegans*. *Cell* 109(5):639-49.
- Janetopoulos C, Jin T and Devreotes P (2001).** Receptor-mediated activation of heterotrimeric G-proteins in living cells. *Science* 291:2408-11.
- Jansen G, Thijssen KL, Werner P, van der Horst M, Hazendonk E and Plasterk RH (1999).** The complete family of genes encoding G proteins of *Caenorhabditis elegans*. *Nat Genet* 21:414-419.
- Jansen G, Weinkove D and Plasterk RH (2002).** The G-protein gamma subunit *gpc-1* of the nema-

tode *C.elegans* is involved in taste adaptation. *EMBO J* 21(5):986-94.

**Jenkins PM, Hurd TW, Zhang L, McEwen DP, Brown RL, Margolis B, Verhey KJ and Martens JR (2006).** Ciliary Targeting of Olfactory CNG Channels Requires the CNGB1b Subunit and the Kinesin-2 Motor Protein, KIF17. *Curr Biol* 16:1211-1216.

**Jin Y.** Synaptogenesis (December 23, 2005), WormBook, ed. The *C. elegans* Research Community, WormBook, doi/10.1895/wormbook.1.44.1, <http://www.wormbook.org>.

**Johnston RJ Jr and Hobert O (2003).** A microRNA controlling left/right neuronal asymmetry in *Caenorhabditis elegans*. *Nature* 426:845-9.

**Johnston RJ Jr, Chang S, Etchberger JF, Ortiz CO and Hobert O (2005).** MicroRNAs acting in a double-negative feedback loop to control a neuronal cell fate decision. *Proc Natl Acad Sci USA* 102(35):12449-54

**Kandel ER and Schwartz JH (1982).** Molecular biology of learning: modulation of transmitter release. *Science* 218(4571):433-43.

**Kerr R, Lev-Ram V, Baird G, Vincent P, Tsien RY and Schafer WR (2000).** Optical imaging of calcium transients in neurons and pharyngeal muscle of *C. elegans*. *Neuron* 26(3):583-94.

**Kindt KS, Quast KB, Giles AC, De S, Hendrey D, Nicastro I, Rankin CH and Schafer WR (2007).** Dopamine mediates context-dependent modulation of sensory plasticity in *C. elegans*. *Neuron* 55(4):662-76.

**Knöpfel T, Tomita K, Shimazaki R and Sakai R (2003).** Optical recordings of membrane potential using genetically targeted voltage-sensitive fluorescent proteins. *Methods* 30(1):42-8.

**Kodama E, Kuhara A, Mohri-Shiomi A, Kimura KD, Okumura M, Tomioka M, Iino Y and Mori I (2006).** Insulin-like signaling and the neural circuit for integrative behavior in *C. elegans*. *Genes Dev* 20(21):2955-60.

**Kwok BH, Kaptein LC, Kim JH, Peterman EJG, Schmidt CE, Kapoor TM (2006).** Allosteric inhibition of kinesin-5 modulates its processive directional motility. *Nat Chem Biol* 9: 480-485.

**Lamprecht R and LeDoux J (2004).** Structural plasticity and memory. *Nat Rev Neurosci.* 5(1), 45-54.

**Lans H, Rademakers S and Jansen G (2004).** A Network of stimulatory and inhibitory G-subunits regulates olfaction in *Caenorhabditis elegans*. *Genetics* 167(4):1677-1688

**Law E, Nuttley WM and van der Kooy D (2004).** Contextual taste cues modulate olfactory learning in *C. elegans* by an occasion-setting mechanism. *Curr Biol* 14(14):1303-8.

**Levenson JM and Sweatt JD (2005).** Epigenetic mechanisms in memory formation. *Nat Rev Neurosci* 6(2):108-18.

**Li C, Kim K and Nelson LS (1999).** FMRFamide-related neuropeptide gene family in *Caenorhabditis elegans*. *Brain Res* 848(1-2):26-34.

**Li W, Kennedy SG, and Ruvkun G (2003).** *daf-28* encodes a *C. elegans* insulin superfamily member that is regulated by environmental cues and acts in the DAF-2 signaling pathway. *Genes Dev.* 17, 844-858.

**Li X, Gutierrez DV, Hanson MG, Han J, Mark MD, Chiel H, Hegemann P, Landmesser LT and**

- Herlitze S (2005).** Fast noninvasive activation and inhibition of neural and network activity by vertebrate rhodopsin and green algae channelrhodopsin. *Proc Natl Acad Sci USA* 102(49):17816-21
- Liedtke W, Tobin DM, Bargmann CI and Friedman JM (2003).** Mammalian TRPV4 (VR-OAC) directs behavioral responses to osmotic and mechanical stimuli in *Caenorhabditis elegans*. *Proc Natl Acad Sci USA* 100 Suppl 2:14531-6.
- Lisman J, Schulman H and Cline H (2002).** The molecular basis of CaMKII function in synaptic and behavioural memory. *Nat Rev Neurosci* 3(3):175-90.
- Marshall WF, Rosenbaum JL (2001).** Intraflagellar transport balances continuous turnover of outer doublet microtubules: implications for flagellar length control. *J Cell Biol* 155: 405-414.
- Marszalek JR, Liu X, Roberts EA, Chui D, Marth JD, Williams DS and Goldstein LS (2000).** Genetic evidence for selective transport of opsin and arrestin by kinesin-II in mammalian photoreceptors. *Cell* 102:175187.
- Matsuki M, Kunitomo H and Iino Y (2006).** Go $\alpha$  regulates olfactory adaptation by antagonizing Gq $\alpha$ -DAG signaling in *Caenorhabditis elegans*. *Proc Natl Acad Sci USA* 103(4):1112-7.
- Matsushime H, Jinno A, Takagi N, Shibuya M (1990).** A novel mammalian protein kinase gene (mak) is highly expressed in testicular germ cells at and after meiosis. *Mol Cell Biol* 10: 2261-2268.
- Mellem JE, Brocki PJ, Zheng Y, Madsen DM and Maricq AV (2002).** Decoding of polymodal sensory stimuli by postsynaptic glutamate receptors in *C. elegans*. *Neuron* 36(5):933-44.
- Mello CC, Kramer JM, Stinchcomb D and Ambros V (1991).** Efficient gene transfer in *C. elegans*: extrachromosomal maintenance and integration of transforming sequences. *EMBO J* 10: 3959-3970
- Mello C and Fire A (1995).** DNA transformation. In *Caenorhabditis elegans: Modern Biological Analysis of an Organism*, H.F. Epstein and D.C. Shakes eds. (Academic Press, San Diego), pp451-482.
- Mesland DA, Hoffman JL, Caligor E and Goodenough UW (1980).** Flagellar tip activation stimulated by membrane adhesions in *Chlamydomonas* gametes. *J Cell Biol* 84:599-617.
- Miesenböck G, De Angelis DA and Rothman JE (1998).** Visualizing secretion and synaptic transmission with pH-sensitive green fluorescent proteins. *Nature* 394:192-5.
- Milani N, Guarin E, Renfer E, Nef P and Andres-Barquin PJ (2002).** Functional expression of a mammalian olfactory receptor in *Caenorhabditis elegans*. *Chem Neurosci* 13:2515-2520.
- Minke B and Cook B (2002).** TRP channel proteins and signal transduction. *Physiol Rev* 82(2):429-72.
- Miyata Y, Akashi M, Nishida E (1999).** Molecular cloning and characterization of a novel member of the MAP kinase superfamily. *Genes Cells* 4: 299-309.
- Miyawaki A, Llopis J, Heim R, McCaffery JM, Adams JA, Ikura M, Tsien RY (1997).** Fluorescent indicators for Ca<sup>2+</sup> based on green fluorescent proteins and calmodulin. *Nature* 388:882-887
- Miyawaki A (2003).** Fluorescence imaging of physiological activity in complex systems using GFP-based probes. *Curr Op Neurobiol* 13(5):591-596.
- Miyawaki A (2005).** Innovations in the Imaging of Brain Functions using Fluorescent Proteins. *Neuron* 48(2):189-199.

**Mori I (1999).** Genetics of chemotaxis and thermotaxis in the nematode *Caenorhabditis elegans*. *Annu Rev Genet* 399-422.

**Murakami M, Koga M and Ohshima Y (2001).** DAF-7/TGF-beta expression required for the normal larval development in *C. elegans* is controlled by a presumed guanylyl cyclase DAF-11. *Mech Dev* 109:27-35.

**Nagai T, Ibata K, Park ES, Kubota M, Mikoshiba K, Miyawaki A (2002).** A variant of yellow fluorescent protein with fast and efficient maturation for cell-biological applications. *Nat Biotech* 20(1):87-90.

**Nagel G, Brauner M, Liewald JF, Adeishvili N, Bamberg E and Gottschalk A (2005).** Light activation of channelrhodopsin-2 in excitable cells of *Caenorhabditis elegans* triggers rapid behavioral responses. *Curr Biol* 15(24):2279-84.

**Nakai J, Ohkura M and Imoto K (2001).** A high signal-to-noise Ca<sup>2+</sup> probe composed of a single green fluorescent protein. *Nat Biotech* 19:137-141.

**Ng M, Roorda RD, Lima SQ, Zemelman BV, Morcillo P and Miesenböck G (2002).** Transmission of olfactory information between three populations of neurons in the antennal lobe of the fly. *Neuron* 36(3):463-74.

**Nguyen RL, Tam LW, Lefebvre PA (2005).** The LF1 gene of *Chlamydomonas reinhardtii* encodes a novel protein required for flagellar length control. *Genetics* 169:1415-1424.

**Nonet ML (1999).** Visualization of synaptic specializations in live *C. elegans* with synaptic vesicle protein-GFP fusions. *J Neurosci Methods* 89(1):33-40.

**Nuttley WM, Harbinder S and van der Kooy D (2001).** Regulation of distinct attractive and aversive mechanisms mediating benzaldehyde chemotaxis in *Caenorhabditis elegans*. *Learn Mem* 8(3):170-81.

**Orozco JT, Wedaman KP, Signor D, Brown H, Rose L and Scholey JM (1999).** Movement of motor and cargo along cilia. *Nature* 398:674.

**Ou G, Blacque OE, Snow JJ, Leroux MR and Scholey JM (2005a).** Functional coordination of intraflagellar transport motors. *Nature* 436:583-587.

**Ou G, Qin H, Rosenbaum JL and Scholey JM (2005b).** The PKD protein qilin undergoes intraflagellar transport. *Curr Biol* 15:R410-411.

**Palmitessa A, Hess HA, Bany IA, Kim YM, Koelle MR and Benovic JL (2005).** *Caenorhabditis elegans* arrestin regulates neuronal G protein signaling and olfactory adaptation and recovery. *J Biol Chem* 280:24649-24662.

**Pan J, Snell WJ (2005).** *Chlamydomonas* shortens its flagella by activating axonemal disassembly, stimulating IFT particle trafficking, and blocking anterograde cargo loading. *Dev Cell* 9(3):431-8.

**Pan J, Wang Q and Snell WJ (2005).** Cilium-generated signaling and cilia-related disorders. *Lab Invest* 85, 452-463.

**Pan J and Snell W (2007).** The primary cilium: keeper of the key to cell division. *Cell* 129(7):1255-7.

**Pan X, Ou G, Civelekoglu-Scholey G, Blacque OE, Endres NF, Tao L, Mogilner A, Leroux MR, Vale RD, Scholey JM (2006).** Mechanism of transport of IFT particles in *C. elegans* cilia by the

concerted action of kinesin-II and OSM-3 motors. *J Cell Biol* 174: 1035-1045.

**Pazour GJ and Witman GB (2003).** The vertebrate primary cilium is a sensory organelle. *Curr Opin Cell Biol* 15, 105-110.

**Pazour GJ, Agrin N, Leszyk J, Witman GB (2005).** Proteomic analysis of a eukaryotic cilium. *J Cell Biol* 170: 103-113.

**Peden EM, and Barr MM (2005).** The KLP-6 kinesin is required for male mating behaviors and polycystin localization in *Caenorhabditis elegans*. *Curr Biol* 15, 394-404.

**Perens EA and Shaham S (2005).** *C. elegans* daf-6 encodes a patched-related protein required for lumen formation. *Dev Cell* 8, 893-906.

**Perkins LA, Hedgecock EM, Thomson JN and Culotti JG (1986).** Mutant sensory cilia in the nematode *Caenorhabditis elegans*. *Dev Biol* 117, 456-487.

**Pierce-Shimumora JT, Faumont S, Gaston MR, Pearson BJ and Lockery SR (2001).** The homeobox gene *lim-6* is required for distinct chemosensory representations in *C. elegans*. *Nature* 410:694-8

**Pierce-Shimomura JT, Morse TM and Lockery SR (1999).** The fundamental role of pirouettes in *Caenorhabditis elegans* chemotaxis. *J Neurosci* 19(21):9557-69.

**Pitcher JA, Freedman NJ and Lefkowitz RJ (1998).** G protein-coupled receptor kinases. *Annu Rev Biochem* 67:653-692.

**Pradayrol L, Jornvall, H, Mutt V and Ribet A (1980).** N-terminally extended somatostatin: the primary structure of somatostatin-28. *FEBS Lett* 109: 55-58.

**Price LA, Kajkowski EM, Hadcock JR, Ozenberger BA and Pausch MH (1995).** Functional coupling of a mammalian somatostatin receptor to the yeast pheromone response pathway. *Mol Cell Biol* 15:6188-6195.

**Price TD, Qvarnström A and Irwin DE (2003).** The role of phenotypic plasticity in driving genetic evolution. *Proc Biol Sci.* 270(1523): 1433-1440.

**Pugacheva EN, Jablonski SA, Hartman TR, Henske EP and Golemis EA (2007).** HEF1-dependent Aurora A activation induces disassembly of the primary cilium. *Cell* 129(7):1351-63.

**Qin H, Burnette DT, Bae YK, Forscher P, Barr MM and Rosenbaum JL (2005).** Intraflagellar transport is required for the vectorial movement of TRPV channels in the ciliary membrane. *Curr Biol* 15:1695-1699.

**Qin H, Diener DR, Geimer S, Cole DG and Rosenbaum JL (2004).** Intraflagellar transport (IFT) cargo: IFT transports flagellar precursors to the tip and turnover products to the cell body. *J Cell Biol* 164:255-266.

**Qin H, Rosenbaum JL and Barr MM (2001).** An autosomal recessive polycystic kidney disease gene homolog is involved in intraflagellar transport in *C. elegans* ciliated sensory neurons. *Curr Biol* 11:457-461.

**Qin H, Wang Z, Diener D and Rosenbaum J (2007).** Intraflagellar Transport Protein 27 Is a Small G Protein Involved in Cell-Cycle Control. *Curr Biol*, 17(3), 193-202

**Rankin CH, Beck CD and Chiba CM (1990).** *Caenorhabditis elegans*: a new model system for the study of learning and memory. *Behav Brain Res* 37:89-92.

**Reed NA, Cai D, Blasius TL, Jih GT, Meyhofer E, Gaertig J, Verhey KJ (2006).** Microtubule acetylation promotes kinesin-1 binding and transport. *Curr Biol* 16: 2166-2172.

**Reiter E and Lefkowitz RJ (2006).** GRKs and beta-arrestins: roles in receptor silencing, trafficking and signaling. *Trends Endocrinol Metab* 17(4):159-65.

**Remy JJ and Hobert O (2005).** An interneuronal chemoreceptor required for olfactory imprinting in *C. elegans*. *Science* 309:787-90.

**Ren P, Lim CS, Johnsen R, Albert PS, Pilgrim D and Riddle DL (1996).** Control of *C. elegans* larval development by neuronal expression of a TGF-beta homolog. *Science* 274, 1389-1391.

**Riddle DL and Albert PS (1997).** Genetic and environmental regulation of dauer larva development. In *C. elegans II*. Riddle, D.L., Blumenthal, T., Meyer, B.J., and Priess, J.R. eds. (Cold Spring Harbor Laboratory Press, New York, NY), pp. 739-768.

**Roayaie K, Crump JG, Sagasti A and Bargmann CI (1998).** The G alpha protein ODR-3 mediates olfactory and nociceptive function and controls cilium morphogenesis in *C. elegans* olfactory neurons. *Neuron* 20(1):55-67.

**Rohatgi R, Milenkovic L and Scott MP (2007).** Patched1 Regulates Hedgehog Signaling at the Primary Cilium. *Science* 317:372-6.

**Rongo C, Whitfield CW, Rodal A, Kim SK and Kaplan JM (1998).** LIN-10 is a shared component of the polarized protein localization pathways in neurons and epithelia. *Cell* 94(6):751-9.

**Rosenbaum JL and Witman GB (2002).** Intraflagellar transport. *Nat. Rev. Mol. Cell Biol.* 3, 813-825.

**Rossi D and Zlotnik A (2000).** The biology of chemokines and their receptors. *Annu Rev Immunol* 18: 217-242.

**Saeki S, Yamamoto M, Iino Y (2001).** Plasticity of chemotaxis revealed by paired presentation of a chemoattractant and starvation in the nematode *Caenorhabditis elegans*. *J Exp Biol* 204(Pt 10):1757-64.

**Sagasti A, Hobert O, Troemel ER, Ruvkun G and Bargmann CI (1999).** Alternative olfactory neuron fates are specified by the LIM homeobox gene *lim-4*. *Genes Dev* 13(14):1794-806.

**Sakai R, Repunte-Canonigo V, Raj CD and Knöpfel T (2001).** Design and characterization of a DNA-encoded, voltage-sensitive fluorescent protein. *Eur J Neurosci* 13(12):2314-8.

**Sanyal S, Wintle RF, Kindt KS, Nuttley WM, Arvan R, Fitzmaurice P, Bigras E, Merz DC, Hebert TE, van der Kooy D, Schafer WR, Culotti JG and Van Tol HH (2004).** Dopamine modulates the plasticity of mechanosensory responses in *Caenorhabditis elegans*. *EMBO J* 23(2):473-82.

**Schafer JC, Haycraft CJ, Thomas JH, Yoder BK and Swoboda P (2003).** *XBX-1* encodes a dynein light intermediate chain required for retrograde intraflagellar transport and cilia assembly in *Caenorhabditis elegans*. *Mol Biol Cell* 14:2057-2070.

**Schneider L, Clement CA, Teilmann SC, Pazour GJ, Hoffmann EK, Satir P and Christensen ST (2005).** PDGFRalpha signaling is regulated through the primary cilium in fibroblasts. *Curr Biol* 15(20):1861-6.

**Scholey, J.M. (2003).** Intraflagellar transport. *Annu. Rev. Cell Dev. Biol.* 19, 423-443.



- Setou M, Nakagawa T, Seog DH and Hirokawa N (2000).** Kinesin superfamily motor protein KIF17 and mLin-10 in NMDA receptor-containing vesicle transport. *Science* 288, 1796-1802.
- Shen K and Bargmann CI (2003).** The immunoglobulin superfamily protein SYG-1 determines the location of specific synapses in *C. elegans*. *Cell* 112(5):619-30.
- Shtonda BB and Avery L (2006).** Dietary choice behavior in *Caenorhabditis elegans*. *J Exp Biol* 209(Pt 1):89-102.
- Sieburth D, Ch'ng Q, Dybbs M, Tavazoie M, Kennedy S, Wang D, Dupuy D, Rual JF, Hill DE, Vidal M, Ruvkun G and Kaplan JM (2005).** Systematic analysis of genes required for synapse structure and function. *Nature* 436(7050):510-7.
- Singla V and Reiter JF (2006).** The primary cilium as the cell's antenna: signaling at a sensory organelle. *Science* 313:629-33.
- Signor D, Wedaman KP, Orozco JT, Dwyer ND, Bargmann CI, Rose LS, and Scholey JM (1999).** Role of a class DHC1b dynein in retrograde transport of IFT motors and IFT raft particles along cilia, but not dendrites, in chemosensory neurons of living *Caenorhabditis elegans*. *J Cell Biol* 147:519-530.
- Slessareva JE, Routt SM, Temple B, Bankaitis VA and Dohlman HG (2006).** Activation of the Phosphatidylinositol 3-Kinase Vps34 by a G Protein Subunit at the Endosome. *Cell* 126, 191-123
- Snow JJ, Ou G, Gunnarson AL, Walker MR, Zhou HM, Brust-Mascher I and Scholey JM (2004).** Two anterograde intraflagellar transport motors cooperate to build sensory cilia on *C. elegans* neurons. *Nat Cell Biol* 6:1109-1113.
- Spitzer NC (2006).** Electrical activity in early neuronal development. *Nature* 444, 707-712.
- Starich TA, Herman RK, Kari CK, Yeh WH, Schackwitz WS, Schuyler MW, Collet J, Thomas JH, Riddle DL (1995).** Mutations affecting the chemosensory neurons of *Caenorhabditis elegans*. *Genetics* 139: 171-188.
- Stolc V, Samanta MP, Tongprasit W, Marshall WF (2005).** Genome-wide transcriptional analysis of flagellar regeneration in *Chlamydomonas reinhardtii* identifies orthologs of ciliary disease genes. *Proc Natl Acad Sci USA* 102: 3703-3707.
- Sutton MA and Schuman EM (2006).** Dendritic protein synthesis, synaptic plasticity, and memory. *Cell* 127(1), 49-58.
- Swoboda P, Adler HT, Thomas JH (2000).** The RFX-type transcription factor DAF-19 regulates sensory neuron cilium formation in *C. elegans*. *Mol Cell* 5: 411-421.
- Tam LW, Dentler WL, Lefebvre PA (2003).** Defective flagellar assembly and length regulation in LF3 null mutants in *Chlamydomonas*. *J Cell Biol* 163: 597-607.
- Teilmann SC and Christensen ST (2005).** Localization of the angiopoietin receptors Tie-1 and Tie-2 on the primary cilia in the female reproductive organs. *Cell Biol Int* 29(5):340-6.
- Teilmann SC, Byskov AG, Pedersen PA, Wheatley DN, Pazour GJ and Christensen ST (2005).** Localization of transient receptor potential ion channels in primary and motile cilia of the female murine reproductive organs. *Mol Reprod Dev* 71(4):444-52.
- Togawa K, Yan YX, Inomoto T, Slaugenhaupt S, Rustgi AK (2000).** Intestinal cell kinase (ICK)



localizes to the crypt region and requires a dual phosphorylation site found in map kinases. *J Cell Physiol* 183: 129-139.

**Tomioka M, Adachi T, Suzuki H, Kunitomo H, Schafer WR and Iino Y (2006).** The insulin/PI 3-kinase pathway regulates salt chemotaxis learning in *Caenorhabditis elegans*. *Neuron* 51(5):613-25.

**Troemel ER, Chou JH, Dwyer ND, Colbert HA and Bargmann CI (1995).** Divergent seven transmembrane receptors are candidate chemosensory receptors in *C. elegans*. *Cell* 83(2):207-18.

**Tsalik EL and Hobert O (2003).** Functional mapping of neurons that control locomotory behavior in *Caenorhabditis elegans*. *J Neurobiol* 56(2):178-97

**Tully T (1996).** Discovery of genes involved with learning and memory: An experimental synthesis of Hirshian and Benzerian perspectives *Proc. Natl. Acad. Sci. USA* 93: 13460- 13467.

**Uchida O, Nakano H, Koga M, Oshima Y (2003).** The *C. elegans* che-1 gene encodes a zinc finger transcription factor required for specification of the ASE chemosensory neurons. *Development* 130: 12151224.

**van Rhee J and Jalink K (2002).** Agonist-induced PIP(2) hydrolysis inhibits cortical actin dynamics: regulation at a global but not at a micrometer scale. *Mol Biol Cell* 13(9):3257-67.

**van der Wal J, Habets R, Vrnai P, Balla T and Jalink K (2001).** Monitoring agonist-induced phospholipase C activation in live cells by fluorescence resonance energy transfer. *J Biol Chem* 276(18):15337-44.

**Veber DF, Hreidlinger RM, Perlow DS, Paleveda WJ Jr, Holly FW, Strachan RG, Nutt RF, Arison BH, Homnick C, Randall WC, Glizter MS, Saperstein R and Hirschmann R (1981).** A potent cyclic hexapeptide analogue of somatostatin. *Nature* 292: 55-58.

**Veber DF, Holly FW, Paleveda WJ, Nutt RF, Bergstrand SJ, Torchiana M, Glizter MS, Saperstein R and Hirschmann R (1978).** Conformationally restricted bicyclic analogs of somatostatin. *Proc Natl Acad Sci USA* 75:2636-2640.

**Wang Q, Pan J and Snell WJ (2006).** Intraflagellar transport particles participate directly in cilium-generated signaling in *Chlamydomonas*. *Cell* 125, 549-562.

**Ward S, Thomson N, White JG, and Brenner S (1975).** Electron microscopical reconstruction of the anterior sensory anatomy of the nematode *Caenorhabditis elegans*. *J. Comp. Neurol.* 160, 313-337.

**Ware RW, Clark D, Crossland K, Russell RL (1975).** The nerve ring of the nematode *C. elegans*: Sensory input and motor output. *J Comp Neurol* 162: 71-110.

**Watts VJ and Neve KA (2005).** Sensitization of adenylate cyclase by  $G\alpha$  i/o-coupled receptors. *Pharmacol Ther* 106, 405 421

**Wes PD and Bargmann CI (2001).** *C. elegans* odour discrimination requires asymmetric diversity in olfactory neurons. *Nature* 410:698-701

**White JG, Southgate E, Thomson JN, and Brenner S (1986).** The structure of the nervous system of the nematode *Caenorhabditis elegans*. *Philos Trans R Soc Lond B Biol Sci* 314:1-340.

**Wicks SR, de Vries CJ, van Luenen HG and Plasterk RH (2000).** CHE-3, a cytosolic dynein heavy chain, is required for sensory cilia structure and function in *Caenorhabditis elegans*. *Dev Biol*

221:295-307.

**Willars GB (2006).** Mammalian RGS proteins: multifunctional regulators of cellular signalling. *Semin Cell Dev Biol* 17(3):363-76

**Witman GB (2003).** Cell motility: deaf *Drosophila* keep the beat. *Curr Biol* 13: R796-798.

**Yang T, Jiang Y, Chen J (2002).** The identification and subcellular localization of human MRK. *Biomol Eng* 19: 1-4.

**Yu JH (2006).** Heterotrimeric G protein signaling and RGSs in *Aspergillus nidulans*. *J Microbiol* 44(2):145-54

**Zhang F, Wang LP, Brauner M, Liewald JE, Kay K, Watzke N, Wood PG, Bamberg E, Nagel G, Gottschalk A and Deisseroth K (2007).** Multimodal fast optical interrogation of neural circuitry. *Nature* 446:633-9.

**Zwaal RR, Mendel JE, Sternberg PW and Plasterk RH (1997).** Two neuronal G proteins are involved in chemosensation of the *Caenorhabditis elegans* Dauer-inducing pheromone. *Genetics* 145, 715-727.

*Was ich noch zu sagen hätte,  
Dauert eine Zigarette,  
Und ein letztes Glas im Steh'n.*

Inga & Wolf

# 8

## Appendix

## 8.1 Summary

All organisms perceive cues from their environment. However, the response to these stimuli depends on their context, on previous experiences, age and developmental stage. This flexibility in responsiveness is called plasticity, and has been found indispensable for many processes in biology, such as development and memory formation. We have studied behavioural and developmental plasticity in the nematode *Caenorhabditis elegans*, to gain insight into the molecular mechanisms of these processes.

We have studied chemosensation of NaCl as a model for behavioural plasticity. Normally, *C. elegans* is attracted to low concentrations of salt. However, when the animals have been exposed to NaCl prior to the assay, they strongly avoid all concentrations of NaCl. This behavioural switch is called gustatory plasticity. We have studied this using behavioural assays and single cell imaging, and found that the altered behaviour after pre-exposure can be explained by decreased sensitivity of the ASE attraction neurons, and an enhanced sensitivity of the ASH avoidance neurons.

In a parallel approach, we have introduced the rat TRP channel VR-1 and the human G-Protein Coupled Receptors (GPCRs) SSTR-2 and CCR-5 in specific sensory neurons of *C. elegans*. By exposing the nematodes to the ligands of these receptors, we were able to activate the transgene expressing cells. This technique allowed us to study the output of these neurons and the intracellular signalling routes.

We have studied the cilia of *C. elegans* as well. Cilia are the only part of the sensory neurons that are exposed to the environment in *C. elegans*, and play an important role in signalling. Therefore, this is a potential site for establishing plasticity. For proper function, cilia need to be maintained at a certain length. We have identified DYF-5, a conserved MAP kinase that plays a role in regulating the length of cilia. Fluorescence and electron microscopy revealed that the cilia of *dyf-5 loss-of-function (lf)* animals are elongated and not properly aligned into the amphid channel. Localization studies and motility measurements showed that DYF-5 is required for proper function of the specialized transport system in the cilia (Intra Flagellar Transport, IFT), and for correct localization of its components.

In addition, we describe the function of the G-protein GPA-3 in cilia. In the constitutively active mutant *gpa-3QL* the cilia are shortened, and the morphology of the cilia is disturbed. In addition, the IFT machinery is perturbed. Interestingly, we found that exposing the animals to dauer pheromone, a compound that induces a developmental switch called dauer formation, results in similar effects on morphology of the cilia and on IFT. We propose that environmental cues signal via G-proteins to regulate the constitution of IFT particles in the cilia, thereby altering its length and/or structure.

## 8.2 Samenvatting

Alle organismen kunnen signalen uit hun omgeving waarnemen en erop reageren. Echter, hoe op het signaal gereageerd wordt hangt af van de context van het signaal, van eerdere ervaringen, van de leeftijd en het ontwikkelingsstadium. Deze flexibiliteit wordt plasticiteit genoemd, en is essentieel voor vele biologische processen, zoals bijvoorbeeld ontwikkeling en geheugen. We hebben plasticiteit in gedrag en ontwikkeling bestudeerd in de nematode *Caenorhabditis elegans*, om zo inzicht te krijgen in de moleculaire mechanismen van deze processen.

We hebben de perceptie van NaCl genomen als model voor gedragsplasticiteit. Normalgesproken is *C. elegans* sterk aangetrokken tot lage concentraties zout. Echter, als deze wormen voor de proef aan NaCl zijn blootgesteld, verandert dit, en vermijden ze alle concentraties NaCl. Deze omschakeling in het gedrag noemen we smaakplasticiteit. Door middel van gedragsproeven en calcium metingen in enkele zenuwcellen hebben we gevonden dat het veranderde gedrag kan worden verklaard door een verminderde gevoeligheid van de ASE attractie cellen, en een toegenomen gevoeligheid van de ASH aversie cellen.

Als alternatieve benadering om dit gedrag te bestuderen, hebben we een TRP kanaal VR-1 uit de rat en G-eiwit gekoppelde receptoren SSTR-2 en CCR-5 uit de mens in specifieke zenuwcellen van *C. elegans* geïntroduceerd. Door de nematoden bloot te stellen aan de stoffen die binden aan deze receptoren kunnen we de cellen activeren waarin deze tot expressie komen. Deze techniek heeft ons in staat gesteld de functie van deze zenuwcellen in gedrag en de signaal routes binnen deze cellen te bestuderen.

We hebben ook de cilia van *C. elegans* bestudeerd. Cilia zijn de enige onderdelen van de sensore zenuwcellen van *C. elegans* die met de buitenwereld in contact staan, en spelen een belangrijke rol in signaaloverdracht. Daarom zou dit een plaats kunnen zijn waar plasticiteit wordt geregeld. Cilia moeten op de juiste lengte gehouden worden, hetgeen belangrijk is voor hun functie. We hebben DYF-5 geïdentificeerd, een eiwit dat een rol speelt in de regulatie van de lengte van de cilia. Door middel van fluorescentie en elektronen microscopie konden we laten zien dat zonder DYF-5 de cilia langer zijn, en niet goed met de buitenwereld in contact staan. Ook hebben we de localisatie en transportsnelheden van verschillende onderdelen van het Intra Flagellaire Transport (IFT) systeem bekeken. Dit liet zien dat DYF-5 belangrijk is voor de coordinatie en localisatie van de motor eiwitten in de cilia.

Daarnaast hebben we de functie van GPA-3 beschreven in de cilia. In de *gpa-3QL* mutant, waarin het GPA-3 eiwit altijd actief is, zijn de cilia korter, en is de morfologie verstoord. Ook is de IFT machinerie ontregeld. Als de wormen worden blootgesteld aan dauer feromoon, een stof die een bepaalde vorm van ontwikkelings plasticiteit teweeg brengt, vinden we soortgelijke effecten op de morfologie van de cilia en het IFT systeem. We stellen voor dat signalen uit de buitenwereld via GPA-3 de samenstelling van IFT partikels regelt, waardoor de lengte en/of structuur van de cilia verandert.

### 8.3 Dankwoord

Nou, dit is em dan: mijn kleine grote boek van wijsheid en geluk! Het heeft eventjes geduurd, en zonder de hulp van de volgende mensen was het er misschien nooit gekomen.

Allereerst de chef: Frank, bedankt dat je me hebt aangenomen om onderzoek te komen doen op jouw afdeling. Gert, Ik ben heel blij dat ik bij jou aan wormen heb mogen werken. De vrijheid die je me hebt gegeven bij het opzetten van de imaging, maar ook de af en toe opgetrokken wenkbrauw bij het tigste wilde plan waren precies goed. Ik wens je alle goeds, en hoop dat de microscopie technieken je daarbij kunnen helpen.

Ik wil ook de andere wormenmensen bedanken. Allereerst Renate, mijn AIO en congres maatje. De haarkleur veranderde dan zo af en toe, maar niet de discussies of gewoon het gezever over wormen, politiek of god weet wat. Ik ben heel blij dat ik je paranimf heb mogen zijn, en wens je heel veel succes en plezier in de rest van je carrière. Suzanne, de alleskunner. Ik heb veel van je geleerd, maar je efficiëntie is gewoon niet te evenaren. Ook het gemak waarmee je zelf dingen oppikt en uitvoert (jouw movies voor de snelheidsmetingen zijn echt top!) is ongelooflijk. Eva, fellow MD: if you ever long for non-flat sceneries: Basel is not far away! En dan waren er nog Hannes en Jan, onafscheidelijk. Oh Hannes, nogmaals bedankt voor Blackbird! Verder de mensen die het lab korter of langer bezocht hebben. Najat, mijn eerste echte eigen student. Helaas is het je ondanks verwoede pogingen niet gelukt een transgene worm te maken. En ook Rowin, Jessica, Noemí, Michelle the whirlwind, Ronald, Souad en Zeli (van de cake!), bedankt voor de leuke tijd.

Ook buiten het wormenlab hebben een heleboel mensen het verblijf op de afdeling Celbiologie en Genetica heel aangenaam gemaakt, teveel om hier te noemen. Natuurlijk hadden we een stel Hoxers in ons lab. Jeroen, danwel fluitend, danwel rochelend, en ook Laura, Begoña en Judith. En dan was er ook nog dat microtubule lab: iNiels, je enthousiasme is aanstekelijk, en het was erg fijn te discussieren over microtubules, appelflappen, microscopen of Macs. Het spijt me dat ik Katha zo af en toe van haar werk heb gehouden. Katha, ik heb de verhalen over de konijnen, jullie verre reizen en (natuurlijk) de FCS en andere data erg op prijs gesteld. Ik ben dan ook blij dat je mijn paranimf wil zijn op deze voor jou toch ook bijzondere dag. Jeff, gepassioneerd over wetenschap en bijna altijd opgewekt. Het was prettig met je te praten en (af en toe) met je te eten. Met de mensen van het lab van Anna (bedankt dat je in mijn grote commissie wilde zitten!) heb ik microscopisch lief en leed kunnen delen. Daniel: veel succes met je nieuwe carrière tussen de luiers, and Ilya, perhaps

you can give him some advice. I really enjoyed your company on the trips to test the fast confocals. The neighbours from lab 1002. Katrin, I appreciated our conversations a lot, and wish you all the best in Cambridge. Catherine, good luck with your first steps as a labhead.

Voor het wormenwerk heb je veel flessen agar nodig, en deze zijn allemaal geautoclaveerd en naar het lab gebracht door de dames van de spoelkeuken. Hartelijk dank daarvoor! Voor de hulp (en een luisterend oor) voor alle mogelijke zaken wil ik graag Melle, Jasperina en Marike bedanken. Marike, het was een eer om je te mogen spelen in de pantomime (For which I want to thank Laura G, you bring out the best in people!). Ook wil ik graag Gerard, Niels en Dies bedanken voor het lezen van mijn proefschrift. Jullie commentaren hebben het een stuk beter gemaakt.

Onontbeerlijk was de steun van die mensen die me zo af en toe weer in de normale wereld wisten te brengen. Mijn ouders en broertjes, maar ook Willem en Anne, Miranda, Henk en Anneke: bedankt!

De laatste is Karin, voor haar is het kusje!

## 8.4 Curriculum Vitae

### Personalia:

Naam: Martinus Petrus Josephus Dekkers (Martijn)  
Geboren: 28 februari 1976 te Velp(Gld.)

### Opleiding:

1988 - 1994: Gymnasium Het Rhedens Lyceum, Rozendaal  
1994 - 2000: Geneeskunde, Erasmus Universiteit Rotterdam  
2000 - 2002: Artsopleiding, Erasmus Universiteit Rotterdam  
2002 - 2007: AIO onderzoek in het lab van Dr Gert Jansen,  
Afdeling Cel Biologie & Genetica, Erasmus Universiteit Rotterdam  
2007 - heden: Post-Doc in het lab van Prof.dr. Yves Barde,  
Biozentrum, Universität Basel

### Publicaties en manuscripten:

**Martijn P.J. Dekkers** and Gert Jansen

*Altered sensitivity of ASE and ASH neurons explains gustatory plasticity in C. elegans*  
Submitted for publication.

Jan Burghoorn\*, **Martijn P.J. Dekkers\***, Suzanne Rademakers, Ton de Jong,  
Rob Willemsen and Gert Jansen

*Mutation of the MAP kinase DYF-5 affects docking and undocking of kinesin-2 motors  
and reduces their speed in the cilia of C. elegans*

Proceedings of the National Academy of Sciences, 2007 Apr 24;104(17):7157-62.  
contributed equally

Teng MS, **Dekkers MP**, Ng B, Rademakers S, Jansen G, Fraser AG, McCafferty J.

*Expression of mammalian GPCRs in C. elegans generates novel behavioural responses  
to human ligands.*

BMC Biology. 2006 Jul 20;4:22.

Hukema RK, Rademakers S, **Dekkers MP**, Burghoorn J, Jansen G.

*Antagonistic sensory cues generate gustatory plasticity in Caenorhabditis elegans.*

EMBO Journal. 2006 Jan 25;25(2):312-22.